Damage evaluation of civil engineering structures under extreme loadings

Bahar Ayhan Tezer

THÈSE DE DOCTORAT

DE L'ÉCOLE NORMALE SUPÉRIEURE DE CACHAN

Présentée par

Bahar AYHAN TEZER

pour obtenir le grade de

DOCTEUR DE L'ÉCOLE NORMALE SUPÉRIEURE DE CACHAN

Domaine :

MÉCANIQUE, GÉNIE MÉCANIQUE, GÉNIE CIVIL

Damage evaluation of civil engineering structures under extreme loadings

Thèse présentée et soutenue le 07/03/2013 devant le jury composé de :

- M. Turgut Kocaturk (rapporteur)
- M. Bostjan Branck (rapporteur)
- M. Adnan Ibrahimbegovic (directeur de thèse)
- M. Hasan Engin (directeur de thèse)
- M. Tuncer Toprak
- M. Reha Artan
- Mme Delphine Brancherie

LMT (Laboratoire de Mécanique et Technologie Cachan)
61, avenue du Président Wilson, 94235 CACHAN CEDEX (France)
ITU Graduate School of Science Engineering and Technology

ISTANBUL TECHNICAL UNIVERSITY ★ GRADUATE SCHOOL OF SCIENCE ENGINEERING AND TECHNOLOGY
ECOLE NORMALE SUPERIEURE DE CACHAN ★ DOCTORAL SCHOOL OF PRACTICAL SCIENCES

DAMAGE EVALUATION OF CIVIL ENGINEERING STRUCTURES UNDER EXTREME LOADINGS

JOINT Ph.D. THESIS

Bahar AYHAN TEZER

Department of Civil Engineering

Structural Engineering Programme

MARCH 2013

ISTANBUL TECHNICAL UNIVERSITY ★ GRADUATE SCHOOL OF SCIENCE ENGINEERING AND TECHNOLOGY
ECOLE NORMALE SUPERIEURE DE CACHAN ★ DOCTORAL SCHOOL OF PRACTICAL SCIENCES

DAMAGE EVALUATION OF CIVIL ENGINEERING STRUCTURES UNDER EXTREME LOADINGS

JOINT Ph.D. THESIS

Bahar AYHAN TEZER
(501052012) (ITU)
(150317) (ENSC)

Department of Civil Engineering

Structural Engineering Programme

Thesis Advisor: Prof. Dr. Hasan ENGİN
Thesis Co-advisor : Prof. Dr. Adnan IBRAHIMBEGOVIC

MARCH 2013

İSTANBUL TEKNİK ÜNİVERSİTESİ ★ FEN BİLİMLERİ ENSTİTÜSÜ

DİNAMİK YÜKLER ALTINDA MÜHENDİSLİK YAPILARINDA HASAR ANALİZİ

ORTAK DOKTORA TEZİ

Bahar AYHAN TEZER
(501052012) (ITU)
(150317) (ENSC)

İnşaat Mühendisliği Anabilim Dalı

Yapı Mühendisliği Programı

Tez Danışmanı: Prof. Dr. Hasan ENGİN
Tez Eşdanışmanı: Prof. Dr. Adnan IBRAHIMBEGOVIC

MARCH 2013

Bahar AYHAN TEZER, a **Ph.D.** student of ITU **Graduate School of Science Engineering and Technology** student ID **501052012** and ENS Cachan **Doctoral School of Practical Sciences** student ID **150317** successfully defended the thesis entitled **"DAMAGE EVALUATION OF CIVIL ENGINEERING STRUCTURES UNDER EXTREME LOADINGS"**, which she prepared after fulfilling the requirements specified in the associated legislations, before the jury whose signatures are below.

Thesis Advisor :	**Prof. Dr. Hasan ENGİN** Istanbul Technical University	.....
Co-advisor :	**Prof. Dr. Adnan IBRAHIMBEGOVIC** Ecole Normale Superieure de Cachan	.....
Jury Members :	**Prof. Dr. Tuncer TOPRAK** Istanbul Technical University	.....
	Prof. Dr. Reha ARTAN Istanbul Technical University	.....
	Prof. Dr. Turgut KOCATÜRK Yıldız Technical University	.....
	Prof. Dr. Bostjan BRANK University of Ljubljana	.....
	Assoc. Prof. Dr. Delphine BRANCHERIE University of Technology of Compiegne	.....

Date of Submission : **31 December 2012**
Date of Defense : **7 March 2013**

To my parents,

FOREWORD

This dissertation is written as completion to the joint doctoral studies in Structural Engineering at Istanbul Technical University and Ecole Normale Superieure de Cachan. The research along this title started at ENS Cachan under supervision of Dr. Adnan Ibrahimbegovic.

I would like to thank my advisor at Istanbul Technical University, Dr. Hasan Engin who made this dissertation possible with his knowledge, support and helpful suggestions in discussion. My heartfelt thanks and sincere regards go to Dr. Adnan Ibrahimbegovic for his meticulous guidance, continuous belief in my ability, constant encouragement and sincere advice all throughout my academic research.

I am also greatfully indebted to Dr. Delphine Brancherie whom I have had the opportunity to have valuable discussions with and help to the difficulties that I faced during the research, also without whom I would not deal with the problems. Thank you for your assistance and patience! I would like to express my appreciation to Dr. Pierre Jehel for his fruitful discussions and his introduction to FEAP codes. Special thanks to Dr. Jaka Dujc, PhD. Candidates Miha Jukic and Ngo Minh for their theoretical discussions and their friendships during our journey in Cachan.

Last but certainly not least, I would like to thank my parents Nilgün and Cem Ayhan and my sister Deniz Ayhan who have supported me in my whole life. I owe a grateful thank to my husband Övünc Tezer for encouranging and keeping me in focus.

I would like to herein appreciate the French Government through the French Embassy in Turkey for supporting me under the protocol of joint doctoral program.

I would also like to acknowledge The Scientific and Technological Research Council of Turkey, TUBITAK-BIDEB-2211 and 2214 from which I was funded by scholarship.

March 2013 Bahar AYHAN TEZER

TABLE OF CONTENTS

Page

LIST OF FIGURES

Page

DAMAGE EVALUATION OF CIVIL ENGINEERING STRUCTURES UNDER EXTREME LOADINGS

SUMMARY

In many industrial and scientific domains, especially in civil engineering and mechanical engineering fields, materials that can be used on the microstructure scale, are highly heterogeneous by comparison to the nature of mechanical behavior. This feature can make the prediction of the behavior of the structure subjected to various loading types, necessary for sustainable design, difficult enough. The construction of civil engineering structures is regulated all over the world: the standards are more stringent and taken into account, up to a limit state, due to different loadings, for example severe loadings such as impact or earthquake.

Behavior models of materials and structures must include the development of these design criteria and thereby become more complex, highly nonlinear. These models are often based on phenomenological approaches, are capable of reproducing the material response to the ultimate level.

Stress-strain responses of materials under cyclic loading, for which many researches have been executed in the previous years in order to characterize and model, are defined by different kind of cyclic plasticity properties such as cyclic hardening, ratcheting and relaxation.

By using the existing constitutive models, these mentioned responses can be simulated in a reasonable way. However, there may be failure in some simulation for the structural responses and local and global deformation. Inadequacy of these studies can be solved by developing strong constitutive models with the help of the experiments and the knowledge of the principles of working of different inelastic behavior mechanisms together.

This dissertation develops a phenomenological constitutive model which is capable of coupling two basic inelastic behavior mechanisms, plasticity and damage by studying the cyclic inelastic features. In either plasticity or damage part, both isotropic and linear kinematic hardening effects are taken into account. The main advantage of the model is the use of independent plasticity versus damage criteria for describing the inelastic mechanisms. Another advantage concerns the numerical implementation of such model provided in hybrid-stress variational framework, resulting with much enhanced accuracy and efficient computation of stress and internal variables in each element.

The model is assessed by simulating hysteresis loop shape, cyclic hardening, cyclic relaxation, and finally a series of ratcheting responses under uniaxial loading responses. Overall, this dissertation demonstrates a methodical and systematic development of a constitutive model for simulating a broad set of cycle responses. Several illustrative examples are presented in order to confirm the accuracy and efficiency of the proposed formulation in application to cyclic loading.

DİNAMİK YÜKLER ALTINDA MÜHENDİSLİK YAPILARINDA HASAR ANALİZİ

ÖZET

Bir çok endüstri ve bilimsel alanda, özellikle inşaat mühendisliği ve makine mühendisliği alanlarında, malzemeler mekanik davranışı itibariyle mikro ölçekte son derece heterojen bır yapıya sahiptirler. Bu özellik nedeniyle, sürdürülebilir tasarım için gerekli olan çeşitli yükleme türleri altında yapının davranışı hakkında tahmin yapmanın yeterince zor, hatta imkansız olduğu söylenebilir.

İnşaat mühendisliği yapılarının davranış kontrolü de maruz kaldığı yükleme çeşitliliği nedeniyle çok karmaşıktır. Yapıların analizi tüm dünyada standartlar ile düzenlenmiştir. Standartlar limit durumlar için deprem, darbe veya kimyasal reaksiyonlar gibi fiziksel etkileri dikkate alan farklı yüklemeleri hesaplara katar.

Malzeme ve yapıların davranış modelleri bu tasarım kriterlerinin geliştirilmesini içermelidir ve bu şekilde daha karmaşık, doğrusal olmayan hale gelir. Bununla birlikte, davranış modeleri genellikle çok ölçekli yaklaşımlara dayalıdır ve fiziksel olaylar dikkate alınır. Davranış yasaları ne kadar hassas ve karmaşık ise, yapıların davranışının sayısal simülasyonun kullanımı sınırlı kalır. Bu modeller genellikle fenomonolojik yaklaşımlara dayanmakta olup, nihai bir seviyeye kadar malzemenin yüklemelere tepki üretme yeteneğine sahiptir.

Tekrarlı yükleme altında malzemelerin gerilme-şekil değiş tirme tepkilerini karakterize etmek ve modellemek iç in önceki yıllarda yapılan birçok araştırmanın yapılmıştır. Bu tepkiler döngüsel pekleşme, şekil değ itirmelerin toplanması (ratcheting) ve ortalama gerilme gevşemesi (relaxation) gibi farklı türde döngüsel plastisite özellikleri ile tanımlanır.

Çevrimsel plastisite, tekrarlayan dış yüklemelere maruz kalan malzemelerin doğrusal olmayan gerilme şekil değiştirme tepkileri ile ilgilidir. Çevrimsel plastik şekil değiştirme, hizmet ömürleri sırasında çeşitli yüklemelere maruz kalan yük taşıyan, yük aktaran birleşimlerde kullanılan mühendislik malzemeleri için genellikle kaçınılmazdır. Çeşitli çevrimsel plastik deformasyonları incelemek mühendislikte kullanılan malzemelerin davranışlarını kavrayabilmek adına yararlı olabilir.

Simetrik şekil değiştirme kontrollü çevrimsel plastikleşme düşük çevrimli yorulma ve asimetrik şekil değiştirme kontrollü çevrimsel plastikleşme ortalama gerilme gevşemesi (mean stress relaxation) gibi malzeme davranışlarını doğurur. Şekil değiştirmelerin birikmesi (ratcheting) gerilme kontrollü asimetrik çevrimsel plastik yükleme sonucudur.

şekil değiştirmelerin birikmesi malzeme ve yapının genelinde ayrı ayrı ortaya çıkabilir. Malzemedeki birikme, yapı üzerine etkiyen gerilme homojen ise veya laboratuvar ortamında incelenen malzeme gibi kusursuz ise ortaya çıkabilir. Bunun dışında, yapıdaki şekil değiştirme birikmesi, malzemede birikme olmaması durumunda dahi

çevrimsel yükleme altında mazleme doğrusal olmayan davranışı dolayısıyla ortaya çıkar. Bu tip şekil değiştirme birikmesi yapıdaki gerilme durumunun homojen olmaması nedeniyle meydana gelir. Bu modellerin genelliğini doğrulamak için şekil değiştirmelerin birikmesi (ratcehting)ile ilgili geniş bir yelpazede tepkilere karşı test edilir. Sonuç olarak, bu bünye modellerin çoğu malzemelerdeki şekil değiştirmelerin birikmesi durumuna dair tepkileri oldukça iyi tahmin edebilir, ama yapılardaki birikme durumunda başarısız olabilir.

Ortalama bir gerilme esas alınarak etkitilen çevrimsel şekil değiştirme için, erken evre yorulma ömrü ortalam gerilme gevşemesi sonuçları ile belirlenir. Bu nedenle yorulma ömrü, simetrik çevrimsel şekil değiştirme ile karşılaştırıldığında ortalama şekil değiştirme tanıtımının sunulması ile kayda değer şekilde etkilenmez.

Farklı tipteki yorulma yüklemeleri altında malzeme şekil değiştirmelerinin birikimi, özelliklerinin bozulması ve dayanımlarının düşmesi ile ilgili kapsamlı bilgi mühendislik yapılarının etkili tasarım için gereklidir.

Gevşeme (relaxation) testleri, yükleme koşulları hizmet yüklerinin düzensizliğine yaklaştığı zaman, değişken büyüklükte yüklemeler için ortalama gerilmelerin çevrimsel gevşeme özellikleri hakkında bilgi edinmek amacıyla yapılmaktadır. Çeşitli plastisite modelleri, gözelenen davranışı elde etmek için incelenenir. Simülasyonlar ömür tahmini için geliştirilen yazılımların uygulaması için karşılaştırılırlar.

Çevrimsel plastisite tpkilerinin modellemesi oldukça karmaşıktır. Deneysel çalışmalar plastik yüklemeler ile akma yüzeylerinin büyüdüğü ve şekil değiştirdiğini göstermiştir.Plastik yükelem sırasında bazı metaller pekleşir, bazıları yumuşar (soften). Bununla birlikte, çevrimsel plastik tepkileri yükleme geçmişine bağlıdır. Mevcut bünye modellerinin çoğu, idealize edilmiş akma yüzeyleri ve pekleşme kuralları gibi bu karmaşık olayları simüle etmekte başarısızdır. Buna ek olarak, şekil değiştirmelerin birikmesi (ratcehting) simülasyonları için çevrimsel plastisite modelleri sınırlı veya basit deneyler verileri kullanılarak doğrulanır ve geliştirilir.

Mevcut bünye modellerini kullanarak, bu bahsedilen tepkiler makul bir şekilde simüle edilebilir. Ancak, yapısal tepkiler, yerel ve toplam deformasyon için bazı hesaplamalarda baş arısızlık olabilir. Bu çalışmaların yetersizliğ i deneyler ve farklı elastik olmayan davranış mekanizmalarının birlikte ç alış ma ilkelerine iliş kin bilgiler yardımıyla güçlü bünye modelleri geliştirerek çözülebilir.

Bu çalışmada, iki temel inelastik davranış plastisite ve hasar mekanizmalarını çift olarak çalıştığı bir fenomenolojik bünye modeli sunuyoruz. Bu model tekrarlı yükleme uygulamalarını hedeflemektedir. Böylece, plastisite veya hasar davranışı için, hem izotropik hem doğrusal kinematik pekleşme etkileri dikkate alınır. Modelin en büyük avantajı, elastik olmayan mekanizmaları tarif etmek için plastikleşme davranışına karşı hasar ölçütlerinin bağımsız olarak kullanılmasıdır. Diğer bir avantajı, her eleman için hibrid-gerilme varyasyonel hesaplamalar çerçevesinde elde edilen, gerilmelerin ve iç değişkenlerin doğru ve etkili hesaplanması ile sonuçlanan, bu modelin sayısal uygulaması ile ilgilidir.

Çevrimsel diyagramlar, geleneksel yöntem olan izotropik pekleşme parametreleri kullanılmasına ek olarak, kinematik pekleşme parametreleri ile plastik davranışa eklenen hasar izotropik pekleşmesi de dahil edilerek oluşturulur. Model, tek eksenli yüklemeler altında çeşitli çevrimsel diyagramlar elde edilmesiyle değerlendirilir. Genel sistematik geliş tirilmesini göstermektedir. Çeşitli örnekler tekrarlı yükleme

olarak, bu çalışma çevrimsel davranışların bir dizi geniş simülasyonu için bünye modelinin metodik ve için önerilen formülasyonun doğruluğu ve verimliliğini teyit etmek amacıyla sunulmaktadır.

DAMAGE EVALUATION OF
CIVIL ENGINEERING STRUCTURES
UNDER EXTREME LOADINGS

RESUME

Dans de nombreux domaines industriels et scientifiques, en particulier dans les domaines du génie civil et de génie mécanique, des matériaux à l'échelle de la microstructure, un très hétérogène par rapport à la nature du comportement mécanique. Cette fonctionnalité peut faire la prédiction du comportement de la structure soumise à différents types de chargement, nécessaires pour la conception durable, assez difficile. Le contrôle du comportement des ouvrages de génie civil est très complexe en raison de la diversité de la charge à laquelle ils sont soumis. La construction est maintenant réglementée partout dans le monde: les normes sont plus strictes et pris en compte, jusqu'à un état limite, en raison de différentes charges, par exemple des charges sévères tels que l'impact ou tremblement de terre.

Modèles de comportement des matériaux et des structures doivent inclure l'élaboration de ces critères de conception et deviennent plus complexe. Ces modèles sont souvent basées sur des approches phénoménologiques, sont capables de reproduire la réponse du matériau au niveau ultime.

Réponses de contrainte-déformation des matériaux sous sollicitations cycliques, dont de nombreuses recherches ont été exécutées dans les années précédentes afin de caractériser et le modèle, sont définies par différents types de propriétés de plasticité cycliques tels que l' écrouissageue, l'effet rochet et de de relaxation.

En utilisant les modèles de comportement existants, ces réponses mentionnées peuvent être simulés d'une manière raisonnable. Cependant, il peut y avoir échec dans certains simulation des réponses structurelles et la déformation locale et globale. Insuffisance de ces études peut être résolu par le développement de solides modèles de comportement à l'aide d'expériences et de la connaissance des principes de fonctionnement des différents mécanismes de comportement inélastique ensemble.

Dans ce travail, nous présentons un modèle phénoménologique constitutive qui est capable de coupler deux principaux mécanismes de comportement inélastique, plasticité et endommagement. Le modèle vise les applications de chargement cycliques. Ainsi, dans une partie de plasticité ou de dommages, les effets de durcissement isotropes et linéaires cinématiques à la fois sont pris en compte. Le principal avantage de ce modèle est l'utilisation de la plasticité indépendante contre les critères de l'endommagement pour décrire les mécanismes inélastiques. Un autre avantage concerne la mise en œuvre numérique d' un tel modèle fourni en hybride-stress variationnel, obtenu avec une précision très améliorée et calcul efficace du stress et des variables internes dans chaque élément. Plusieurs exemples sont présentés afin de confirmer l'exactitude et l'efficacité de la formulation proposée en application à un chargement cyclique.

1. INTRODUCTION

1.1 Problem Statement

Design of structures for various cyclic loading conditions that may cause inelastic behavior, such as earthquake ground motion, rotating machinery, etc. requires full understanding of inelastic phenomena of material, such as plasticity and damage, which may give correct interpretation of material failure. Persistent slip bands, rearrangement of dislocation system void nucleation etc. are the examples of changes that occur within the material which can be represented by plasticity model. Given our special interest in for cyclic loading, two main features of plasticity model ought to be represented. The first one is isotropic hardening, which is chosen to represent the saturation type behavior, and the second is the kinematic hardening, which is selected to capture the strain cycling effects.

For mechanical components subjected to asymmetric cyclic loading leading to plastic strain, most materials exhibit the phenomenon of either mean stress relaxation or strain ratchetting, or a combination of the two, depending on the applied load and structure geometry. If the maximum and minimum strains are fixed, then stress relaxation will occur. The initially non-zero mean stress will progressively shift towards zero as cyclic loading is applied, as sketched in Figure 1.1a. This is analogous to stress relaxation under monotonic loading with fixed strain, except it is induced by the cyclic loading rather than the elapsed time. On the other hand, if the maximum and minimum stresses are controlled, then the so called strain ratchetting will take place, as shown schematically in Figure 1.1b.

Again, this is similar to creep under constant monotonic stress, but it is caused by the cyclic straining and the existence of a non-zero mean stress. Both strain ratchetting and mean stress relaxation are characterised by unclosed hysteresis loops, and plastic shakedown refers to the steady state reached after a certain number of cycles. For a component with geometrical discontinuities, such as holes, cut-outs, notches and fillets, neither the stress nor the strain at the notch root is under control. Instead, the

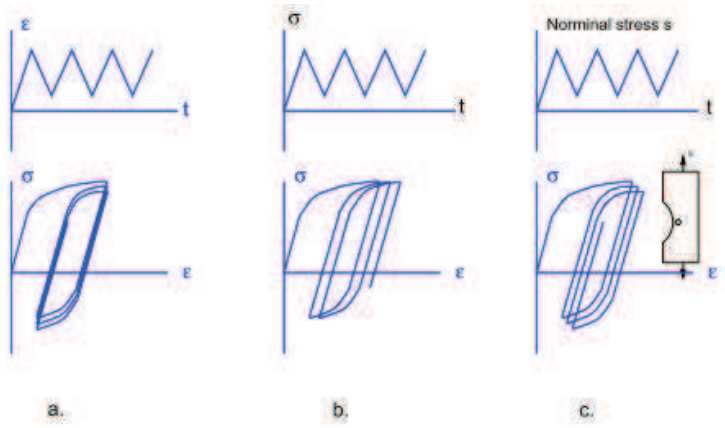

Figure 1.1: Cyclic behavior models.

remote stress or strain is prescribed, while the local stress and strain are governed by the geometry of the discontinuity and the behaviour of the material. In this case both strain ratchetting and mean stress relaxation occur simultaneously. As ratchetting depends on the existence of a nonzero mean stress, it can be anticipated that the local mean stress will gradually relax, and that eventually the stress-strain loop will stabilize with a zero mean stress [1].

1.2 Background and Literature Review

The plasticity models of this kind are presented in classical works of [2], [3] and [4]. In these works, the typical one of yield criteria, which defines the domain where the elastic response does not change in elastic loading and unloading, is the criterion of von Mises. This kind of criterion pertaining to deviatoric part of stress provide a plasticity that is suitable for metals and alloys. However, if we also want to account for gradual reduction of the elastic stiffness due to cyclic loading, we need a damage model. The continuum damage model is presented in detail in literature (e.g. see [5] or [6]). Elastic response is changed by damage model without residual deformation upon loading. The response of porous metals and alloys, as well as the cracking of concrete are phenomena that can be represented by using the damage model. Damage phenomenon is a irreversible process that occurs in material microstructure and its presence affects the material constitutive response at meso/macro scale. Damage accumulation occurs as a result of micro-cracking induced plastic deformation and this cyclic accumulation results in failure of the material.

Researchers are developing advanced constitutive model in order to define complex behavior of materials in cyclic loading. A constitutive model that is capable of coupling both basic types of inelastic behavior, plasticity and damage, is presented by [7] and [8]). These two basic constitutive models can be coupled into a single model, which can be used for metals with voids by [9], concrete compaction by [10] and plain concrete by [11]. There are two independent associated flow rules for plasticity and damage in the previous works done by [12] and [13].

Many oher recent works deal with the different facets of this complex problem, of providing the consititutive behavior characterized by damage and plasticity for different types of material (e.g. see [14]; [15]; [16]; [17]; [18]; [19]; [20]; [21]; [22]; [14]).This kind of models have not been extended to cycling loading.

Some have developed the constitutive models of plasticity under cyclic loading conditions which are also taken into account in this paper. The complicated behavior of material, such as plastic strain accumulation (ratcheting) or progressive relaxation of the stress, has been explained (e.g. [23] and [24]).

Cyclic behavior and its governing mechanims were also observed in recent years (e.g. see [25]; [26]; [27]; [28]; [29]; [30]; [31]; [32]; [33]; [34]).

In this work, we further extend these models to add a damage component, so to be able to account for elastic stiffness reduction. Strain energy is chosen as quadratic form with state variables, which are total strain, elastic strain, damage strain and strainlike variables. Yield criterion is also constructed as a quadratic form with dual variables, which are stress-like variables for both plasticity and damage. For this purpose, the principle of maximum plastic dissipation is used. The equations of evolution for plastic and damage internal variables are obtained by using the implicit backward Euler scheme. This model hypothesis was first presented in the study of [8].However, this presentation is here slightly modified to allow for using stress as one of the other state variables.

Contrary to this mentioned paper A. Ibrahimbegovic, D. Markovic and F. Gatuingt (Revue europeenne des elements finis [2003]) paper, we here proposed the direct stress interpolations and not the classical FE displacement interpolations presented previously by [8], AI, DM and FG [2003]), which allows us to remove the local

iterative procedure in computing the stress and internal variable of plasticity and damage. Hence, the proposed formulation is more efficent computationally, and for that reason we have also provided the details of the computational procedure.

Whereas, some researchers have employed the plasticity criteria on the effective stress obtained by damage model (e.g. [35] and [36])

Stress-based formulation of coupled damage-plasticity in the study of [37] is chosen herein,since it is very useful for solving simultaneously the equations at each numerical integration point.Once the values of internal variables are obtained the equilibrium equations are solved for the whole structure. Hellinger-Reissner type mixed variational type is constructed in which the interpolation functions are elaborated for displacement and stress fields independently. The first presentation of this kind is given in [37] for 1D problem. Here in this study, we target two-dimensional problems for membrane structure made of metallic materials and also the corresponding applications for cyclic loadings. Thus, the Pian-Sumihara finite element formulation is used in order to define the stress field.

1.3 Scope and Objectives

The cyclic constitutive behavior of mild steel under elastoplastic-damage deformation has been investigated in this research. Numerical simulations were performed under strain- controlled and stress-controlled cyclic loading, respectively, with a view to quantify the phenomena of mean stress relaxation and strain ratchetting. To mathematically describe the observed cyclic stress-strain behaviour, the framework of constitutive theory for rate-independent plasticity has been reviewed. A detailed discussion has been presented for a class of constitutive models which uses nonlinear differential equations to describe the isotropic hardening and also the kinematic hardening, using a back stress. A comparison to the experimental result shows that the model can provide very good representation of the material stress strain behavior under cyclic loading.

Responses under cyclic loading, e.g. cyclic hardening/softening, ratcheting, relaxation, and their dependence on strain range determine the stress-strain responses of materials under cyclic loading. Numerous efforts have been made in the past decades to characterize and model these responses. Many of these responses can be simulated

reasonably by the existing constitutive models, but the same models would fail in simulating the structural responses, local stress-strain, or global deformation. One of the reasons for this deficiency is that the constitutive models are not robust enough to simulate the cyclic plasticity responses when they interact with each other. This deficiency can be understood better or resolved by developing and validating constitutive models against a broad set of experimental responses and two or more of the responses interacting with each other. This dissertation develops a unified constitutive model by studying the cyclic plasticity features in an integrated manner and validating the model by simulating a broad set of cyclic plasticity responses.

1.4 Outline

The thesis outline is as follows. In Chapter 2, we describe the basic concepts of the inelastic phenomenon. A discussion is given from the elastic limit state througout the inelastic behavior, e.g. plasticity at first. The most common material inelastic behaviors are described. Also, control of the behavior from the elastic to plastic state are explained.

Chapter 3 gives the thermodynamically consistent theoretical formulations for the coupled damage-plasticity phenomenon. Internal variables which determines the material behavior are introduced by using the dissipation law and free strain energy. Hardening rules, which are important for the cyclic behavior are defined.

In Chapter 4, the finite element formulation is described. Pian Sumihara stress interpolation function beside the displacement shape function are used for the discretization of the problem. Computational algorithm (Operator Split Method) is presented, along with the numerical implementation and the corresponding variational formulation. The results of numerical examples are also given in order to further illustrate a very satisfying performance of the proposed solution scheme. Computer codes that describes the hardening models with the internal variables are implemented into the FEAP (Finite Element Program Analysis) in order to obtain hysteresis diagrams.

The results and conclusion are presented in Chapter 5.

2. FUNDAMENTAL CONCEPTS

2.1 Observations Elastic Limit

Assuming, we have a prismatic rod made of a ductile material, subjected to a uniaxial tensile stress, for which loading is quasi-static. A problem arises in order to determine the elastic limit: it is only when the limit is overleapt that we can determine where the limit was. So in theory, a certain level of stress should br applied, returned to zero, the deformation is measured. As the deformation at the end of the cycle is zero, the behavior of the material is said to be elastic. When the final deformation is measured as non-zero value for the maximum applied stress level, we get out of the elastic domain: the elastic limit is between the last two levels of imposed stress during the test. This procedure is very long and the precision of the limit depends on the difference between two successive levels of stress. It is not known that stress level corresponds to the limit, it is seen a posteriori that there is an irreversible deformation and it is deduced that the elastic domain of the material is quitted.

In practice, we proceed differently. Monotonic loading is performed at a given speed and the stress-strain curve is plotted. The elastic limit is determined by a suitable treatment of the points of this curve. Determining this limit is difficult and depends on the accuracy of measurement instruments. The conventional use of elastic limit is resorted; the most used idea is that the value which corresponds to a permanent deformation of $0,2$. If the material had never been subjected to this level of stress, the yield (elastic limit) is called initial. If we continue to increase the stress on the specimen beyond the elastic limit, there is material hardening: its elastic limit increases. This is why we have introduced earlier the initial yield. All stress levels between the initial yield and limit at failure are out elastic limits. The theory of plasticity is the mathematical theory of irreversible deformations independent of time.

If loading-unloading cycles are carried out by imposing in each cycle a stress exerted greater than in the previous cycle, the same curve is obtained as have been obtained without such intermediate unloading and loading.

The slope for these intermediate unloading and loading is constant up to a certain stress level and equal to the initial slope at the origin, that means that the modulus does not change while the structure plasticize and that the material hardens. The modulus of elasticity decreases beyond this stress called damage threshold. The deformation of the structure under loading, total deformation, called ε^t, is the sum of the elastic deformation ε^e and plastic deformation ε^p. The elastic deformation is determined from both the current point and the modulus of elasticity, which is equal to the ratio of stress modulus of elasticity. The plastic deformation is determined from both the total deformation and the elastic deformation. When the specimen was hardened in tension, and then it is compressed enough to reach the limit in compression, we see that for some materials, this limit has been reduced by hardening: it is the Bauschinger effect. For others, the increase in yield tensile is accompanied by an increase in the compression limit. Plastic deformations are, for most materials, incompressible: plastic flow occurs without volume change. Since the variation in volume associated with plastic deformations is zero, the modulus is infinite so Poisson's ratio is equal to $\frac{1}{2}$ for the plastic deformations.

$$\begin{aligned} \frac{V-V_0}{V_0} &\approx (\boldsymbol{\varepsilon}^t_{xx}+\boldsymbol{\varepsilon}^t_{yy}+\boldsymbol{\varepsilon}^t_{zz}) = 0 \\ \Rightarrow \kappa &= \frac{\sigma_{xx}+\sigma_{yy}+\sigma_{zz}}{3(\boldsymbol{\varepsilon}^t_{xx}+\boldsymbol{\varepsilon}^t_{yy}+\boldsymbol{\varepsilon}^t_{zz})} \\ &= \frac{E}{3(1-2\nu^p)} \\ \Rightarrow \nu^p &= \frac{1}{2} \end{aligned} \tag{2.1}$$

When a tensile test is performed on a specimen made of a ductile material, for sufficiently small values of the deformation, it is not useful to specify what kind of measurement is used to characterize the stress and strain: the curves are superimposables whatever the kind of measure is chosen. But when we leave this field, it may be important to make a difference in Figure 2.1.

On the conventional curve, peak point corresponds to the maximum load and the maximum stress, which the structure and the material can withstand. On the rational curve, the maximum stress does not appear at the peak but at the rupture. It is therefore important to specify on which curve is referred to the maximum or rupture stress. The peak point is characterized by the peak point coefficient.

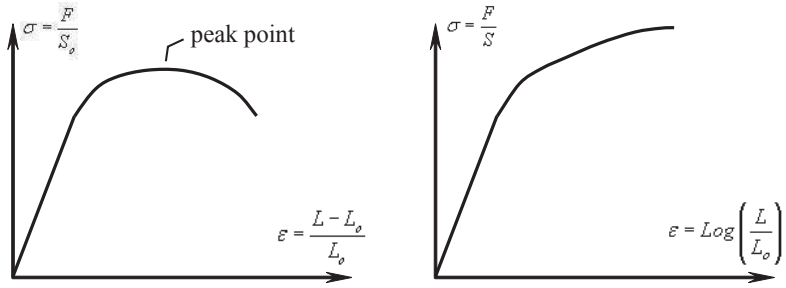

Figure 2.1: Curves in tension, ductile material. At left side, conventionel (nominal) curve At right side rational (real) curve.

$$Z = \frac{S_0 - S_{rupture}}{S_0}(en\%) \tag{2.2}$$

At the necking point, the abrupt decrease of the section is no longer compensated by hardening: the conventional curve passes through its maximum and the stress has no derivative with respect to the stretching (deformation). On the rational curve, there is a pinch point when the Cauchy stress is equal to its derivative with respect to deformation. σ^C is the Cauchy stress, γ is the deformation (stretching), Π is the stress PK1(Piola-Kirshoff 1), ε^C the Cauchy deformation , we write:

$$\begin{aligned}
\sigma^C = \gamma\Pi \rightarrow \frac{d\sigma^C}{d\gamma} &= \frac{d\Pi}{d\gamma}\gamma + \Pi \\
\varepsilon^C = Ln(\gamma) \rightarrow d\varepsilon^C = \frac{1}{\gamma}d\gamma \rightarrow \frac{d\gamma}{d\varepsilon^C} &= \gamma \\
\frac{d\sigma^C}{d\varepsilon^C} = \frac{d\sigma^C}{d\gamma}\frac{d\gamma}{d\varepsilon^C} &= (\frac{d\Pi}{d\gamma}\lambda + \Pi)\gamma = (0 + \Pi)\gamma = \sigma^C
\end{aligned} \tag{2.3}$$

Unless the deformations are the order of 2 or 3 %, there is no difference between the various steps of the deformation. A steel bar subjected to tension is out of the elastic range when its deformation is the order of 0.1 %. Deformation of 3 % is already high, few structural studies have been realized for the determination of metal behavior until failure. Consider now a test sample which is hardened in traction and hardened in compression, hardened again in tension and is subjected finally to a discharge elastic until the applied stress is zero in Figure 2.2. At point D, the plastic deformation is the same as the one going on during the first discharge or the second. However, the yield is not the same as it has been hardening between the two pathways through the point D. A law relating strain and stress is not conceivable. One of the difficulties of plasticity is the history effect(integration of all previous states) related to the irreversibility of

certain phenomena, so that there is no more simple and direct relationship between stress and strain. Thus, plasticity requires incremental laws dependent to parameters describing the hardening and parameters describing the state of plastic deformation from the current state. The laws of variation are infinitesimal and are taken into account in comparison to the current state. They provide the relationship between infinitesimal increase in deformation $d\varepsilon$ and infinitesimal increase in stress $d\sigma$ associated.

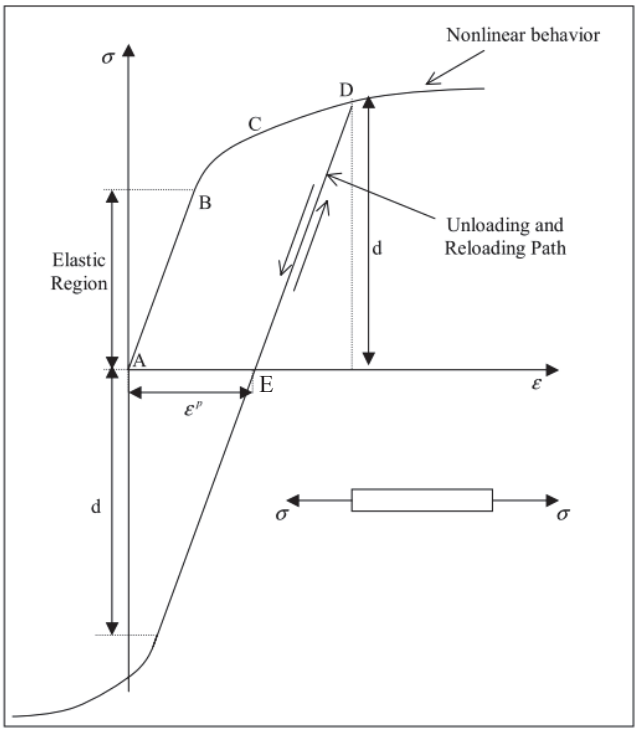

Figure 2.2: Stress-Strain curve for uniaxial loading.

In this study, we are interested in the macroscopic aspect of the plasticity, in models that represent this aspect and in numerical problems related to these models in commercial programs for calculation of structure [2]. During the calculation of the internal forces and tangent matrix, what is needed is to be able to calculate the stresses and tangent constitutive law from the state of deformation and internal variables of material. For plasticity, material nonlinearities are independent of time. This means that the nonlinear effects are instantaneous: deformation and stress have a simultaneous development; there is no delay of one with respect to the other. Creep and relaxation are not taken into account by standard plastic models. To calculate the behavior of a structure that plastifies, it reveals the concept of time. This is an auxiliary variable, which can give the chronology of events and study the behavior of the structure for a series of quasi-static equilibrium.

2.2 Materials and Behavior Models

A metal bar is subjected to a uniform uniaxial tension, the load gradually increases. Depending on the materials, there are various behavior models to represent the experimental curve. Material has an elastoplastic behavior if we can represent the experimental stress strain curve by a first segment that is straight line and then by a curve possibly rectilinear in Figure 2.3. If a discharge is performed in a point, the discharge is carried out by the initial Young's modulus.

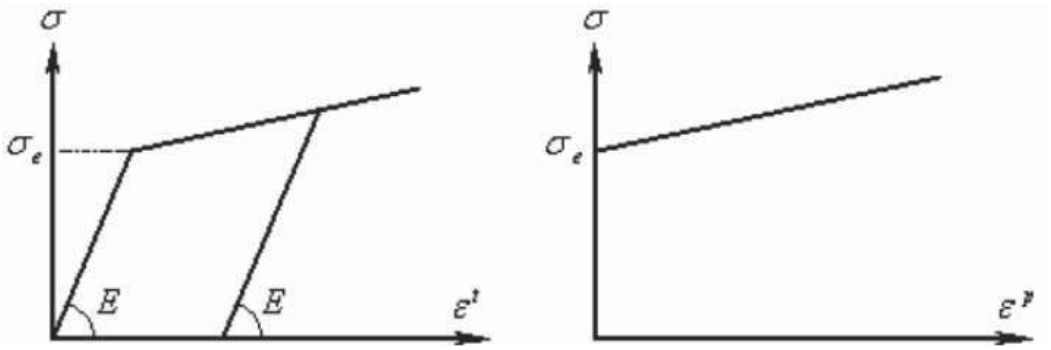

Figure 2.3: Model of elastoplasticity behavior.

There is hardening of the material, that means, variation in its yield with its plastic deformation. As the applied stress is less than the elastic limit σ_e, the behavior is elastic. When the applied stress reaches the yield stress and the loading is continued to increase, the plastic deformation and the elastic limit increase. When the plastic strain increases, the elastic range is enlarged, the length of the slope segment E increases. But more the yield increases more the material becomes brittle because the increase in the field of elasticity decreases the field of plasticity and increases sensitivity to stress concentrations due to small manufacture defects, the cavities caused by small one-off shocks. In the case of uniaxial tension, we can directly compare the applied stress on the elastic limit as the stress field has a nonzero component in the loading direction. Material has a perfect elastoplastic behavior if the experimental stress-strain curve can be represented by a first straight segment whose slope is the modulus of elasticity, and a horizontal segment. As the applied stress is less than the elastic limit σ_e, the behavior is elastic. When the applied stress reaches the elastic limit and the loading continues to increase. The total deformation increases but not the stress; there is no hardening

of the material in Figure 2.4. When the plastic strain is increased, the elastic field cannot grow; the length of the slope segment E is constant. If a discharge is performed in a point, it is carried out with the initial Young's modulus. This model of perfectly elastoplastic behavior is adapted in the stretching bearing area for materials such as mild steel.

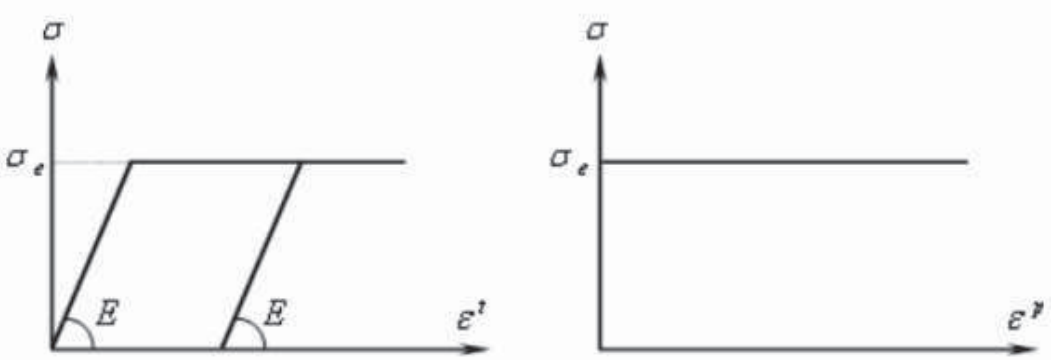

Figure 2.4: Model of perfectly elastoplasticity behavior.

2.3 Control of Plasticity

Assuming that a point in stress space represents the stress state in a material point of the structure. It is within the volume delimited by the surface plasticity. The material has an elastoplastic behavior, the viscosity is not taken into account. Three cases can occur during a load increment in Figure 2.5a.

- The point representing the new state of stress is in the volume defined by the surface plasticity,
- The point representing the new stress state is on the surface of plasticity,
- The point representing the new stress state is outside the volume limited by the surface of plasticity.

  In the first case, the behavior was elastic and it still is. For the second, the behavior was elastic and he became plastic. For the third, the behavior was elastic and became inadmissible. The plasticity surface must evolve so that the new point is on a new surface: this is the work hardening of the material. Assume now a point of the stress space representing the stress state in a material point of the structure. It is on the surface in Figure 2.5b.

- The point representing the new stress state came back to the volume delimited by the surface plasticity,
- The point representing the new stress state remains on the plasticity surface,
- The point representing the new stress is outside the volume delimited by the surface plasticity.

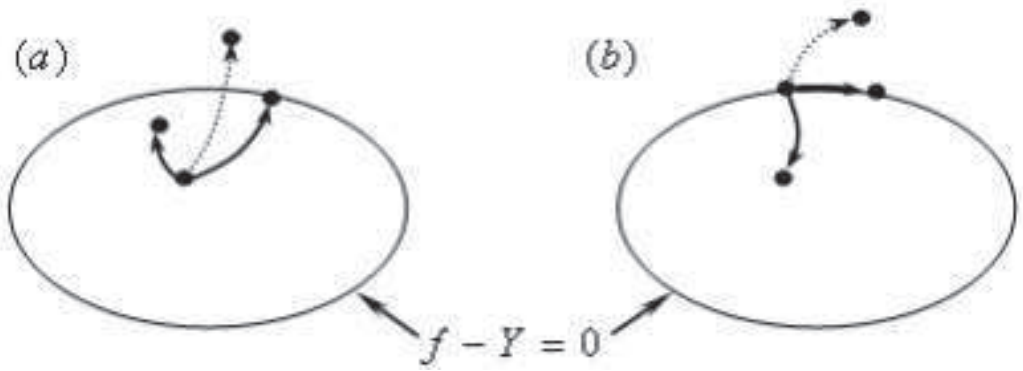

Figure 2.5: Representation of the possible configurations for a loading.

For the first case, we have an elastic discharge. For the second, loading is neutral. For the third, the behavior was plastic and it became inadmissible. The plasticity surface must evolve so that the new point is on a new surface: this is the work hardening of the material. Three types of data are needed to treat elastoplasticity:

- The plasticity criterion,
- The flow rule,
- The hardening rule

The plasticity criterion allows determining the value of the equivalent stress from the components of the stress tensor. If the elastic limit is exceeded by the value of the equivalent stress, the stress state is inadmissible. Plasticity came up or it has developed. A criterion allows determining when the plasticity appears but provides no information about the nature of the plastic behavior. To describe the plasticity surface and its evolution when there is hardening, it is necessary to know the flow law which expresses the relation between increased plastic deformation and increased stress. In the case of plasticity associated, hypothesis of the elastoplasticity theory generally well suited to

represent the behavior of metals, the function F, which describes the equation of the plasticity surface, is also called the plastic potential, plastic potential and plasticity surface being identical. The flow law is the relationship between the strain increment and increased stress. The hardening law gives the variation of plasticity with the stress state.

In practice, the current yield is compared to the equivalent stress that is evaluated for the current loading. When viscoplasticity is not taken into account, a point representing a stress state cannot be outside the volume defined (delimited) by the plasticity surface. If the estimated stress during a calculation of iteration is beyond this envelope, the stress state is not physical. The hardening is not involved to exceed the limit but to push it so that the stress reaches the new limit and is therefore admissible. In stress space, work harden a material is to modify its surface plasticity. Surface plasticity ϕ or intrinsic surface is written in the general form:

$$f(\sigma_{ij}, \alpha ij) - \sigma_y(\bar{\varepsilon}^p) = \phi(\sigma_{ij}, \alpha_{ij}, \bar{\varepsilon}^p) = 0 \qquad \textbf{(2.4)}$$

σ_y is the yield limit of the material which depends only on the equivalent plastic strain. f is the equivalent stress. α_{ij} are the coordinates of the center of the plasticity surface in the stress space. $\phi > 0$ is an unacceptable condition. If $\phi < 0$, the material has an elastic behavior in the vicinity of considered material, loading may continue until $\phi = 0$, the material in the vicinity of the considered material point has plastic behavior under the loading. In order that there is flow, the loading must be continued and is such that in Figure 2.6.

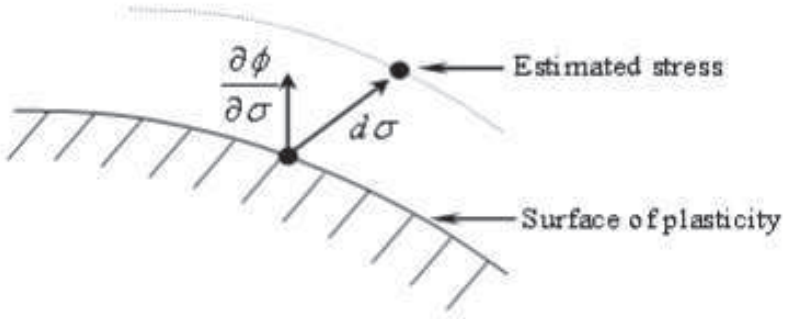

Figure 2.6: Plasticity Surface.

$$\phi = 0 \quad \frac{\partial \phi}{\partial \sigma} d\sigma \, 0 \qquad \textbf{(2.5)}$$

This relationship expresses that the projection of increased stress is in the direction of the outward normal at the current point of the plasticity surface, gradient $\frac{\partial \phi}{\partial \sigma}$ giving the direction and the direction of the maximum increase of the function ϕ. When there is flow, the starting point satisfies $\phi = 0$, the end point also: plasticity surface evolves but ϕ continues to be zero regardless the loading that produces the flow. The rule of consistency is deduced:

$$d\phi = 0 \tag{2.6}$$

If $\phi = 0$ and $\frac{\partial \phi}{\partial \sigma} d\sigma < 0$, the projection of increased stress on the gradient is negative, we return to the inside of plasticity surface, we are dealing with an elastic unloading. If $\phi = 0$ and $\frac{\partial \phi}{\partial \sigma} d\sigma = 0$, the projection of increased stress on the gradient is zero, we stay on the plasticity surface, we are dealing with a neutral loading.

When plasticity increases, increased plastic deformation is orthogonal to the plasticity surface at the considered point, it is the normality rule. It is written, $d\gamma$ being a scalar to be determined is called plastic multiplier:

$$d\varepsilon_{ij}^{p} = d\gamma \frac{\partial \phi}{\partial \sigma_{ij}} \tag{2.7}$$

In other words, we know how to evaluate the plastic deformation, but not how much. Whatever increase in stress σ, which expand the plasticity, it is accompanied by an increase in plastic deformation which is always orthogonal to the plasticity surface at the point where it is situated. The $d\gamma$ depends on the increase in loading, but the direction of change of plastic deformation does not depend on it, it depends on where it is located on the plasticity surface. In the case where the Von Mises criterion is used to define the equivalent stress, plasticity surface is given by:

$$\begin{aligned} \phi &= \sqrt{\frac{1}{2}[2\sigma_I^2 + 2\sigma^2 II + 2\sigma_{III}^2 - 2\sigma_I\sigma_{II} - 2\sigma_{II}\sigma_{III} - 2\sigma_{III}\sigma_I]} - \sigma_e \\ &= f - \sigma_e = 0 \end{aligned} \tag{2.8}$$

One can calculate the change in volume due to plastic deformation.

$$\begin{aligned} \frac{\partial \phi}{\partial \sigma_I} &= \frac{1}{2f}(2\sigma_I - \sigma_{II} - \sigma_{III}) \\ \frac{\partial \phi}{\partial \sigma_{II}} &= \frac{1}{2f}(-\sigma_I + 2\sigma_{II} - \sigma_{III}) \\ \frac{\partial \phi}{\partial \sigma_{III}} &= \frac{1}{2f}(-\sigma_I - \sigma_{II} + 2\sigma_{III}) \end{aligned} \tag{2.9}$$

The use of von Mises criterion involves the confirmation of experimental results obtained for metals, namely that plastic deformations are incompressible.

$$\begin{aligned} d\varepsilon_{ii}^{p} &= d\varepsilon_{I}^{p} + d\varepsilon_{II}^{p} + d\varepsilon_{III}^{p} \\ &= d\gamma\left(\frac{\partial\phi}{\partial\sigma_{I}} + \frac{\partial\phi}{\partial\sigma_{II}} + \frac{\partial\phi}{\partial\sigma_{III}}\right) = 0 \end{aligned} \tag{2.10}$$

2.4 The Criterion of Plasticity

Various tests with different stress states are performed and it is determined for each of them when the plasticity appears, which is arranged after a test of points cloud in the plane of the two principal stresses (σ_I, σ_{II}). We can then look for what is the equation of the curve that goes best with this scatter plot, or the equation of the surface in the stress space. This equation can always be put in the form, σ representing the principal constraints or constraints [3] as follows:

$$f(\sigma) = \sigma_y \quad \text{or} \quad f(\sigma, \sigma_y) = 1 \tag{2.11}$$

The function f defines the equivalent stress which is nothing other than a scalar obtained by more or less complicated mixing of components of the stress tensor, scalar, which has the advantage of being easily compared to the elastic limit. Mixing rule is called plasticity criterion. For a given material, a criterion passes better through the experimental points than others, but there is not a criterion better than another, suitable for all materials. It was only after development of material and mechanical tests that we are able to say which plasticity criterion is the most appropriate for this material. In the case of a uniform tension, which is the simplest mechanical test to perform and therefore the most common, the equivalent stress must be equal to the tensile stress applied to the specimen. σ_y is the yield strength of the material. The curve or surface equation is called plasticity surface.

$$f - \sigma_y = 0 \tag{2.12}$$

In the space of principal stresses, principal stresses are conventionally arranged in descending algebraic order, the surface of plasticity defined by the criterion Tresca (1864) is a right cylinder whose axis has equation $\sigma_I = \sigma_{II} = \sigma_{III}$, and whose cross section is independent of hydrostatic stress. In a plane deviator, which is a perpendicular plane to the axis of equation $\sigma_I = \sigma_{II} = \sigma_{III}$, all points on the surface of plasticity for a yield given is a regular hexagon. Projected in a plan of principal stresses, this set of points is a hexagon non regular in Figure 2.7 This is simply the intersection of a right hexagonal cylinder whose axis has equation $\sigma_I = \sigma_{II} = \sigma_{III}$ with a plane nonorthogonal to this axis. One difficulty with this criterion in terms

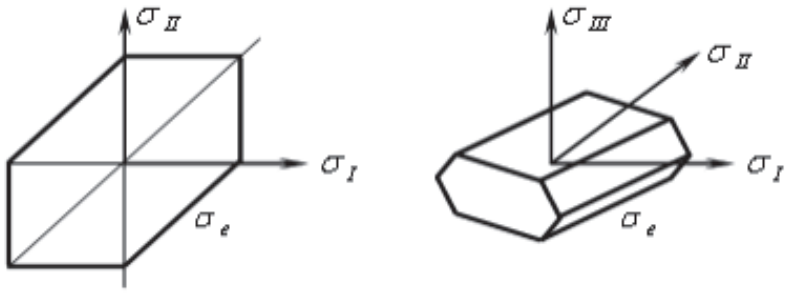

Figure 2.7: Representation of the plasticity surface defined by the Tresca criterion.

of numerical modeling is that the surface of plasticity, which this criterion defines, is not differentiable, important property for the representation of hardening. Equivalent stress of Tresca, based on the maximum shear stress that the material can withstand, is defined by the following equation.

$$\sigma_{eqT} = \sigma_I - \sigma_{III} \tag{2.13}$$

When the stress is reduced to a nonzero component σ_I, the equivalent stress is equal to the applied stress or to its opposite when the applied stress is negative. A material has an elastic behavior according to the criterion Tresca as the equivalent stress is less than or equal to the yield point.

$$\sigma_{eqT} \leqslant \sigma_e \tag{2.14}$$

The three basic invariants of the stress tensor from which all others can be written are:

$$\begin{aligned} I_1 &= \sigma_I + \sigma_{II} + \sigma_{III} \\ I_2 &= \sigma_I\sigma_{II} + \sigma_{II}\sigma_{III} + \sigma_I\sigma_{III} \\ I_3 &= \sigma_I\sigma_{II}\sigma_{III} \end{aligned} \tag{2.15}$$

The stress tensor is separated into two parts. σ_0 is the hydrostatic stress, the spherical part (or hydrostatic part) and the deviatoric part of the stress tensor are respectively defined by:

$$\sigma_0 = \frac{1}{3}(\sigma_I + \sigma_{II} + \sigma_{III}) \tag{2.16}$$

$$\begin{bmatrix} \sigma_{xx} & \sigma_{xy} & \sigma_{zx} \\ \sigma_{xy} & \sigma_{yy} & \sigma_{zy} \\ \sigma_{xz} & \sigma_{yz} & \sigma_{zz} \end{bmatrix} = \begin{bmatrix} \sigma_0 & 0 & 0 \\ 0 & \sigma_0 & 0 \\ 0 & 0 & \sigma_0 \end{bmatrix} + \begin{bmatrix} \sigma_{xx} - \sigma_0 & \sigma_{xy} & \sigma_{zx} \\ \sigma_{xy} & \sigma_{yy} - \sigma_0 & \sigma_{zy} \\ \sigma_{xz} & \sigma_{yz} & \sigma_{zz} - \sigma_0 \end{bmatrix} \tag{2.17}$$

The principal directions of the deviator are parallel to those of the stress tensor, the principal stress of the deviator are noted s_1, s_2, s_3. We introduce the invariants J, with

the same expression as I, but as the function of the deviatoric stress. The J_2 invariant can be expressed in terms of principal stress of deviator or function of the principal stresses:

$$J_2 = \frac{1}{2}(s_1^2 + s_1^2 + s_1^2) = \frac{1}{6}[(\sigma_I - \sigma_{II})^2 + (\sigma_{II} - \sigma_{III})^2 + (\sigma_{III} - \sigma_I)^2] = I_2 \qquad \textbf{(2.18)}$$

The most used and best known equivalent stress, suitable for most metallic materials is the von Mises (1913). It is based on the invariant J_2 and the fact that a finite amount of material can only store a limited amount of distortion energy. In the principal coordinate of stresses, the equivalent stress is expressed as:

$$\sigma_{eqVM} = \frac{1}{\sqrt{2}}\sqrt{(\sigma_I - \sigma_{II})^2 + (\sigma_{II} - \sigma_{III})^2 + (\sigma_{III} - \sigma_I)^2} \qquad \textbf{(2.19)}$$

A material has an elastic behavior according to the von Mises criterion as long as the equivalent stress is less than or equal to the yield point.

$$\sigma_{eqVM} \leqslant \sigma_e \qquad \textbf{(2.20)}$$

When the stress is reduced to a single non-zero component σ_I, the equivalent stress is equal to the applied stress, or to its opposite when the applied stress is negative. In the space of principal stresses, plasticity surface defined by the Von Mises criterion is a right cylinder of constant radius, independent of the hydrostatic stress and the axis has equation $\sigma_I = \sigma_{II} = \sigma_{III}$. In a deviator plane, which is a plane perpendicular to the previous axis, the set of points on the surface of plasticity for a yield limit given is a circle whose radius is independent of hydrostatic stress. Projected in a plane of principal stresses, this set of points is an ellipse whose major axis is the bisector of the first quadrant in Figure 2.8. This is simply the intersection of a right circular cylinder whose axis has equation $\sigma_I = \sigma_{II} = \sigma_{III}$ and a plane non-orthogonal to the mentioned axis.

The von Mises criterion is based on three assumptions.

- It assumes the isotropy of the material because all stresses have the same symmetric function.
- It is independent of the hydrostatic pressure, which makes it well suited for isotropic crystalline materials deforming by slip. But under the effect of hydrostatic

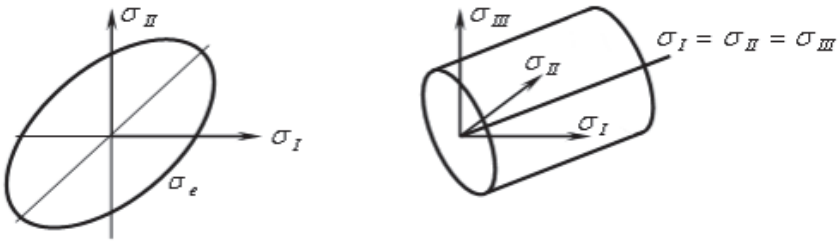

Figure 2.8: Representation of the plasticity surface defined by the von Mises criterion.

compression, the equivalent Von Mises stress is always zero and therefore, always remains below the elastic limit of the materials: the von Mises criterion is not suitable, among others, for the soil mechanics.

- If we replace the stresses by their opposite, the von Mises equivalent stress does not change: the criterion does not differentiate the traction from the compression.

For an orthotropic material, the criteria are developed in the orthotropic coordinate of material, which is directly related to the behavior of the material, rather than the coordinate of the principal stresses. This is particularly the case for the criterion of Hill and that of Tsai. F, G, H, L, M and N are the six parameters characterizing the hardening of the material, the equivalent stress in the sense of [2], dimensionless, is written:

$$\begin{aligned} F(\sigma_{11}-\sigma_{22})^2+G(\sigma_{22}-\sigma_{33})^2+H(\sigma_{33}-\sigma_{11})^2 \\ +2L\tau_{23}^2+2M\tau_{31}^2+2N\tau_{12}^2=\sigma_{eqH} \end{aligned} \tag{2.21}$$

If the limits are equal in all directions of space, the criterion of von Mises and Hill are identical. Material has an elastic behavior according to the criterion of Hill as long as;

$$\sigma_{eqH} \leqslant 1 \tag{2.22}$$

The limits are different according to the directions of orthotropy, the equivalent stress is no longer compared with the yield limit but with the expression above, equal to 1. When the normalized equivalent stress σ_{eqH} reaches the tensile yield stress in direction 1 and in direction 2 for another test, in the direction 3 for another test, there are respectively:

$$\begin{aligned} F\sigma_{e11}^2+H\sigma_{e11}^2=1 \\ F\sigma_{e22}^2+G\sigma_{e22}^2=1 \\ G\sigma_{e33}^2+H\sigma_{e33}^2=1 \end{aligned} \tag{2.23}$$

This system gives the coefficients F, G and H, the functions of the elastic limits in different directions. Shear tests allow the determination of the coefficients L, M and N. This criterion is suitable for anisotropic materials, it is an extension of the von Mises criterion. But this criterion is based on two assumptions: the hydrostatic stress has no effect on the equivalent stress and there is no differentiation between tension and compression.

The equivalent stress within the meaning of Tsai-Hill (1968), is written without dimension in the orthotropic axes of material;

$$\begin{aligned}\sigma_{eqTH} = {} & a(\sigma_{11}-\sigma_{22})^2 + b(\sigma_{22}-\sigma_{33})^2 + c(\sigma_{33}-\sigma_{11})^2 \\ & + g(\sigma_{11}-\sigma_{22}) + h(\sigma_{22}-\sigma_{33}) + i(\sigma_{33}-\sigma_{11}) \\ & + d\tau_{23}^2 + e\tau_{31}^2 + f\tau_{12}^2\end{aligned} \tag{2.24}$$

It takes into account linear terms, to differentiate tension from compression, but it does not include the hydrostatic stress. Material has an elastic behavior according to the Tsai-Hill criterion [38] as long as;

$$\sigma_{eqTH} \leqslant 1 \tag{2.25}$$

More expressions take part for coefficients, more mechanical tests are necessary to identify them. The von Mises criterion is based on a decomposition of the deformation energy, involving explicitly the spherical part and the deviatoric part of the stress tensor: there is a physical approach behind this criterion. For glues and adhesives, the behavior is generally different in tension and compression. One possible criterion is the criterion of Raghava (1973) [39] which is defined by the relation:

$$\sigma_{eqR} = \frac{I_1(s-1) + \sqrt{I_1^2(s-1)^2 + 12J_2 s}}{2s} \leqslant \sigma_e \tag{2.26}$$

I_1 is the first invariant of the stress tensor, that is to say a simple function of the hydrostatic stress. J_2 is the second invariant of the deviatoric stress, thus independent of the hydrostatic stress. C is the absolute value of the yield stress in compressive and T is limit stress in traction; s is the ratio between C and T. For adhesives, the parameter s is of the order of 1,3. This criterion implies the isotropy of the material but manages the differences between tension and compression. It is suitable for modeling the behavior of certain metal alloys, having the same limits of elasticity according to the direction

of the load. There are other criteria in which the expression is more complex, taking into account the anisotropy, the hydrostatic stress, defining distinguishable surfaces or not. The plasticity surface is dependent on principal stress or components of the stress tensor. The equation is in the form

$$f(\sigma) = \sigma_y \quad \text{ou} \quad f(\sigma, \sigma_y) = 1 \tag{2.27}$$

Is the limit surface that separate the admissible behavior (all set of interior points of the volume delimited by the surface) from the inadmissible behavior (all set of points outside the volume limited by the surface). For the points such as the stress state satisfies the equation $f(\sigma) < \sigma_y$ or $f(\sigma, \sigma_y) < 1$ according to the criteria, the material has an elastic behavior. For the points such as the stress state satisfies the equation $f(\sigma) = \sigma_y$ or $f(\sigma, \sigma_y) = 1$ according to the criteria, the material has a plastic behavior.

3. COUPLED DAMAGE-PLASTICITY MODEL : THEORY

3.1 Introduction

Dislocation theory first studied by [40], [41], [42], can explain plastic deformation of ductile materials. After the yield stress limit, which is the critical point for paasing through the inelastic behavior, dislocations are generating, moving, storing. Thus, hardening of material starts to occur with the moving dislocations, whose density in the material begins to form, and therefore an increase in stress for additional plastic deformation starts.

The accumulation of micro cracks and micro voids with loading can be caused the change of damage surface. In order to describe the phenemenon, a damage material model can be used by defining the evolution of a damage tensor through a damage criterion. The change in size, shape, position of the damage are taken into account in addition to damage surface. A $J2$ damage criterion is used with isotropic hardening corresponding to the change in size of the damage surface.

The constitutive model is derived using consistent thermodynamics in this chapter for a classical rate-independent continuum J2 coupled plasticity damage model. Based on the first law of thermodynamics, the Helmholtz free energy , which is function of the strain and the internal state variables under consideration, is introduced to describe the current state of energy in the material [43] and [44].

3.2 Continuum Mechanics and Thermodynamics

3.2.1 Equations of states

In this section we present the main ingredients for the formulation of a coupled damage-plasticity model in the framework of the thermodynamics of continuum media. In order to describe evolution of elastic properties due to damage and hardening of the material due to plasticity, we consider five different internal variables, namely: $\boldsymbol{\varepsilon}^d$ is the plastic strain, ξ^p a scalar that controls the isotropic hardening, $\boldsymbol{\kappa}^{\boldsymbol{p}}$, a deviatoric

second order tensor controlling the kinematic hardening, damage compliance tensor $\boldsymbol{D}$ and ξ^d, which is a scalar hardening like variable related to damage.

In order to derive governing equations of the model, we consider the following main three groups of ingredients:

- additive decomposition of strain into elastic, damage and plastic strains:

$$\boldsymbol{\varepsilon} = \boldsymbol{\varepsilon}^e + \boldsymbol{\varepsilon}^p + \boldsymbol{\varepsilon}^d \tag{3.1}$$

where $\boldsymbol{\varepsilon}^p$ corresponds to the unrecoverable strain at zero stress, $\boldsymbol{\varepsilon}^e$ corresponds to the recoverable part of strains when unloading with the initial elastic modulus. Finally, $\boldsymbol{\varepsilon}^d$ corresponds to the additional recoverable part of strains due to the evoloution of the elastic modulus during damage. A schematic representation is given in Figure 3.1 for a 1D model.

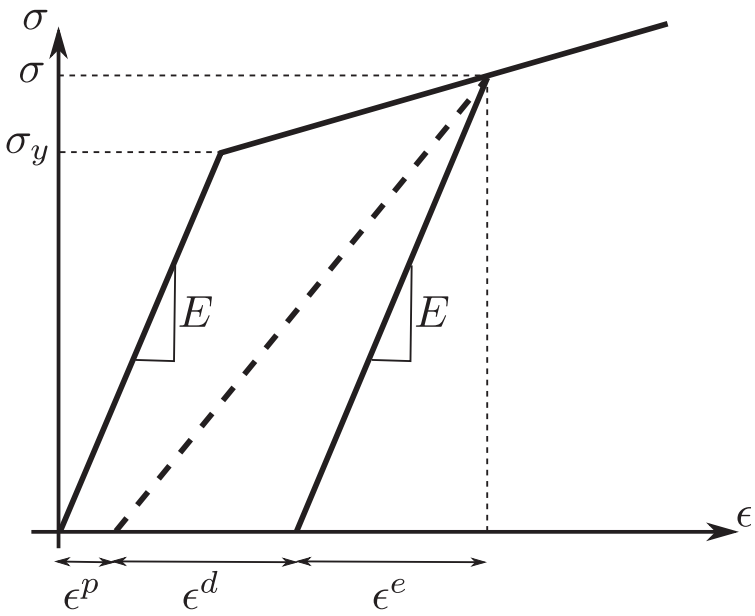

Figure 3.1: Schematic representation of the involved strains for a 1D model.

Strictly speaking, the damage strain $\boldsymbol{\varepsilon}^d$ is not new internal variable, but rather a vehicle of ensuring the coupling the plasticity on one side and damage on another side in constructing the joint inelastic response of this kind of model.

- total strain energy with contribution of both plasticity and damage:

$$\begin{aligned}\psi(\boldsymbol{\varepsilon}, \boldsymbol{\varepsilon}^d, \boldsymbol{D}, \xi^d, \boldsymbol{\varepsilon}^p, \xi^p, \boldsymbol{\kappa^p}) = &\psi^e(\boldsymbol{\varepsilon}^e) + \psi^d(\boldsymbol{\varepsilon}^d, \boldsymbol{D}) \\ &+ \Xi^p(\xi^p) + \Xi^d(\xi^d) + \Lambda^p(\boldsymbol{\kappa^p})\end{aligned} \tag{3.2}$$

where $\Xi^p(\xi^p)$, $\Lambda^p(\boldsymbol{\kappa^p})$ and $\Xi^d(\xi^d)$ are the plastic and damage hardening functions. The elastic strain energy is defined as:

$$\psi^e(\boldsymbol{\varepsilon}^e) = \frac{1}{2}\boldsymbol{\varepsilon}^e : \boldsymbol{C}^e : \boldsymbol{\varepsilon}^e = \boldsymbol{\sigma} : \boldsymbol{\varepsilon}^e - \chi^e(\boldsymbol{\sigma}) \tag{3.3}$$

and the term related to damage strain energy is given by using the Legendre transformation (see [45]),

$$\psi^d(\boldsymbol{\varepsilon}^d, \boldsymbol{D}) = \boldsymbol{\sigma} : \boldsymbol{\varepsilon}^d - \chi^d(\boldsymbol{\sigma}, \boldsymbol{D}); \quad \chi^d(\boldsymbol{\sigma}, \boldsymbol{D}) = \frac{1}{2}\boldsymbol{\sigma} : \boldsymbol{D} : \boldsymbol{\sigma} \tag{3.4}$$

- yield and damage criteria defining the elastic domain are final ingredients given as:

$$\phi^p(\boldsymbol{\sigma}, q^p, \boldsymbol{\alpha}) \leq 0; \quad \phi^d(\boldsymbol{\sigma}, q^d) \leq 0 \tag{3.5}$$

where q^p, $\boldsymbol{\alpha}$ and q^d denote respectively the dual variables associated to ξ^p, $\boldsymbol{\kappa^p}$ and ξ^d defined previously:

$$\begin{aligned} q^p &= -\frac{\partial \Xi^p}{\partial \xi^p} = -K^p \xi^p + (\sigma_\infty - \sigma_y)(1 - \mathrm{e}^{-b^p \xi^p}) \\ \boldsymbol{\alpha} &= -\frac{\partial \Lambda^p}{\partial \boldsymbol{\kappa}^p} = -H \boldsymbol{\kappa}^p \\ q^d &= -\frac{\partial \Xi^d}{\partial \xi^d} = -K^d \xi^d + (\sigma_{f\infty} - \sigma_{fy})(1 - \mathrm{e}^{-b^d \xi^d}) \end{aligned} \tag{3.6}$$

where K^p,K^d and H are the modulus for the relating inelastic behavior, also b^p and b^d are the hardening parameters of plasticity and damage, respectively. Furthermore, σ_y and σ_∞ are the yield stress and saturation stress for the isotropic hardening behavior of the plasticity. σ_{fy} and $\sigma_{f\infty}$ are the fracture stress and saturation stress of the damage phenomenon.

3.2.2 Dissipation potential

Considering in addition the principle of maximum plastic/damage dissipation will allow to obtain the internal variables evolution equations and constitutive equations. Namely, the second principle of the thermodynamics imposes that the total dissipation produced by the model remains positive [3], so that we can write:

$$
\begin{aligned}
0 \leq \dot{\mathscr{D}} &= \boldsymbol{\sigma} : \dot{\boldsymbol{\varepsilon}} - \dot{\psi} \\
&= \boldsymbol{\sigma} : (\dot{\boldsymbol{\varepsilon}}^e + \dot{\boldsymbol{\varepsilon}}^p + \dot{\boldsymbol{\varepsilon}}^d) - \frac{\partial}{\partial t}[\psi^e(\boldsymbol{\varepsilon}^e) + \psi^d(\boldsymbol{\varepsilon}^d, D) + \Xi^p(\xi^p) + \Xi^d(\xi^d) + \Lambda^p(\boldsymbol{\kappa^p})] \\
&= \dot{\boldsymbol{\varepsilon}}^e : (\boldsymbol{\sigma} - \frac{\partial \psi^e}{\partial \boldsymbol{\varepsilon}}) - \dot{\boldsymbol{\sigma}} : (\boldsymbol{\varepsilon}^d - \frac{\partial \chi^d}{\partial \boldsymbol{\sigma}}) \\
&\quad + \underbrace{\boldsymbol{\sigma} : \dot{\boldsymbol{\varepsilon}}^p - \frac{\partial \Xi^p}{\partial \xi^p}\dot{\xi}^p - \frac{\partial \Lambda^p}{\partial \boldsymbol{\kappa}^p} : \dot{\boldsymbol{\kappa}}^p}_{\dot{\mathscr{D}}^p} + \underbrace{\frac{\partial \chi^d}{\partial \boldsymbol{D}} : \dot{\boldsymbol{D}} - \frac{\partial \Xi^d}{\partial \xi^d}\dot{\xi}^d}_{\dot{\mathscr{D}}^d} \geq 0
\end{aligned}
\tag{3.7}
$$

For an elastic process with no evolution of plastic and damage variables and no plastic or damage dissipation, the last equation gives the state equations for the stress and damage strain:

$$
\boldsymbol{\sigma} = \frac{\partial \psi^e}{\partial \boldsymbol{\varepsilon}^e} = \boldsymbol{C}^e : \boldsymbol{\varepsilon}^e; \quad \boldsymbol{\varepsilon}^d = \frac{\partial \Xi^d}{\partial \boldsymbol{\sigma}} = \boldsymbol{D} : \boldsymbol{\sigma} \tag{3.8}
$$

Assuming that the state equations (3.6) and (3.8) remain valid for a plastic process, the total dissipation can be rewritten and decomposed into a plastic and a damage part, so that we obtain the two following inequalities:

$$
\dot{\mathscr{D}}^p = \boldsymbol{\sigma} : \dot{\boldsymbol{\varepsilon}}^p + q^p \dot{\xi}^p + \boldsymbol{\alpha} : \dot{\boldsymbol{\kappa}}^p \geq 0 \tag{3.9}
$$

and

$$
\dot{\mathscr{D}}^d = \frac{1}{2}\boldsymbol{\sigma} : \dot{\boldsymbol{D}} : \boldsymbol{\sigma} + q^d \cdot \dot{\xi}^d \geq 0 \tag{3.10}
$$

The evolution equations of internal variables for such a process can be obtained by appealing to the principle of maximum plastic dissipation. The latter can be defined as the choice of both admissible stress and dual hardening variables $(\boldsymbol{\sigma}, q^p, \boldsymbol{\alpha}, q^d)$ which maximize the total dissipation. Finally, due to the separation of the total dissipation into (3.10)and (3.9), we can treat separately the two behaviors and search for the set $(\boldsymbol{\sigma}, q^p, \boldsymbol{\alpha})$ maximizing the plastic dissipation and the variable q^d maximizing the damage dissipation. Those maximization problems can be recast as minimization problems under constraint and treated by introducing Lagrange multipliers and the corresponding Lagrangian. For such minimization problems, the Kuhn-Tucker optimality conditions will provide the evolution equations and loading/unloading conditions. The two following subsections detail all those procedures for the plastic and damage part of the model, respectively.

3.2.2.1 Plasticity model: yield criterion and consistency condition

The plastic internal variables evolution equations are obtained considering the plastic part of the total dissipation and introducing the plastic Lagrangian and associated plastic Lagrange multiplier $\dot{\gamma}^p$. The maximization problem is then recast as a minimization problem as:

$$\max_{\dot{\gamma}^p>0} \min_{(\boldsymbol{\sigma}^*, q^{p*}, \boldsymbol{\alpha}^*)} \mathscr{L}^p(\boldsymbol{\sigma}^*, q^{p*}, \boldsymbol{\alpha}^*, \dot{\gamma}^p) \tag{3.11}$$

where

$$\begin{aligned} \mathscr{L}^p(\boldsymbol{\sigma}, q^p, \boldsymbol{\alpha}, \dot{\gamma}^p) &= -\mathscr{D}^p(\boldsymbol{\sigma}, q^p) + \dot{\gamma}^p \phi(\boldsymbol{\sigma}, q^p, \boldsymbol{\alpha}) \\ &= -\boldsymbol{\sigma} : \dot{\boldsymbol{\varepsilon}}^p - q^p \dot{\xi}^p - \boldsymbol{\alpha} : \dot{\boldsymbol{\kappa}}^p + \dot{\gamma}^p \phi(\boldsymbol{\sigma}, q^p, \boldsymbol{\alpha}) \end{aligned} \tag{3.12}$$

We obtain the associated Kuhn-Tucker optimality conditions as follows:

$$\begin{aligned} \frac{\partial \mathscr{L}^p}{\partial \boldsymbol{\sigma}} &= -\dot{\boldsymbol{\varepsilon}}^p + \dot{\gamma}^p \frac{\partial \phi^p}{\partial \boldsymbol{\sigma}} = 0 \rightarrow \dot{\boldsymbol{\varepsilon}}^p = \dot{\gamma}^p \frac{\partial \phi^p}{\partial \boldsymbol{\sigma}} \\ \frac{\partial \mathscr{L}^p}{\partial q^p} &= -\dot{\xi}^p + \dot{\gamma}^p \frac{\partial \phi^p}{\partial q^p} = 0 \rightarrow \dot{\xi}^p = \dot{\gamma}^p \frac{\partial \phi^p}{\partial q^p} \\ \frac{\partial \mathscr{L}^p}{\partial \boldsymbol{\alpha}} &= -\dot{\boldsymbol{\kappa}}^p + \dot{\gamma}^p \frac{\partial \phi^p}{\partial \boldsymbol{\alpha}} = 0 \rightarrow \dot{\boldsymbol{\kappa}}^p = \dot{\gamma}^p \frac{\partial \phi^p}{\partial \boldsymbol{\alpha}} \end{aligned} \tag{3.13}$$

The evolution equations in (3.13) are also accompanied by the loading/unloading conditions, which can be written as:

$$\begin{aligned} \phi^p(\boldsymbol{\sigma}, q^p, \boldsymbol{\alpha}) = &\parallel dev(\boldsymbol{\sigma}) + \boldsymbol{\alpha} \parallel - \sqrt{\frac{2}{3}}(\boldsymbol{\sigma}_y - q^p) \leq 0 \\ &\dot{\gamma}^p \geq 0 \quad \text{and} \quad \dot{\gamma}^p \phi^p = 0 \end{aligned} \tag{3.14}$$

where $\phi^p(\boldsymbol{\sigma}, \boldsymbol{\alpha}, q^p)$ is here chosen as the von Mises criterion with isotropic and kinematic hardening that is used to characterize the elastoplastic behavior of the material, $\boldsymbol{\alpha}$ is the back stress, a second order deviatoric tensor ($tr(\boldsymbol{\alpha}) = \mathbf{0}$), $dev\boldsymbol{\sigma} = \boldsymbol{\sigma} - \frac{1}{3} tr(\boldsymbol{\sigma})\mathbf{I}$ and $\parallel \bullet \parallel = \sqrt{\bullet : \bullet}$.

Taking into account the characteristic form of the von Mises yield criterion, the derivative of the yield function ϕ^p with respect to the stress and back stress are given by:

$$\frac{\partial \phi^p}{\partial \boldsymbol{\sigma}} = \frac{dev(\boldsymbol{\sigma}) + \boldsymbol{\alpha}}{\parallel dev(\boldsymbol{\sigma}) + \boldsymbol{\alpha} \parallel} : (\mathbf{I} - \frac{\mathbf{1}}{\mathbf{3}} \mathbf{1} \otimes \mathbf{1}) = \boldsymbol{\nu} \tag{3.15}$$

$$\frac{\partial \phi^p}{\partial \boldsymbol{\alpha}} = \frac{dev(\boldsymbol{\sigma}) + \boldsymbol{\alpha}}{\parallel dev(\boldsymbol{\sigma}) + \boldsymbol{\alpha} \parallel} = \boldsymbol{\nu} \tag{3.16}$$

where $\boldsymbol{\nu}$ is a second order tensor which is defined as the normal to the yield surface $\phi^p = 0$. The explicit form of the evolution equations (3.13)are then readily obtained as;

$$\begin{aligned} \dot{\boldsymbol{\varepsilon}}^p &= \dot{\gamma}^p \boldsymbol{\nu} \\ \dot{\xi}^p &= \sqrt{\frac{2}{3}}\dot{\gamma}^p \\ \dot{\boldsymbol{\kappa}}^p &= \dot{\gamma}^p \boldsymbol{\nu} \end{aligned} \tag{3.17}$$

During the plastic loading, $\dot{\gamma}^p > 0$ has to be computed to obtain the evolution of internal variables. This is reached by using the consistency condition in order to guarantee the admissibility of the subsequent states:

$$\dot{\gamma}^p > 0 \quad , \quad \phi^p(\boldsymbol{\sigma}, q^p, \boldsymbol{\alpha}) = 0 \quad , \quad \dot{\phi}^p(\boldsymbol{\sigma}, q^p, \boldsymbol{\alpha}) = 0 \tag{3.18}$$

which gives:

$$\dot{\phi}^p(\boldsymbol{\sigma}, q^p, \boldsymbol{\alpha}) = \frac{\partial \phi^p}{\partial \boldsymbol{\sigma}} : \dot{\boldsymbol{\sigma}} + \frac{\partial \phi^p}{\partial q^p}\dot{q}^p + \frac{\partial \phi^p}{\partial \boldsymbol{\alpha}} : \dot{\boldsymbol{\alpha}} = 0 \tag{3.19}$$

By introducing equations (3.8)and (3.17)into the consistency condition we finally obtain the Lagrange multiplier as:

$$\dot{\gamma}^p = -\frac{\frac{\partial \phi^p}{\partial \boldsymbol{\sigma}} : \dot{\boldsymbol{\sigma}}}{\frac{\partial \phi^p}{\partial q^p}\frac{\partial q^p}{\partial \dot{\xi}^p}\frac{\partial \phi^p}{\partial q^p} + \frac{\partial \phi^p}{\partial \boldsymbol{\alpha}} : \frac{\partial \boldsymbol{\alpha}}{\partial \dot{\boldsymbol{\kappa}}^p} : \frac{\partial \phi^p}{\partial \boldsymbol{\alpha}}} \tag{3.20}$$

This result can then be used to obtain the stress rate constitutive equations in the plastic regime.

$$\dot{\boldsymbol{\sigma}} = \left\{ \boldsymbol{C}^e - \frac{\boldsymbol{C}^e \frac{\partial \phi^p}{\partial \boldsymbol{\sigma}} \frac{\partial \phi^p}{\partial \boldsymbol{\sigma}} \boldsymbol{C}^e}{\frac{\partial \phi^p}{\partial \boldsymbol{\sigma}} \boldsymbol{C}^e \frac{\partial \phi^p}{\partial \boldsymbol{\sigma}} + \frac{\partial \phi^p}{\partial q^p}\frac{dq^p}{d\xi^p}\frac{\partial \phi^p}{\partial q^p} + \frac{\partial \phi^p}{\partial \boldsymbol{\alpha}} : \frac{\partial \boldsymbol{\alpha}}{\partial \boldsymbol{\kappa}^p} : \frac{\partial \phi^p}{\partial \boldsymbol{\alpha}}} \right\} (\dot{\boldsymbol{\varepsilon}} - \dot{\boldsymbol{\varepsilon}}^d) \tag{3.21}$$

3.2.2.2 Damage model: damage criterion and consistency condition

The procedure to obtain damage internal variables evolution is very similar to the one presented for plasticity. We start by constructing the minimization problem by using the damage dissipation already obtained in the previous section and $\dot{\gamma}^d$ as Lagrange multiplier.

$$\max_{\dot{\gamma}^d > 0} \min_{(\boldsymbol{\sigma}^*, q^{d*})} \mathscr{L}^d(\boldsymbol{\sigma}^*, q^{d*}, \dot{\gamma}^d) \tag{3.22}$$

where

$$\begin{aligned}\mathscr{L}^d(\boldsymbol{\sigma},q^d,\dot{\gamma}^d) &= -\dot{\mathscr{D}}^d(\boldsymbol{\sigma},q^d)+\dot{\gamma}^d\phi(\boldsymbol{\sigma},q^d)\\ &= -\frac{1}{2}\boldsymbol{\sigma}:\dot{\boldsymbol{D}}:\boldsymbol{\sigma}+q^d\xi^d+\dot{\gamma}^d\phi(\boldsymbol{\sigma},q^d)\end{aligned} \tag{3.23}$$

The Kuhn-Tucker optimality conditions for the damage behavior can then be written as:

$$\begin{aligned}\frac{\partial\mathscr{L}^d}{\partial\boldsymbol{\sigma}} = -\boldsymbol{\sigma}:\dot{\boldsymbol{D}}+\dot{\gamma}^d\frac{\partial\phi^d}{\partial\boldsymbol{\sigma}} = 0 \rightarrow \boldsymbol{\sigma}:\dot{\boldsymbol{D}} = \dot{\gamma}^d\frac{\partial\phi^d}{\partial\boldsymbol{\sigma}}\\ \frac{\partial\mathscr{L}^d}{\partial q^d}-\dot{\xi}^d+\dot{\gamma}^d\frac{\partial\phi^d}{\partial q^d} = 0 \rightarrow \dot{\xi}^d = \dot{\gamma}^d\frac{\partial\phi^d}{\partial q^d}\end{aligned} \tag{3.24}$$

along with the loading/unloading condition for damage components:

$$\phi^d(\boldsymbol{\sigma},q^d) = \frac{1}{3}Tr(\boldsymbol{\sigma})-(\boldsymbol{\sigma}_f-q^d)\leq 0,\quad \dot{\gamma}^d\geq 0\quad\text{and}\quad\dot{\gamma}^d\phi^d = 0 \tag{3.25}$$

We finally use consistency condition to obtain the damage multiplier needed to compute the damage internal variables evolution and constitutive equations.

$$\dot{\gamma}^d = -\frac{\frac{\partial\phi^d}{\partial\boldsymbol{\sigma}}:\boldsymbol{D}^{-1}:\dot{\boldsymbol{\varepsilon}}^d}{\frac{\partial\phi^d}{\partial\boldsymbol{\sigma}}:\boldsymbol{D}^{-1}:\frac{\partial\phi^d}{\partial\boldsymbol{\sigma}}+\frac{\partial\phi^d}{\partial q^d}\frac{\partial q^d}{\partial\xi^d}\frac{\partial\phi^d}{\partial q^d}} \tag{3.26}$$

This result can be used to obtain the stress rate constitutive equation for damage component.

$$\dot{\boldsymbol{\sigma}} = \left\{\boldsymbol{D}^{-1}-\frac{\boldsymbol{D}^{-1}\frac{\partial\phi^d}{\partial\boldsymbol{\sigma}}\frac{\partial\phi^d}{\partial\boldsymbol{\sigma}}\boldsymbol{D}^{-1}}{\frac{\partial\phi^d}{\partial\boldsymbol{\sigma}}\boldsymbol{D}^{-1}\frac{\partial\phi^d}{\partial\boldsymbol{\sigma}}+\frac{\partial\phi^d}{\partial q^d}\frac{dq^d}{d\xi^d}\frac{\partial\phi^d}{\partial q^d}}\right\}\dot{\boldsymbol{\varepsilon}}^d \tag{3.27}$$

3.2.2.3 Coupling model: elasto-plastic-damage tangent modulus

In this section, the elasto-plastic-damage tangent moculus will be obtained by using the incremental stress and the total incremental strain.

Enforcing the equality of stress computed from the coupled model components in (3.21) and (3.27) , we obtain;

$$\mathbf{C}^{ep}(\dot{\boldsymbol{\varepsilon}}-\dot{\boldsymbol{\varepsilon}}^d) = \mathbf{C}^{ed}\dot{\boldsymbol{\varepsilon}}^d \rightarrow \dot{\boldsymbol{\varepsilon}}^d = [\mathbf{C}^{ep}+\mathbf{C}^{ed}]^{-1}\mathbf{C}^{ep}\dot{\boldsymbol{\varepsilon}} \tag{3.28}$$

where

$$\mathbf{C}^{ep} = \boldsymbol{C}^e-\frac{\boldsymbol{C}^e\frac{\partial\phi^p}{\partial\boldsymbol{\sigma}}\frac{\partial\phi^p}{\partial\boldsymbol{\sigma}}\boldsymbol{C}^e}{\frac{\partial\phi^p}{\partial\boldsymbol{\sigma}}\boldsymbol{C}^e\frac{\partial\phi^p}{\partial\boldsymbol{\sigma}}+\frac{\partial\phi^p}{\partial q^p}\frac{dq^p}{d\xi^p}\frac{\partial\phi^p}{\partial q^p}+\frac{\partial\phi^p}{\partial\boldsymbol{\alpha}}:\frac{\partial\boldsymbol{\alpha}}{\partial\boldsymbol{\kappa}^p}:\frac{\partial\phi^p}{\partial\boldsymbol{\alpha}}} \tag{3.29}$$

$$\mathbf{C}^{ed} = \boldsymbol{D}^{-1} - \frac{\boldsymbol{D}^{-1}\frac{\partial \phi^d}{\partial \boldsymbol{\sigma}}\frac{\partial \phi^d}{\partial \boldsymbol{\sigma}}\boldsymbol{D}^{-1}}{\frac{\partial \phi^d}{\partial \boldsymbol{\sigma}}\boldsymbol{D}^{-1}\frac{\partial \phi^d}{\partial \boldsymbol{\sigma}} + \frac{\partial \phi^d}{\partial q^d}\frac{dq^d}{d\xi^d}\frac{\partial \phi^d}{\partial q^d}} \tag{3.30}$$

The latter provides the stress rate constitutive equation of the coupled model.

$$\dot{\boldsymbol{\sigma}} = \underbrace{\frac{\mathbf{C}^{ed}\mathbf{C}^{ep}}{\mathbf{C}^{ep} + \mathbf{C}^{ed}}}_{\mathbf{C}^{epd}} \dot{\boldsymbol{\varepsilon}} \tag{3.31}$$

From (3.21) and (3.27) we can see the explicitly the consistent tangent modulus $\mathbf{C}^{epd}$. The graphic illustration for 1D case is shown in Figure 3.2.

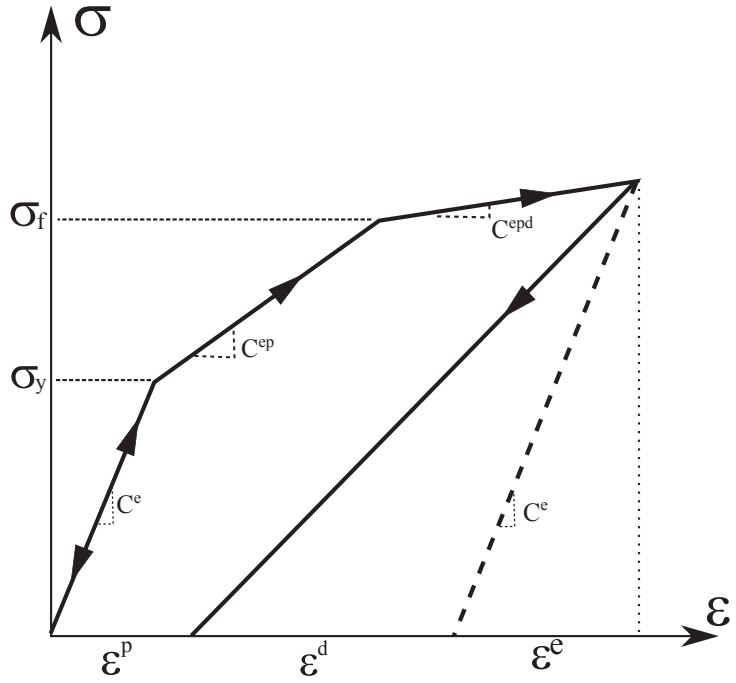

Figure 3.2: Stress-strain diagram for the coupled damage-plasticity model.

3.2.3 Hardening models

When there is hardening, plasticity surface changes. It can change the volume, change position, change shape or any combination of these three evolutions. In this work, we do not consider the change in shape of the plasticity surface, which is the case when the experimental curves in different directions are not proportional. The hardening is called isotropic if the center of the plasticity surface is not affected by hardening. Plasticity surface changes by scaling (homothety); it retains the shape of the surface and has uniform expansion in all directions: there is no Bauschinger effect. The increase in the tensile elastic limit is equal to the increase of the yield in compression

in Figure 3.3. In the case of the Von Mises criterion, the plasticity surface has, in a deviatoric plane, a circle whose center does not change but whose radius increases by work hardening. In terms of principal stresses, an expansion of the ellipse in all directions has occured. The plasticity surface is defined by the relation:

$$f(\sigma_{ij} - \sigma_y(\bar{\varepsilon}^p)) = \phi(\sigma_{ij}, \bar{\varepsilon}^p) = 0 \tag{3.32}$$

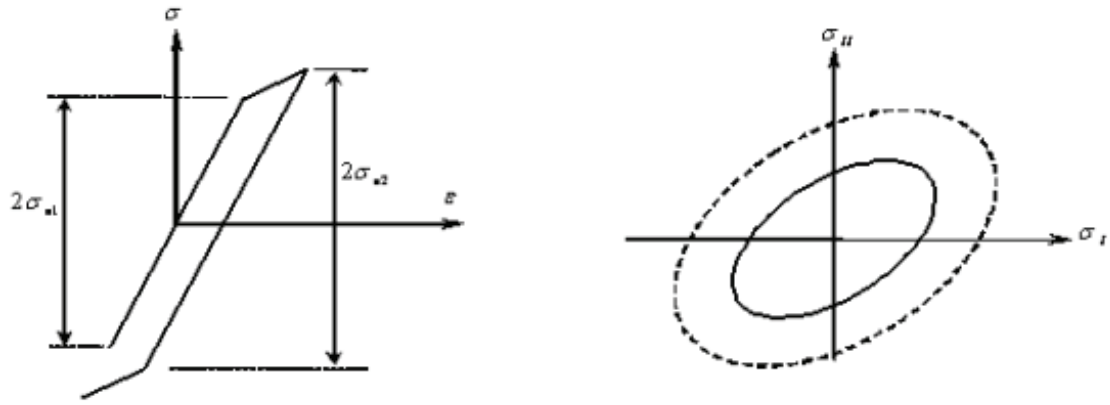

Figure 3.3: Representation of isotropic hardening.

It is said that it's kinematic hardening if only the center of the plasticity surface changes during the hardening. There is no extension of the area in the plasticity surface but only in the area of tensile stress space: there is then a Bauschinger effect in Figure 3.4.

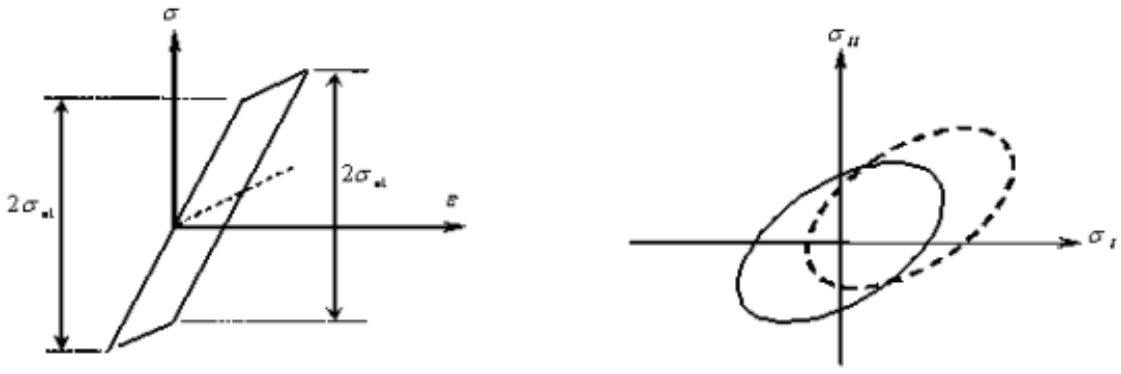

Figure 3.4: Representation of kinematic hardening.

The increase in the tensile elastic limit strength is equal to the reduction of the elastic limit in compression. The plasticity surface is defined by the relation:

$$f(\sigma_{ij}, \gamma_{ij}) - \sigma_y = \phi(\sigma_{ij}, \gamma_{ij}) = 0 \tag{3.33}$$

According to Prager model of kinematic hardening, plasticity surface translates in the direction of the normal to the considered point on this surface. Depending on Ziegler model of kinematic hardening, translation is done in the direction which passes through the updated center of the plasticity surface and the considered point on the surface in Figure 3.5.

In the case of Von Mises criterion, the plasticity surface being a circle in the deviatoric plane, the normal direction and the central direction are confused; there is therefore no need to differentiate between these two models of kinematic hardening.

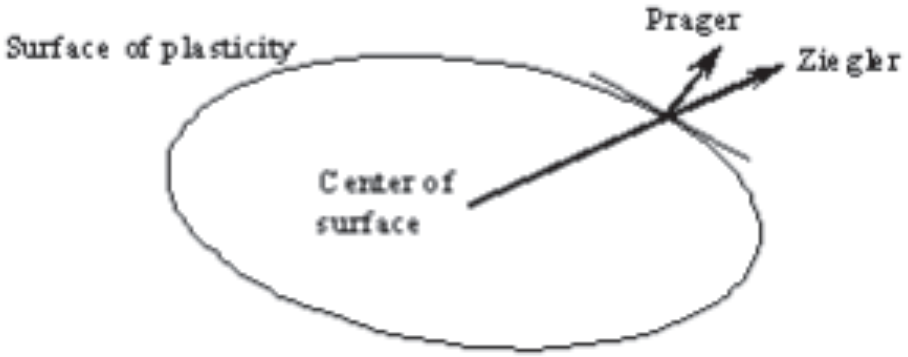

Figure 3.5: Displacement directions of the plasticity surface.

The difference between the isotropic and kinematic hardening only appears during a loading cycle because it is the amplitude of the descent that changes depending on the type of behavior. For a large number of tests, the specimen is subjected to a monotonically increasing tensile loading until failure, or traction followed by a return to zero load. It is not possible to know the type of hardening. Therefore, it is generally assumed to be isotropic, which is easier to define than the kinematic hardening as the center of the plasticity surface is then invariant. According to the extent of elastic area compared to the plastic range, if the loading has an increase in stress and returns to zero which does not induce a compression level which plasticize the material, it is not possible to specify the model of hardening in the numerical model.

The hardening is called mixed if it is a combination of isotropic hardening and kinematic hardening, in which case it is necessary to determine the proportion of each type of hardening.

3.2.4 Flow rule

The flow law is the relationship between increase in plastic deformation and increase in stress. The behavior of many materials can be regarded as isotropic, in order to limit the characterization tests necessary to determine the material properties, it reduces to a uniaxial equivalent curve and scalar law, simple to use. The flow law of material is in theory the link between the growth of components of the strain tensor and the growth of components of stress tensor. In the case of isotropic hardening, the plasticity surface changes according to a variable called the equivalent plastic strain. An equivalent stress is a scalar that represents the state of triaxial stress at a point. An equivalent plastic strain is a scalar that represents the state of triaxial plastic deformation at a point. The variation of equivalent plastic strain can be defined in two ways. The first is to define a simple relationship between the variation of equivalent plastic strain and plastic strain tensor. This is the strain hardening. In this case, we define the increment of equivalent plastic strain by:

$$d\bar{\varepsilon} = \sqrt{\frac{2}{3}(d\varepsilon_{ij}^{p} d\varepsilon_{ij}^{p})} \tag{3.34}$$

By definition, an increment of equivalent plastic strain is always positive or zero. The second is to make equal the work dissipated by the triaxial state, and the equivalent stresses and strains. This is called work hardening:

$$W_p(uniaxial) = W_p(multiaxial) \rightarrow Y d\bar{\varepsilon}^{p} = \sigma_{ij} = d\varepsilon_{ij}^{p} \tag{3.35}$$

In the case of a Von Mises criterion, the two definitions of the variation of equivalent plastic strain are equivalent. Equivalent plastic strain is obtained by integration of the variation of the equivalent plastic strain, regardless of the definition:

$$\bar{\varepsilon}^{p} = \int_{0}^{\varepsilon_{ij}^{p}} d\bar{\varepsilon}^{p} \tag{3.36}$$

This quantity is always positive or zero, it reflects the history of plastic deformation. When the equivalent plastic strain is zero, the material did not plasticize at the point where it was calculated. If it is positive, there were material plastification at the

considered point. It only increases except during an elastic step on which it remains constant. Any multidimensional evolution can be expressed more simply using the work hardening curve between equivalent stress and equivalent plastic strain. In the case of a uniaxial tensile test according to direction 1 performed on a specimen of cylindrical section, knowing that plastic deformations are incompressible for metals and Poisson's ratio associated with plastic deformation is $\frac{1}{2}$, the equivalent plastic strain is equal to the plastic deformation $\frac{2}{3}$ which permit to find the result for the hardening in deformation. The work hardening leads the same result.

$$d\varepsilon_{11}^{p} + d\varepsilon_{22}^{p} + d\varepsilon_{32}^{p} = 0 \rightarrow d\varepsilon_{22}^{p} = d\varepsilon_{33}^{p} = -\frac{1}{2} d\varepsilon_{11}^{p} \tag{3.37}$$

$$\sqrt{\frac{2}{3}(d\varepsilon^{p2}_{11} + d\varepsilon^{p2}_{22} + d\varepsilon^{p2}_{33})} = \sqrt{\frac{2}{3}\frac{3}{2} d\varepsilon^{p2}_{11}} = d\varepsilon_{11}^{p} \tag{3.38}$$

3.3 Conclusion

In this chapter, a framework of the coupled damage-plasticity has been shown. Thermodynamically consistent theoretical formulations have been constructed by starting the Helmholtz free strain energy, which consists of two parts, one is for plasticity and other is for damage. From that point, all the internal variables for plasticity and damage component are described. It is defined at the end how to obtain the elasto-plastic-damage tangent modulus, which is used to find the stress-strain relationship.

4. COUPLED DAMAGE-PLASTICITY MODEL : NUMERICAL ASPECTS

4.1 Integration Algorithm

The previous equations allow finding the variation of stresses as a function of an increase in infinitely small deformations. In practice, during a finite element analysis, on a computation step, the variation of deformation is not infinitely small. The previous equations must be considered. In this section, we consider an integration point which we know all the features (stress, strain, state variables ...) at step (n) and deformations at the step $(n+1)$ or variations of the total strain between the steps n and $(n+1)$. At this stage, we are looking for the stresses at the step $(n+1)$ corresponding to these new strains. The equilibrium is obtained by global iterations on the structure.

First solution for determining the stresses consist in calculating and using the tangential material rule to at the step (n). The stress at the step $(n+1)$ is calculated simply by:

$$\sigma_{n+1} = \sigma_n + C^e_{T,n}\Delta\varepsilon \tag{4.1}$$

If there was a flow at the step, the stresses at the point (n+1) does not obey the plasticity criterion because increase in deformation is finite and not infinitesimal, and the evolution of the tangential material rule has not been taken account at the step. The stresses must be brought on the new surface whose actual equation is $\phi = 0$. It may be possible to cut the variation in deformation at different intervals in order to reduce the error introduced by this scheme. Another commonly used scheme is the elastic predictor / plastic corrector.

The first step (predictor) is to calculate test stress elastically under the assumption that the behavior is elastic at the step: C^e is the matrix of Hooke of material (elastic behavior), increase in total strain is an increase in elastic deformation.

$$\sigma^{TR} = \sigma_n + C^e\Delta\varepsilon \tag{4.2}$$

The second step (corrector) is to compare the stress calculated from these test stress at the initial elastic limit if the material has not been hardened yet, at the current yield if the material has been hardened:

$$\phi = f(\sigma^{TR} - \sigma_y(\bar{\varepsilon}_n^p)) \tag{4.3}$$

If $\phi < 0$, the step is elastic for the considered integration point and stresses at the step $(n+1)$ are equal to test stresses. If $\phi > 0$, the plasticity criterion does not obey at $(n+1)$, there is plastic flow in order to check the criterion, accompanied by a change in plastic deformation. Part of the variation in total strain is elastic, the other plastic but at this stage we do not know yet their proportions.

Since there is the flow, increase in real stress is not equal to increase in estimeted stress by assuming that the increase in total deformation is entirely elastic. Therefore the stresses must be brought on the plasticity criterion.To do this, a plastic corrector is used, the stress at the step $(n+1)$ is given by:

$$\sigma_{n+1} = \sigma_n + C^e(\Delta\varepsilon^e) = \sigma^{TR} - \Delta\gamma C^e \frac{\partial f}{\partial \sigma} \tag{4.4}$$

The variation of plastic deformation is calculated according to the stresses at the step (n+1). It also requires that the plasticity criterion is respected at the step $(n+1)$. This leads to a system of nonlinear equations at each integration point, which is generally solved by a Newton method at the integration point. 7 unknowns of this system of seven equations are six components of the stress tensor and the scalar $\delta\gamma$ which has the same interpretation as $d\gamma$ in the theoretical formulation but is not infinitely small:

$$\sigma_{n+1} = \sigma^{TR} - \Delta\gamma C^e \frac{\partial f}{\partial \sigma_{n+1}} \tag{4.5}$$

$$f(\sigma_{n+1}) - \sigma_y(\bar{\varepsilon}_n^p + \Delta\bar{\varepsilon}^p) = 0 \quad where \quad \bar{\varepsilon}^p = \frac{1}{\sigma_y}\sigma\frac{\partial f}{\partial \sigma}\Delta\gamma \tag{4.6}$$

In general, local convergence is achieved rapidly. It is an implicit integration. The above relationships are used to determine the expression of the stress equation at the step $(n+1)$ as a function of increasing strain.

The equations of the stress at $(n+1)$ in accordance with the increase in deformation. Differentiating these relations with respect to deformations, we obtain the tangent rule which corresponds to the integration scheme used to calculate the stresses. We talk about consistent tangent rule, it is different from the theoretical tangent rule. The use of consistent tangent rule improves the convergence at the Newton-Raphson scheme used for the equilibrium of the structure.

4.2 Tangent Matrice, Numerical Integration

In the case of a finite element whose material behavior is elastic and linear, Hooke matrix that appears in the calculation of the stiffness matrix (or the tangent stiffness matrix for nonlinear geometric analysis) is not only constant for any analysis, but it is uniform in each element. With traditional notations, we can write integral form for the element e:

$$K^e = \int\int\int B^T HBdV \tag{4.7}$$

This matrix is evaluated by numerical integration according to various rules: each term k_{ij} matrix is obtained by sampling the m integration points of the element

$$k_{ij}^e = \int\int\int B^T HNdV = \sum [B_i]_m^T H_m [B_j]_m \omega_m \tag{4.8}$$

H_m is the Hooke matrix at the point m: it is the same at any point. W_m is the weight function associated with the integration point multiplied by the determinant of the Jacobian matrix of the element. In the case of an analysis in which the plasticity appears, the construction of the stiffness matrix is different. From that point of integration, the equivalent stress is such that there is a plastification, Hooke's law is replaced by the material tangent law to integration point(s) having plasticity, the law that evolves the level of hardening and stress state as shown The material tangent law in an element is different in each integration point of the element as it depends on the stress level of each integration point. The evaluation of the terms of the tangent stiffness matrix is much more complex than in the case where the material has a linear elastic behavior. The variation of the element terms to be integrated in the tangent stiffness matrix is more important in plasticity than in elasticity. We can therefore ask whether it is advantageous to increase the number of integration points on the

element to get a better accuracy. If we increase the number of points, the integral can be better evaluated, but it is a false precision. The plastic solution is less regular than the elastic solution. If we want to increase the precision, it is better to increase the number of elements, because increasing the number of integration points does not change the degree of the deformation field that depends on displacements and not stresses. However, the instant when plasticity begins will be better identified if the number of integration points is increased. Indeed, a linear element with a large strain gradient is considered. If only one point of integration is used, the plasticity begins when the plasticity criterion is reached in the middle of the element. If two points are used, it is when it is achieved about one-quarter of the element. More the number of integration points are big, more they are near the end and the beginning of plasticity is detected. To illustrate this point, there is a quadrangular membrane with an integration rule of $2x2$ points. Plasticity must arrive at point P in order to be detected and $\frac{1}{4}$ of the element is then plastic. Plasticity is in fact already appeared in the element, and when the plasticity begins, it is possible that the plasticity is physically won over a quarter of the element , or less than a quarter depending on how it advances into the element as a function of the loading. With a rule 3x3 points for the same item, simply it arrives at point P in order to be detected and ninth element is then plastic . The increase in the number of integration points has significant influence on the cost of calculating the tangent matrix and storage space. And experience shows that this increase does not significantly change the global non-linear behavior. We must ask ourselves what is the purpose of the plastic calculation: determining when the structure begins to plasticize or know how to redistribute the stresses in the spread of plasticity. In the first case, an elastic calculation with a good post-treatment may suffice. In the second case, provided that the mesh is sufficiently fine and is accountable for the development of plasticity, the number of integration points per element has little influence. Anyway, the mesh is not a solution provider, but a developer solution. The calculation code user should know what he wants and where and how the mesh used to represent what he wants.

In the case of an elastoplastic behavior, plasticity develops first on the surface. The analytical integration performed for an elastic material is replaced by a numerical integration for a plastic material because the stress is no longer a linear evolution in the thickness of the element as soon as the plasticity appears. In addition to the

surface integration scheme which has been explained, there is an integration scheme on the thickness of the shell. Since we do not increase the number of items on the thickness, the deformation field is linear on the thickness. It takes a sufficient number of integration points on thickness to represent the inflectional behavior. Depending on the type of scheme adopted, there may have or not integration points on the surface of the shell. In general, we recommend between 5 and 7 points on the thickness, regardless of the integration in surface. Less, the numerical solution dismiss many physical behavior; in addition, it may risk to penalize the performance in terms of disk space and memory to gain false precision.

4.3 Numerical Implementation and Operator Split Method for Coupled Damage-Plasticity Model

We use three different levels of computation in order to solve the problem. These levels are separated into global, element and local level. The operator split method (see e.g. [46]) is employed in order to simplify the calculation of the three-level computational task in which the nonlinear equations must be solved. Thus, the Newton iterative procedure is applied until we reach a required convergent tolerance at each level.

4.3.1 Discretization of the problem

Firstly, we should define the variational formulation, which is based on Hellinger-Reissner potential (e.g.see [47]) by putting aside the hardening effect to simply notation, the latter can be defined as;

$$
\begin{aligned}
&\Pi(\boldsymbol{\sigma},\boldsymbol{u}) = \\
&= \int_\Omega \psi^e(\boldsymbol{\varepsilon}^e) + \psi^d(\boldsymbol{\varepsilon}^d,\boldsymbol{D}) d\Omega - \int_\Gamma \bar{t}\boldsymbol{u}\, d\Gamma - \int_\Omega \boldsymbol{f_v}\boldsymbol{u}\, d\Omega \\
&= \int_\Omega \left\{ \boldsymbol{\sigma} : \boldsymbol{\varepsilon}^e - \chi^e(\boldsymbol{\sigma}) + \boldsymbol{\sigma} : \boldsymbol{\varepsilon}^d - \chi^d(\boldsymbol{\sigma},\boldsymbol{D}) \right\} d\Omega - \int_\Gamma \bar{t}\boldsymbol{u}\, d\Gamma - \int_\Omega \boldsymbol{f_v}\boldsymbol{u}\, d\Omega \\
&= \int_\Omega \left\{ -\chi^e(\boldsymbol{\sigma}) - \chi^d(\boldsymbol{\sigma},\boldsymbol{D}) + \boldsymbol{\sigma} : \underbrace{(\boldsymbol{\varepsilon}^d + \boldsymbol{\varepsilon}^e)}_{\boldsymbol{\varepsilon}-\boldsymbol{\varepsilon}^p} \right\} d\Omega - \int_\Gamma \bar{t}\boldsymbol{u}\, d\Gamma - \int_\Omega \boldsymbol{f_v}\boldsymbol{u}\, d\Omega \\
&= \int_\Omega \left\{ -\chi^e(\boldsymbol{\sigma}) - \chi^d(\boldsymbol{\sigma},\boldsymbol{D}) + \boldsymbol{\sigma} : (\nabla^s \boldsymbol{u} - \boldsymbol{\varepsilon}^p) \right\} d\Omega - \int_\Gamma \bar{t}\boldsymbol{u}\, d\Gamma - \int_\Omega \boldsymbol{f_v}\boldsymbol{u}\, d\Omega
\end{aligned}
\tag{4.9}
$$

where the expressions of the elastic and damage strain energy in terms of dual variables have been used (see (3.3) and (3.4)

At equilibrium, the minimal free energy condition is valid for the potential stationarity given by;

$$\delta\Pi(\boldsymbol{\sigma},\boldsymbol{u}) = \frac{\partial\Pi}{\partial\boldsymbol{u}}\delta\boldsymbol{u} + \frac{\partial\Pi}{\partial\boldsymbol{\sigma}}\delta\boldsymbol{\sigma} = 0 \tag{4.10}$$

We subsequently obtain the two following equations;

$$\begin{aligned}
\frac{\partial\Pi}{\partial\boldsymbol{u}}\delta\boldsymbol{u} &= \int_\Omega(\boldsymbol{\sigma}\nabla^s\delta\boldsymbol{u})d\Omega - \int_\Gamma(\bar{t}\delta\boldsymbol{u})d\Gamma - \int_\Omega(\boldsymbol{f_v}\delta\boldsymbol{u})d\Omega = 0 \\
\frac{\partial\Pi}{\partial\boldsymbol{\sigma}}\delta\boldsymbol{\sigma} &= \int_\Omega\left\{-\frac{\partial\chi^e}{\partial\boldsymbol{\sigma}} - \frac{\partial\chi^d}{\partial\boldsymbol{\sigma}} + \nabla^s\boldsymbol{u} - \boldsymbol{\varepsilon}^p\right\}\delta\boldsymbol{\sigma}d\Omega = 0
\end{aligned} \tag{4.11}$$

The first equation in (4.11) can be easily seen as the weak form of equilibrium equation. The second equation in (4.11) leads us towards the weak form of the decomposition of total strain $\boldsymbol{\varepsilon} = \boldsymbol{\varepsilon}^e + \boldsymbol{\varepsilon}^p + \boldsymbol{\varepsilon}^d$.

We use a hybrid stress finite element method in order to approximate the unknown fields, the displacement $\mathbf{u}$ and the stress $\boldsymbol{\sigma}$. First, we introduce an operator $\mathscr{L}$ which allows to take advantage of the symmetry and rewrite two symmetric second order tensors components in more compact matrix notation.

$$\boldsymbol{\sigma} = [\sigma_{ij}]_{(i,j)\in[1,2]} \rightarrow \mathscr{L}(\sigma) := \begin{pmatrix} \sigma_{11} \\ \sigma_{22} \\ \sigma_{12} \end{pmatrix} \tag{4.12}$$

and

$$\boldsymbol{\varepsilon} = [\varepsilon_{ij}]_{(i,j)\in[1,2]} \rightarrow \mathscr{L}(\varepsilon) := \begin{pmatrix} \varepsilon_{11} \\ \varepsilon_{22} \\ 2\varepsilon_{12} \end{pmatrix} \tag{4.13}$$

Considering an element Ω^e of the finite element mesh of $\Omega = \bigcup_{e=1}\Omega^e$, we provide the following approximation for the unknown fields.

$$\boldsymbol{u}^h|_{\Omega^e} = \mathbf{N}(x)\boldsymbol{d}^e(t)\mathscr{L}(\boldsymbol{\sigma}^h)|_{\Omega^e} = \mathbf{S}(x)\boldsymbol{\beta}^e(t) \tag{4.14}$$

where $\mathbf{N}$ is a displacement field interpolation function constructed from usual isoparametric approximation for two dimensional element and $\mathbf{S}$ is the stress

interpolation function proposed by Pian-Sumihara (eg. [48] and [49]). Detailed explanation is done in the appendixe B.

It can be shown that, for $\mathbf{A}$ and $\mathbf{B}$, which are two symmetric terms, $\mathbf{A} : \mathbf{B} = \mathscr{L}(A) \cdot \mathscr{L}(B)$. Moreover, we define $\mathbf{B}$ as the second order tensor that satisfies $\mathscr{L}(\mathbf{D}^s(\mathbf{N}) \cdot \mathbf{d}^e) = \mathbf{B}\mathbf{d}^e$, in which $\mathbf{D}^s$ represent the symmetric part of the displacement gradient.

Thus, equations (4.11) can be rewritten in an explicit form by using the interpolation functions.

$$\begin{aligned} \int_{\Omega^e} \delta \boldsymbol{d}^{eT} \mathbf{B}^T \mathbf{S} \boldsymbol{\beta}^e d\Omega^e - \int_{\Gamma_\sigma^e} \delta \boldsymbol{d}^{eT} \mathbf{N}^T \bar{\mathbf{t}} d\Gamma^e - \int_{\Omega^e} \delta \boldsymbol{d}^{eT} \mathbf{N}^T \mathbf{f}_v d\Omega^e = \mathbf{0} \\ \int_{\Omega^e} \delta \boldsymbol{\beta}^{eT} \mathbf{S}^T (\mathbf{B}\mathbf{d}^e - \hat{\boldsymbol{\varepsilon}}(\boldsymbol{\beta}^e)) d\Omega^e = \mathbf{0} \end{aligned} \tag{4.15}$$

Because the equations $(4.15)_1$ and $(4.15)_2$ hold for any $\delta\mathbf{d}^e$ and $\delta\boldsymbol{\beta}^e$, we obtain;

$$\begin{aligned} \mathbf{G}^T \boldsymbol{\beta}^e(t) - \int_{\Omega^e} \mathbf{N}^T \mathbf{f}_v d\Omega^e - \int_{\Gamma_\sigma^e} \mathbf{N}^T \bar{\mathbf{t}} d\Gamma^e = \mathbf{0} \\ \mathbf{G}\mathbf{d}^e(t) - \int_{\Omega^e} \mathbf{S}^T \hat{\boldsymbol{\varepsilon}}(\boldsymbol{\beta}^e) d\Omega^e = \mathbf{0} \end{aligned} \tag{4.16}$$

with

$$\mathbf{G} = \int_\Omega \mathbf{S}^T \mathbf{B} d\Omega \tag{4.17}$$

The problem of finite element approach is governed by equation (4.16) . In the case of an elastoplastic-damage material model, we have;

$$\hat{\boldsymbol{\varepsilon}}(\boldsymbol{\beta}) = \mathscr{L}(\mathbf{C}^{-1})(\mathbf{S}\boldsymbol{\beta}) + \mathscr{L}(\boldsymbol{\varepsilon}^p) + \gamma^p \mathscr{L}(\frac{\partial \phi^p}{\partial \boldsymbol{\sigma}}) + \mathscr{L}(\boldsymbol{D})(\mathbf{S}\boldsymbol{\beta}) + \gamma^d \mathscr{L}(\frac{\partial \phi^d}{\partial \boldsymbol{\sigma}}) \tag{4.18}$$

where $\mathbf{C}$ and $\boldsymbol{D}$ are the fourth order elasticity tensor and compliance tensor, respectively. Considering that $\mathbf{C}_{ijkl} = \mathbf{C}_{klij}$ and that $\mathbf{C}_{ijkl} = \mathbf{C}_{ijlk}$, we can define in 2D here for illustration, $\mathscr{L}(\mathbf{C})$ as;

$$\mathscr{L}(\mathbf{C}) = \begin{bmatrix} C_{1111} & C_{1122} & C_{1112} \\ & C_{2222} & C_{2212} \\ sym & & C_{1212} \end{bmatrix} \tag{4.19}$$

For a homogeneous isotropic material, $\mathscr{L}(\mathbf{C})$ is invertible.

To solve the nonlinear set of equations in (4.16) , we use the Newton iterative procedure and consequently define the following residuals.

$$\begin{aligned}
\mathbf{r}_d^e(\mathbf{d}_{n+1}^e) &= \mathbf{G}^T\boldsymbol{\beta}_{n+1}^e - \int_{\Omega^e}\mathbf{N}^T\mathbf{f}_v d\Omega^e - \int_{\Gamma^e}\mathbf{N}^T\bar{\mathbf{t}}d\Gamma^e \\
\mathbf{r}_\beta^e(\boldsymbol{\beta}_{n+1}^e) &= \mathbf{G}\mathbf{d}_{n+1}^e - \int_{\Omega^e}\mathbf{S}^T\Big(\mathscr{L}(\mathbf{C}^{-1})\mathbf{S}\boldsymbol{\beta}_{n+1}^e + \mathscr{L}(\boldsymbol{\varepsilon}_n^p) + \gamma_{n+1}^p\mathscr{L}(\frac{\partial\phi_{n+1}^p}{\partial\boldsymbol{\sigma}_{n+1}}) \\
&\quad + \mathscr{L}(D_n)(\mathbf{S}\boldsymbol{\beta}_{n+1}^e) + \gamma_{n+1}^d\mathscr{L}(\frac{\partial\phi_{n+1}^d}{\partial\boldsymbol{\sigma}_{n+1}})\Big)d\Omega^e
\end{aligned} \tag{4.20}$$

4.3.2 Global computation

Global equations are obtained by the finite element assembly procedure, which should enforce the equilibrium of structure. Displacement field is given for stresses obtained from the element level computation and the values of internal state variables provided by the local iterative procedure described in the next subsections for both plasticity and damage model in order to check the convergence.

The Newton equation for $\mathbf{r}_d^e$ is solved.

$$\begin{aligned}
\mathbf{r}_d^{e(j+1)} &= \mathbf{r}_d^{e(j)} + \mathbf{D}^{(j)}(\mathbf{r}_d^e)\Delta\mathbf{d}^{e(j)} = \mathbf{0} \\
\mathbf{D}^{(j)}(\mathbf{r}_\mathbf{d}^\mathbf{e})\Delta\mathbf{d}^{e(j)} &= \big(\mathbf{G}^T\frac{\partial\boldsymbol{\beta}^{e(j)}}{\partial\mathbf{d}^e}\big)\Delta\mathbf{d}^{e(j)} = \mathbf{K}^{e(j)}\Delta\mathbf{d}^{e(j)}
\end{aligned} \tag{4.21}$$

To compute $\frac{\partial\boldsymbol{\beta}^e}{\partial\mathbf{d}^e}\Big|^{(j)}$, we derive $\mathbf{r}_\beta^e = \mathbf{0}$ and obtain(see Eq. (4.20));

$$\frac{\partial\mathbf{r}_\beta^e}{\partial\boldsymbol{\beta}_{n+1}^e} = \mathbf{G}\frac{\partial\mathbf{d}_{n+1}}{\partial\boldsymbol{\beta}_{n+1}} - \mathbf{H}_n^e - \mathbf{E}_{n+1}^p - \mathbf{E}_{n+1}^d = \mathbf{0} \tag{4.22}$$

where

$$\begin{aligned}
\mathbf{H}_n^e &= \int_{\Omega^e}\mathbf{S}^T(\mathscr{L}(\mathbf{C}^{-1}) + \mathscr{L}(D_n))\mathbf{S}d\Omega^e \\
\mathbf{E}_{n+1}^p &= \int_{\Omega^e}\mathbf{S}^T\left\{-\mathscr{L}(\frac{\partial\phi_{n+1}^p}{\partial\boldsymbol{\sigma}_{n+1}})\hat{\mathbf{C}}_{n+1}^{(1)}\mathscr{L}^T(\frac{\partial\phi_{n+1}^p}{\partial\boldsymbol{\sigma}_{n+1}}) + \gamma_{n+1}^p\mathscr{L}(\frac{\partial^2\phi_{n+1}^p}{\partial\boldsymbol{\sigma}_{n+1}^2})\right\}\mathbf{S}d\Omega^e \\
\mathbf{E}_{n+1}^d &= \int_{\Omega^e}\mathbf{S}^T\left\{-\mathscr{L}(\frac{\partial\phi_{n+1}^d}{\partial\boldsymbol{\sigma}_{n+1}})\hat{\mathbf{C}}_{n+1}^{(2)}\mathscr{L}^T(\frac{\partial\phi_{n+1}^d}{\partial\boldsymbol{\sigma}_{n+1}}) + \gamma_{n+1}^d\mathscr{L}(\frac{\partial^2\phi_{n+1}^d}{\partial\boldsymbol{\sigma}_{n+1}^2})\right\}\mathbf{S}d\Omega^e
\end{aligned} \tag{4.23}$$

Here, we must define the values of $\hat{\mathbf{C}}_{n+1}^{(1)}$ and $\hat{\mathbf{C}}_{n+1}^{(2)}$, respectively.

$$\hat{\mathbf{C}}^{(1)}_{n+1} = \left\{ \frac{\partial \phi^p_{n+1}}{\partial \boldsymbol{\alpha}^p_{n+1}} : \frac{\partial \boldsymbol{\alpha}^p_{n+1}}{\partial \boldsymbol{\kappa}^p_{n+1}} : \frac{\partial \phi^p_{n+1}}{\partial \boldsymbol{\alpha}^p_{n+1}} + \frac{\partial \phi^p_{n+1}}{\partial q^p_{n+1}} \frac{dq^p_{n+1}}{d\xi^p_{n+1}} \frac{\partial \phi^p_{n+1}}{\partial q^p_{n+1}} \right\}^{-1}$$
$$\hat{\mathbf{C}}^{(2)}_{n+1} = \left\{ \frac{\partial \phi^d_{n+1}}{\partial q^d_{n+1}} \frac{dq^d_{n+1}}{d\xi^d_{n+1}} \frac{\partial \phi^d_{n+1}}{\partial q^d_{n+1}} \right\}^{-1} \tag{4.24}$$

Thus, we obtain:

$$\frac{\partial \boldsymbol{\beta}_{n+1}}{\partial \mathbf{d}_{n+1}} = \left\{ \mathbf{H}^e_n + \mathbf{E}^p_{n+1} + \mathbf{E}^d_{n+1} \right\}^{-1} \mathbf{G} \tag{4.25}$$

$$\mathbf{K}^{e(j)}_{n+1} = \mathbf{G}^T \left\{ \mathbf{H}^e_n + \mathbf{E}^p_{n+1} + \mathbf{E}^d_{n+1} \right\}^{-1} \mathbf{G} \tag{4.26}$$

Finally, the structural tangent stiffness matrix and residual vector are obtained by the classical finite element procedure.

4.3.3 Element computation

For $\mathbf{d}^e_{n+1}(t)$ given, the Newton equation for $\mathbf{r}_\beta$;

$$\mathbf{r}^{e(k+1)}_\beta = \mathbf{r}^{e(k)}_\beta + \mathbf{D}^{(k)}(\mathbf{r}^e_\beta \Delta \boldsymbol{\beta}^{e(k)}) = \mathbf{0} \tag{4.27}$$

is solved and the generalized stress vector is updated.

$$\boldsymbol{\beta}^{e(k+1)} = \boldsymbol{\beta}^{e(k)} + \Delta \boldsymbol{\beta}^{e(k)}$$

In (**4.27**) above, $\mathbf{D}^{(k)}(\mathbf{r}_\beta)\Delta\boldsymbol{\beta}^{(k)} = \frac{d}{d\zeta}\Big|_{\zeta=0} \mathbf{r}_\beta(\boldsymbol{\beta}^{e(k)} + \zeta \Delta \boldsymbol{\beta}^{e(k)})$ is the directional derivative and takes the following expression for the elastoplastic problem.

$$\begin{aligned}
\mathbf{D}^{(k)}(\mathbf{r}_\beta)\Delta\boldsymbol{\beta}^{(k)} = \int_{\Omega^e} \mathbf{S}^T \Big(& -(\mathscr{L}(\mathbf{C})^{-1} + \mathscr{L}(\boldsymbol{D}))\mathbf{S}\Delta\boldsymbol{\beta}^{e(k)} \\
& - \gamma^{p(k)} \mathscr{L}\Big(\frac{\partial^2 \phi^{p(k)}}{\partial \boldsymbol{\sigma}^{(k)^2}}\Big)\mathbf{S}\Delta\boldsymbol{\beta}^{e(k)} - \mathscr{L}\Big(\frac{\partial \gamma^{p(k)}}{\partial \boldsymbol{\sigma}^{(k)}}\Big)\mathscr{L}^T\Big(\frac{\partial \phi^{p(k)}}{\partial \boldsymbol{\sigma}^{(k)}}\Big)\mathbf{S}\Delta\boldsymbol{\beta}^{e(k)} \\
& - \gamma^{d(k)} \mathscr{L}\Big(\frac{\partial^2 \phi^{d(k)}}{\partial \boldsymbol{\sigma}^{(k)^2}}\Big)\mathbf{S}\Delta\boldsymbol{\beta}^{e(k)} - \mathscr{L}\Big(\frac{\partial \gamma^{d(k)}}{\partial \boldsymbol{\sigma}^{(k)}}\Big)\mathscr{L}^T\Big(\frac{\partial \phi^{d(k)}}{\partial \boldsymbol{\sigma}^{(k)}}\Big)\mathbf{S}\Delta\boldsymbol{\beta}^{e(k)} \Big) d\Omega^e
\end{aligned} \tag{4.28}$$

Moreover, we have for the von Mises plastic criteria from the equations (3.20) and (3.26) ,

$$\frac{\partial \gamma^p}{\partial \boldsymbol{\sigma}} = -\frac{\partial \phi^p}{\partial \boldsymbol{\sigma}}\Big(\frac{\partial \phi^p}{\partial \boldsymbol{\alpha}^p} : \frac{\partial \boldsymbol{\alpha}^p}{\partial \boldsymbol{\kappa}^p} : \frac{\partial \phi^p}{\partial \boldsymbol{\alpha}^p} + (\frac{\partial \phi^p}{\partial q^p})^2 \frac{\partial q}{\partial \xi^p}\Big)^{-1}$$
$$\mathscr{L}(\frac{\partial^2 \phi}{\partial \boldsymbol{\sigma} \partial \boldsymbol{\sigma}}) = \mathbf{0} \tag{4.29}$$

$$\frac{\partial \gamma^d}{\partial \boldsymbol{\sigma}} = -\frac{\partial \phi^d}{\partial \boldsymbol{\sigma}}\Big(\frac{\partial \phi^d}{\partial \boldsymbol{\sigma}} : \boldsymbol{D}^{-1} : \frac{\partial \phi^d}{\partial \boldsymbol{\sigma}} + \frac{\partial \phi^d}{\partial q^d}\frac{\partial q^d}{\partial \dot{\xi}^d}\frac{\partial \phi^d}{\partial q^d}\Big)^{-1} \tag{4.30}$$

We finally obtain;

$$\begin{aligned}\Delta \boldsymbol{\beta}^{e(k)} = \Big[\mathbf{H}^e &+ \int_{\Omega^e} \mathbf{S}^T \mathscr{L}(\frac{\partial \phi^p}{\partial \boldsymbol{\sigma}}) \hat{\mathbf{C}}^{(1)} \mathscr{L}^T(\frac{\partial \phi^p}{\partial \boldsymbol{\sigma}}) \\ &+ \int_{\Omega^e} \mathbf{S}^T \mathscr{L}(\frac{\partial \phi^d}{\partial \boldsymbol{\sigma}}) \hat{\mathbf{C}}^{(2)} \mathscr{L}^T(\frac{\partial \phi^d}{\partial \boldsymbol{\sigma}}) \mathbf{S} d\Omega^e \Big]^{-1} \mathbf{r}_\beta^{e(k)}\end{aligned} \tag{4.31}$$

4.3.4 Local computation and implicit backward Euler scheme

The evolution equations of the internal variables are obtained in each time step by using Backward Euler time integration scheme at the local material level, in each Gauss integration point accordingly.

4.3.4.1 Plasticity computation

In order to compute $\dot{\gamma}^p_{n+1}$ and $\boldsymbol{\varepsilon}^p_{n+1} = \hat{\boldsymbol{\varepsilon}}(\boldsymbol{\sigma}_{n+1})$ for a given displacement $\mathbf{d}^{e(j+1)}$ and a given stress state $\boldsymbol{\sigma}^{(k+1)}$, we first rewrite the evolution equations (3.13) and (3.14) in a discrete form, appealing to the implicit backward Euler integration scheme;

$$\begin{aligned}\boldsymbol{\varepsilon}^p_{n+1} &= \boldsymbol{\varepsilon}^p_n + \dot{\gamma}^p_{n+1}\Delta t_{n+1}\frac{\partial \phi^p_{n+1}}{\partial \boldsymbol{\sigma}_{n+1}} \\ \xi^p_{n+1} &= \xi^p_n + \dot{\gamma}^p_{n+1}\Delta t_{n+1}\frac{\partial \phi^p_{n+1}}{\partial q^p_{n+1}} \\ \boldsymbol{\kappa}^p_{n+1} &= \boldsymbol{\kappa}^p_n + \dot{\gamma}^p_{n+1}\Delta t_{n+1}\frac{\partial \phi^p_{n+1}}{\partial \boldsymbol{\alpha}_{n+1}}\end{aligned} \tag{4.32}$$

$$\dot{\gamma}^p_{n+1}\Delta t_{n+1} \geq 0, \quad \phi^p_{n+1} \leq 0, \quad \text{and} \quad \dot{\gamma}^p_{n+1}\Delta t_{n+1}\phi^p_{n+1} = 0 \tag{4.33}$$

In order to simplify notation, we denote in the following, $\dot{\gamma}^p_{n+1}\Delta t_{n+1} = \gamma^p_{n+1}$. The local problem reduces then to the computation of γ^p_{n+1}. To that aim,

- We start with $\gamma^{p(l=0)}_{n+1} = 0$ and compute $\phi^{p(0)}_{n+1} = \phi^p\big(\boldsymbol{\sigma}_{n+1}, q^p(\xi^{p(0)}_{n+1}), \boldsymbol{\alpha}^p(\boldsymbol{\kappa}^{p(0)}_{n+1})\big)$
- If $\phi^{p(0)}_{n+1} \leq 0$, the loading/unloading conditions are satisfied and the local problem is solved. Otherwise, we iteratively look for the value of γ^p_{n+1} that would satisfy

$\phi^p\left(\boldsymbol{\sigma}_{n+1}, q^p(\xi_{n+1}^{p(l)}), \boldsymbol{\alpha}^p(\boldsymbol{\kappa}_{n+1}^{p(l)})\right) = 0$ (for instance with the Newton procedure) and update the internal variables according to the expression in (4.32).

4.3.4.2 Damage computation

The calculation is very analogous to the plasticity.

In order to compute $\dot{\gamma}_{n+1}^d$ and $\boldsymbol{\varepsilon}_{n+1}^d = \hat{\boldsymbol{\varepsilon}}(\boldsymbol{\sigma}_{n+1})$ for a given displacement $\mathbf{d}^{e(j+1)}$ and a given stress state $\boldsymbol{\sigma}^{(k+1)}$, we first rewrite the evolution equations (3.24) and (3.25) in a discrete form, appealing to the implicit backward Euler integration scheme:

$$\begin{aligned} \boldsymbol{D}_{n+1}^d \boldsymbol{\sigma}_{n+1} &= \boldsymbol{D}_n^d \boldsymbol{\sigma}_{n+1} + \dot{\gamma}_{n+1}^d \Delta t_{n+1} \frac{\partial \phi_{n+1}^d}{\partial \boldsymbol{\sigma}_{n+1}} \\ \xi_{n+1}^d &= \xi_n^d + \dot{\gamma}_{n+1}^d \Delta t_{n+1} \frac{\partial \phi_{n+1}^d}{\partial q_{n+1}^d} \end{aligned} \tag{4.34}$$

$$\dot{\gamma}_{n+1}^d \Delta t_{n+1} \geq 0, \quad \phi_{n+1}^d \leq 0, \quad \text{and} \quad \dot{\gamma}_{n+1}^d \Delta t_{n+1} \phi_{n+1}^d = 0 \tag{4.35}$$

In order to simplify notation, we denote in the following, $\dot{\gamma}_{n+1}^d \Delta t_{n+1} = \gamma_{n+1}^d$. The local problem reduces then to the computation of γ_{n+1}^d. To that aim,

- We start with $\gamma_{n+1}^{d(l=0)} = 0$ and compute $\phi_{n+1}^{d(0)} = \phi^d\left(\boldsymbol{\sigma}_{n+1}, q^d(\xi_{n+1}^{d(0)})\right)$
- If $\phi_{n+1}^{d(0)} \leq 0$, the loading/unloading conditions are satisfied and the local problem is solved. Otherwise, we iteratively look for the value of γ_{n+1}^d that would satisfy $\phi^d\left(\boldsymbol{\sigma}_{n+1}, q^d(\xi_{n+1}^{d(l)})\right) = 0$ (for instance with the Newton procedure) and update the internal variables according to the expression in (4.34) .

4.4 Numerical Examples

In this section, several numerical simulations are presented in order to illustrate the performance of the proposed constitutive model of inelastic behavior, taking into account both plasticity and damage. The loading level is chosen so that both isotrope and kinematic hardening phenomena are activated in the calculations of the material response. Numerical simulations are performed by using two dimensional finite element based on the variational formulation of Hellinger-Reissner type, which is implemented into a research version of Finite Element Analysis Program [48]. The

following material properties of mild steel are chosen for all examples; the Young modulus $E = 210GPa$, Poisson ratio is $\nu = 0.3$, the yield stress $\sigma_y = 235MPa$, the saturation stress is $\sigma_\infty = 360MPa$, the modulus $K^p = 1.0\text{x}10^3 MPa$ for linear isotropic hardening and the parameter $b^p = 1.0\text{x}10^4$ for saturation isotropic hardening and $H = 1.0\text{x}10^2 MPa$ for the kinematic hardening, the fracture stress $\sigma_{fy} = 285MPa$, the saturation stress $\sigma_{f\infty} = 360MPa$, the damage modulus $K^d = 1.0\text{x}10^3 MPa$, the damage saturation parameter $b^d = 1.0\text{x}10^4$.

4.4.1 Steel sheet in simple tension test under cycling loading

In the first example, we present the results describing the response of a plane deformation membrane in Figure 4.1, which is made of mild steel, under different types of cyclic loadings applied.

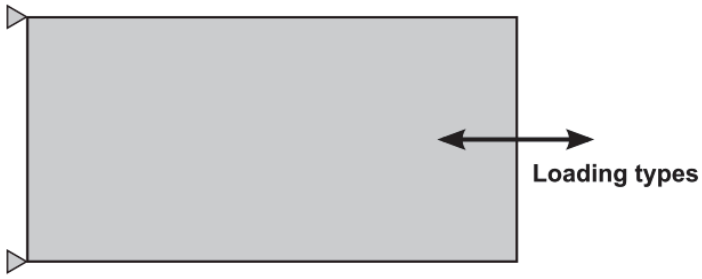

Figure 4.1: Simple tension test specimen with coupled plasticity-damage constitutive model, clamped at the left side, submitted by different kinds of loading at the right side.

First, a comparison of the number of finite elements will be done in Figure 4.2 to show the model capability for representing appropriately the displacement, strain and stress fields.

Secondly, another comparison with the the results of the experiments done by [50] is shown in the Figure 4.3.

A cyclic loading history with symmetric cycles with respect to tension-compression with the max/min values of imposed displacement $\pm 0.07m$ as shown in Figure 4.4, is applied on the element in order to illustrate the behavior of the proposed material model.

The two hysteresis curves are shown in Figure 4.5, with marked difference of activated mechanisms of the coupled model. While only the plasticity is activated for one,

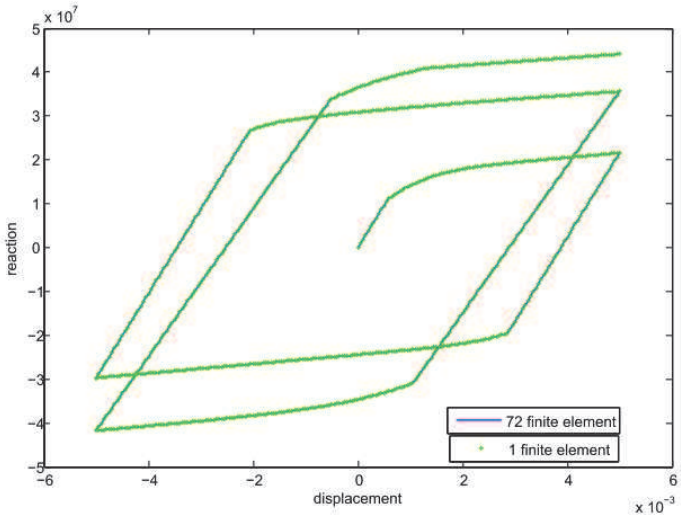

Figure 4.2: The number of finite elements considering coupled plasticity-damage constitutive model.

.

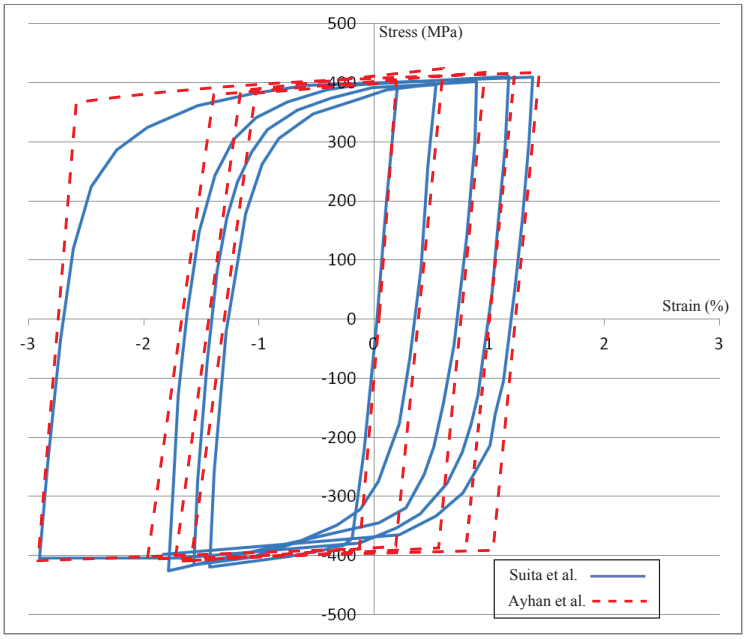

Figure 4.3: Cyclic test on a rectangular member (100*50 cm).

the coupled plasticity-damage behavior is activated for another. It is clearly shown in the figure that the coupled behavior affects the tangent modulus of the material. Furthermore, membrane element, for which the coupled behavior is taken into account with the same imposed displacement interval, reaches smaller value of stress in comparison to the one produced by only plasticity activation.

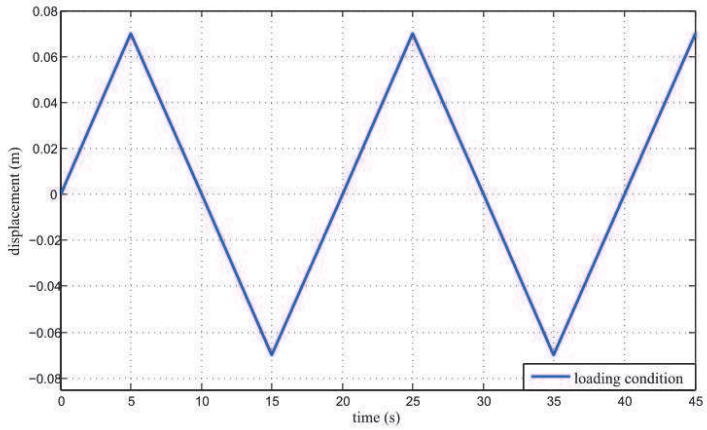

Figure 4.4: Symmetrical cyclic loading conditions with respect to time.

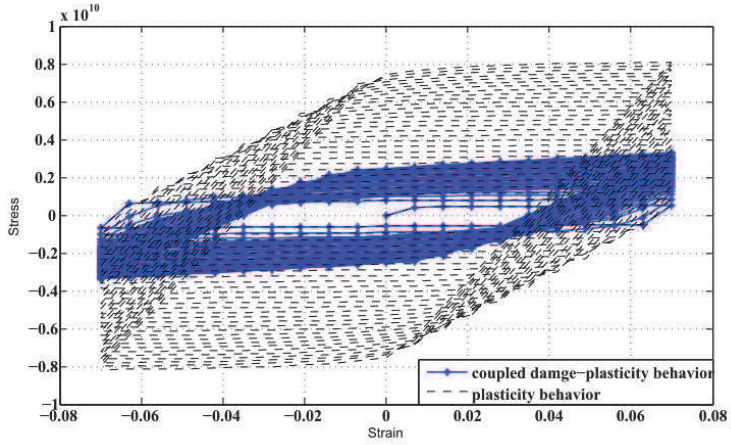

Figure 4.5: Strain-stress diagrams for both proposed coupled damage-plasticity model and plasticity alone.

In order to furher illustrate the contribution of damage mechanism in this model, we carry on with a very large number of cycles in the same test. The corresponding results for the strain-stress diagram are given in Figure 4.5 and the cumulative damage contribution with respect to number of cycles in Figure 4.6.

With the effect of coupled plasticity-damage behavior at hand, we now go on with an example, which shows the progressive relaxation effect for the inelastic behaviors mentioned previously. The chosen time history of imposed displacement is pictured in Figure 4.7.

It is observed in Figure 4.8 that the average of limiting stresses in the cycle relaxes progressively and shift towards zero value under fixed strain limits, whose average is

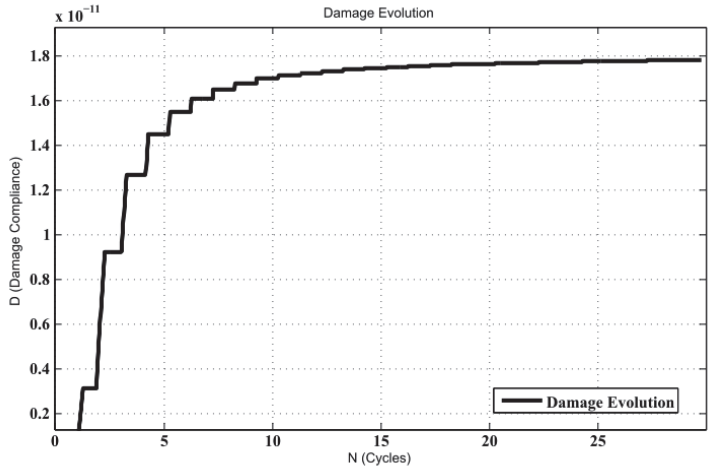

Figure 4.6: Damage Evolution during the loading process in Figure 4.4.

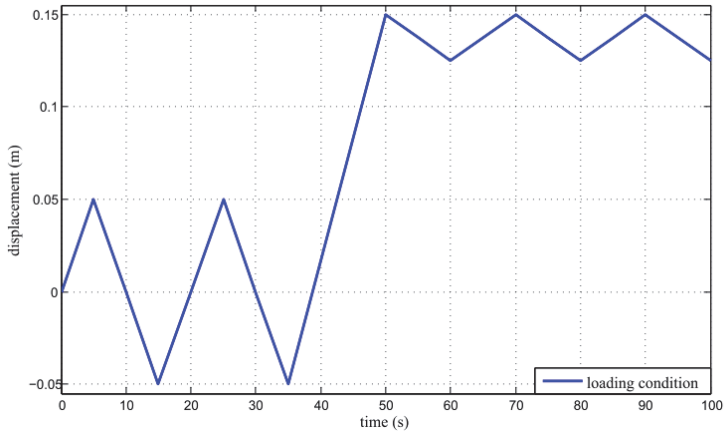

Figure 4.7: Loading conditions.

not zero. More precisely, in the Figure 4.8 the average value of stress at the A3, A4, A5 and B3, B4, B5 tends to zero.

Another phenomenon that the proposed material model can represent the ratcheting effect. The stress cycling between the fixed value in tension and compression, whose average is not zero, is applied as seen in the Figure 4.9. It is important to note that in each example the specimen is pushed well into the plastic range.

For more precise and clearer effect of ratcheting, we focus upon the end of response time history shown in Figure 4.9.

In this particular example the ratcheting occurs with the average of the stresses that remains positive, whereas minimum and maximum values of strain in each cycle increase progressively (see Figure 4.11).

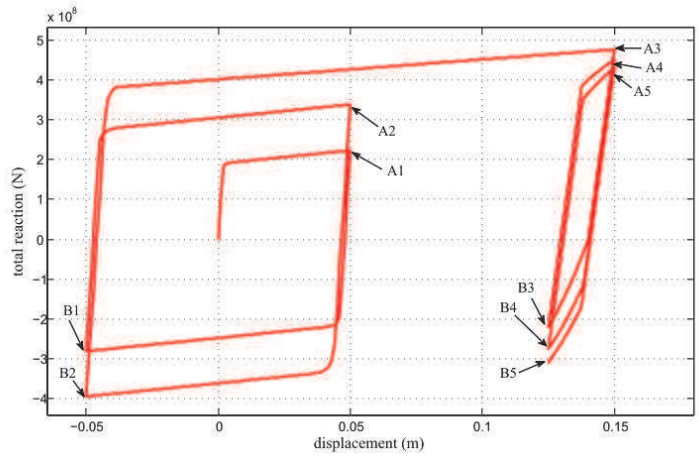

Figure 4.8: Progressive relaxation to zero of the mean stress between A3-B3, A4-B4, A5-B5, ...

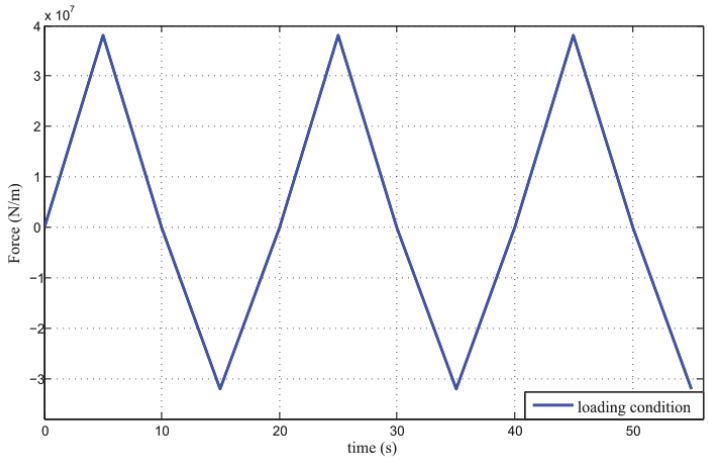

Figure 4.9: Loading conditions.

This example with number of cycles, which allowed us to show that the coupled plasticity-damage response can also lead to saturation in damage compliance, for the case where the plasticity dominates for ratcheting effects as seen in Figure 4.12.

4.4.2 Steel sheet in bending and shear tests under cyclic loading

This example considers the tests under heterogeneous stress. In this example, we show the chosen specimen geometric data and the applied loading conditions in Figure 4.13. All the material properties characterizing the inelastic behaviors of mild steel are the same as in the previous example. The two loading conditions are applied on the right side of the element as a quasi-static load varying in the chosen the time interval. First, we can thus illustrate the capabilities of the proposed model to describe quite well the coupled damage-plasticity response under more complex loading program. Second,

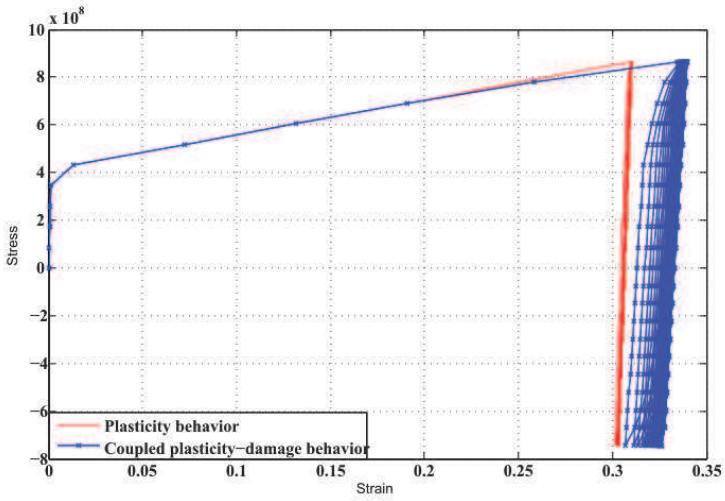

Figure 4.10: Ratcheting behavior reproduced by the proposed material model.

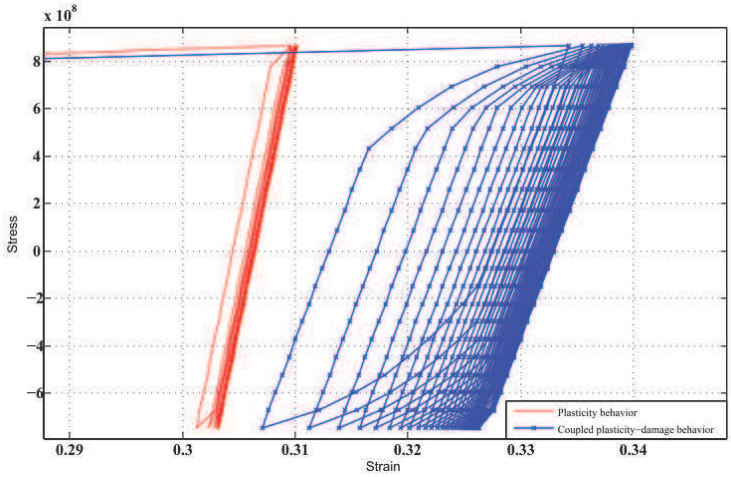

Figure 4.11: Ratcheting behavior of the material due to imposed forces.

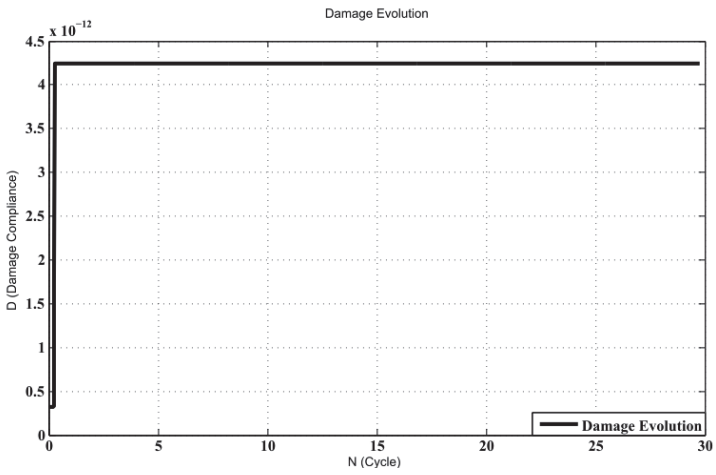

Figure 4.12: Damage Evolution during the loading process in Figure 4.9.

we can also illustrate a very satisfying performance of the developed finite element model to handle in a robust way the finite element mesh.

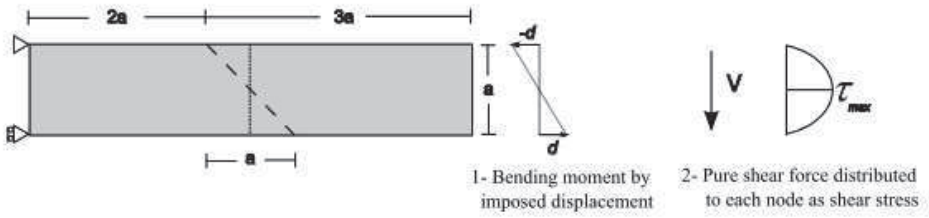

Figure 4.13: Structure with mesh distortion, fixed at the left end, subject to the two types of loading represented in the right side, and made of the proposed coupled plasticity-damage constitutive model.

Contours of plasticity (q^p) and damage (q^d) are examined. First analysis is performed on the element undergoing a pure bending deformation obtained by imposing the displacement $d = \pm 0.05$ as shown in Figure 4.13. The same example is used for studies of mesh distortion effect; the chosen mesh distortion parameter is proportional to the $a = l/5$. A comparison is done for both distorted and undistorted geometry. The finite element mesh refinement is carried out in computations starting from the 2-element mesh. We observe that by using fine mesh solutions there is not much difference in the plastic (Figure 4.14) and damage (Figure 4.15) zones between the distorted and undistorted geometry and the values q^p and q^d are very close.

4.4.2.1 Bending test

For the plastic zone in Figure 4.14 we find the strong spreading in the direction of the top and bottom fibers of the structure, while the damage zone in Figure 4.15 the zone is limited to the the bottom part.The results of this kind are due to the characteristics of the chosen yield criteria taken for each behavior, plasticity and damage.

4.4.2.2 Shear test

The same example is repeated for another loading condition of shear force applied at the right end of the structure. Values of shear stress due to shear shear force applied at each node is calculated from $V = 3.0\text{x}10^3 N$. As seen in the figures 4.16 and 4.17 the

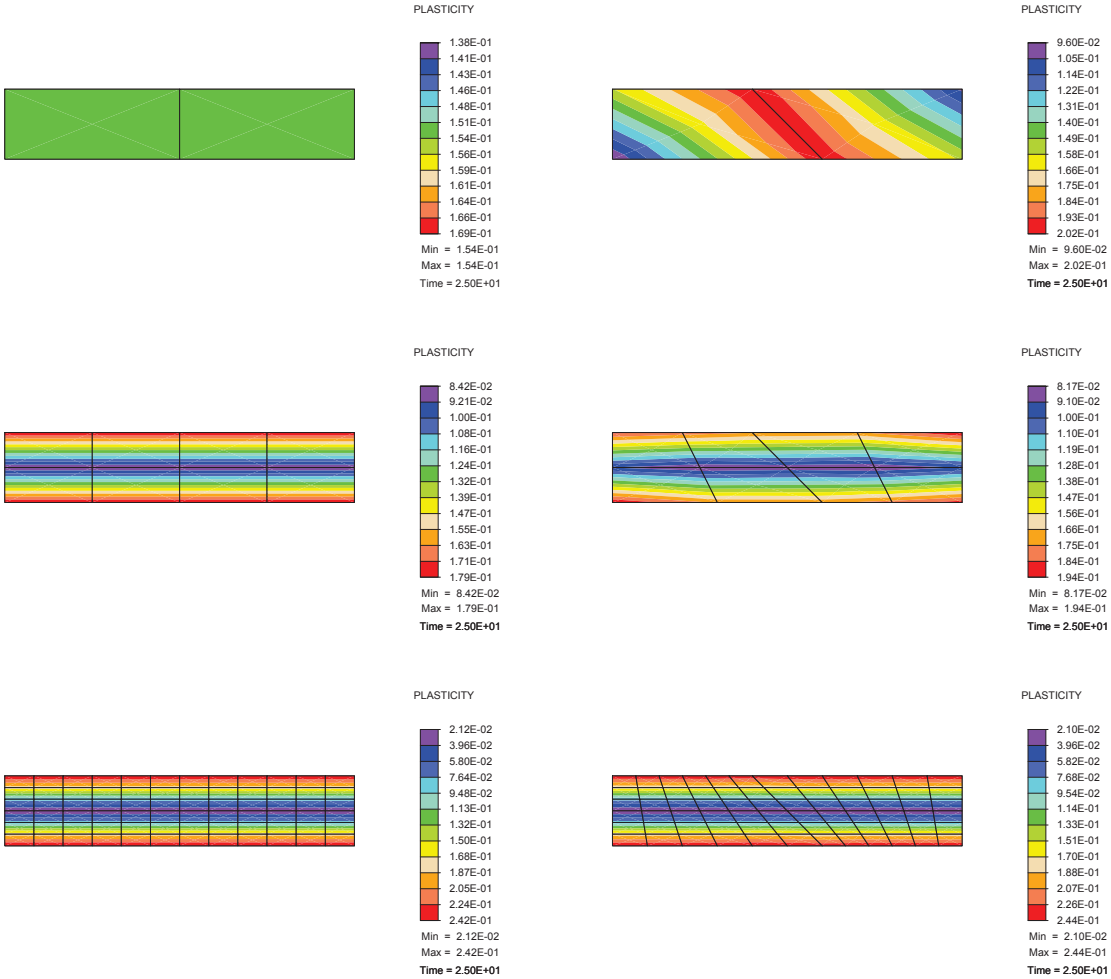

Figure 4.14: Yield contour of plasticity behavior q^p due to imposed bending loading for distorted and undistorted meshes.

plastic and damage zones are becoming very similar as the mesh refinement is carried out. The zones of these two types are accumulated around the boundary points.

Both plastic and damage zones are concentrated near the built-in support, with the spreading typical of plastic hinge. Moreover, we observe in Figure 4.16 and Figure 4.17 that the developed used stress based formulation considering the Pian-Sumihara interpolation functions for the stress variable has a very efficient performance for the distorted shape of mesh. Even in the plasticity or damage range, which generalizes the similar findings for elastic response computation with hybrid-stress elements (eg. see [51]).

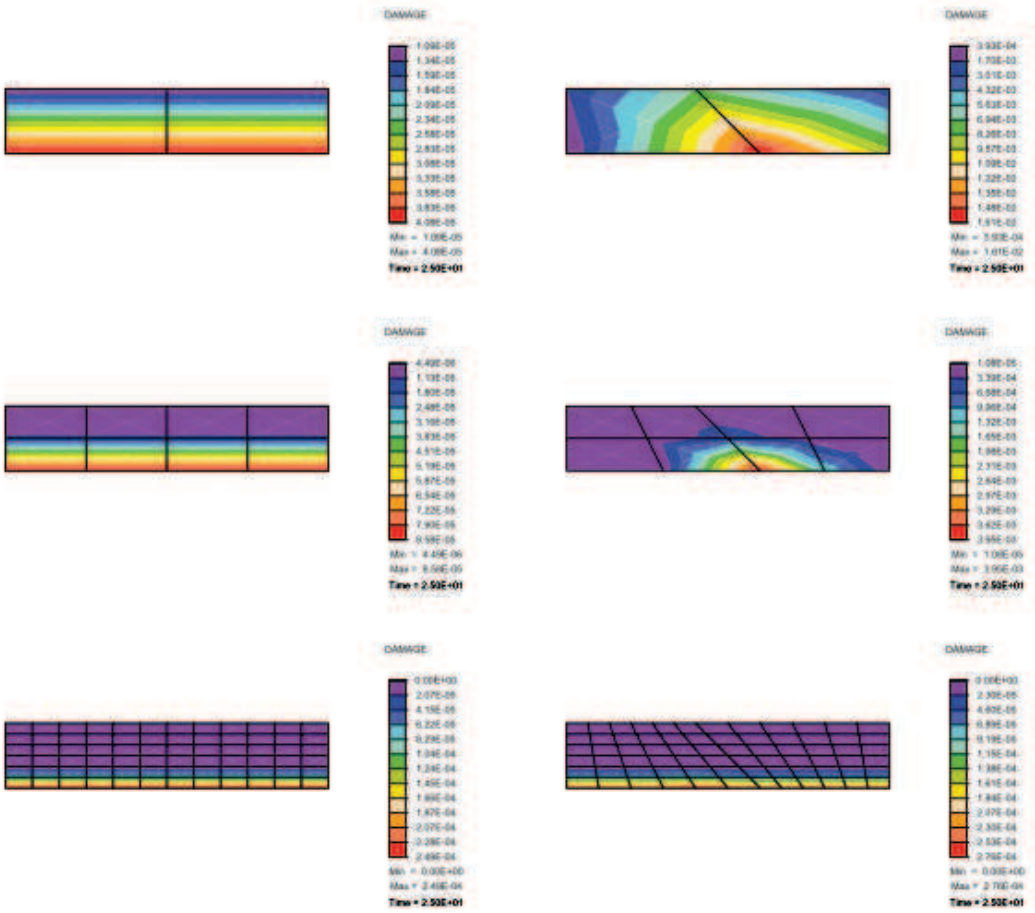

Figure 4.15: Yield contour of damage behavior q^d due to imposed bending loading for distorted and undistorted meshes.

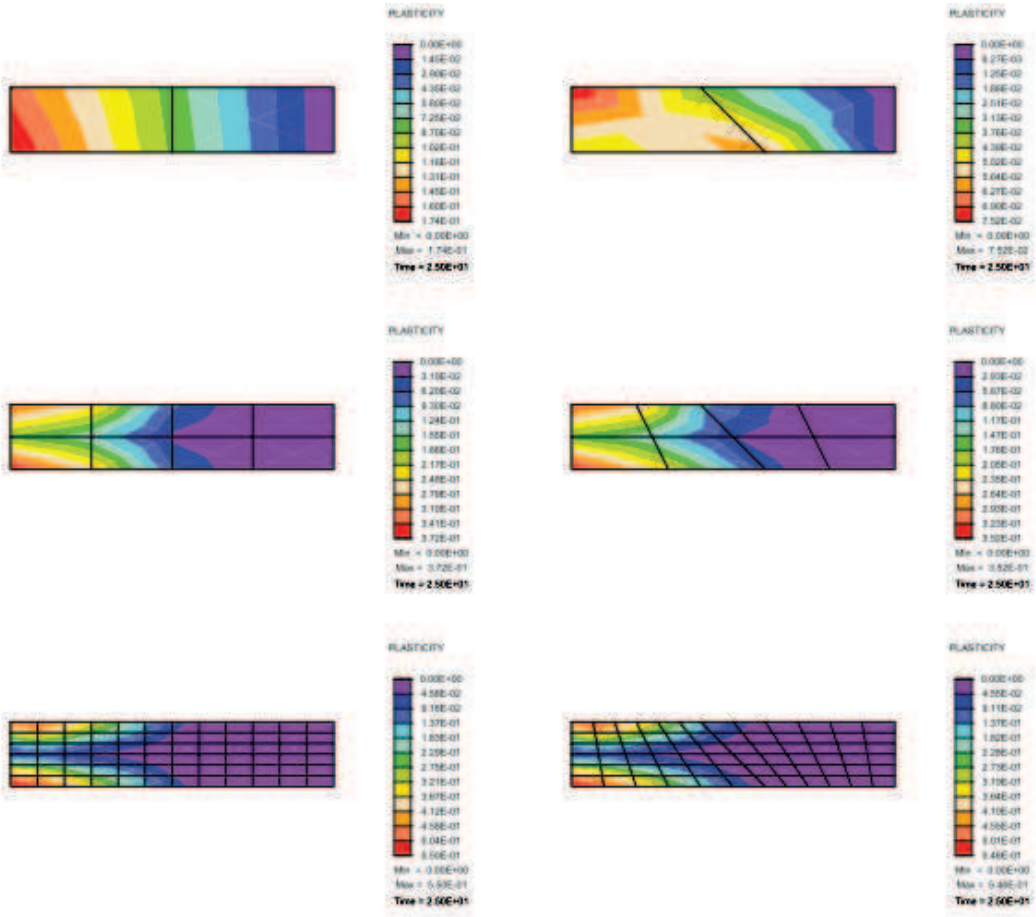

Figure 4.16: Yield contour of plasticity behavior q^p due to imposed shear loading for distorted and undistorted meshes.

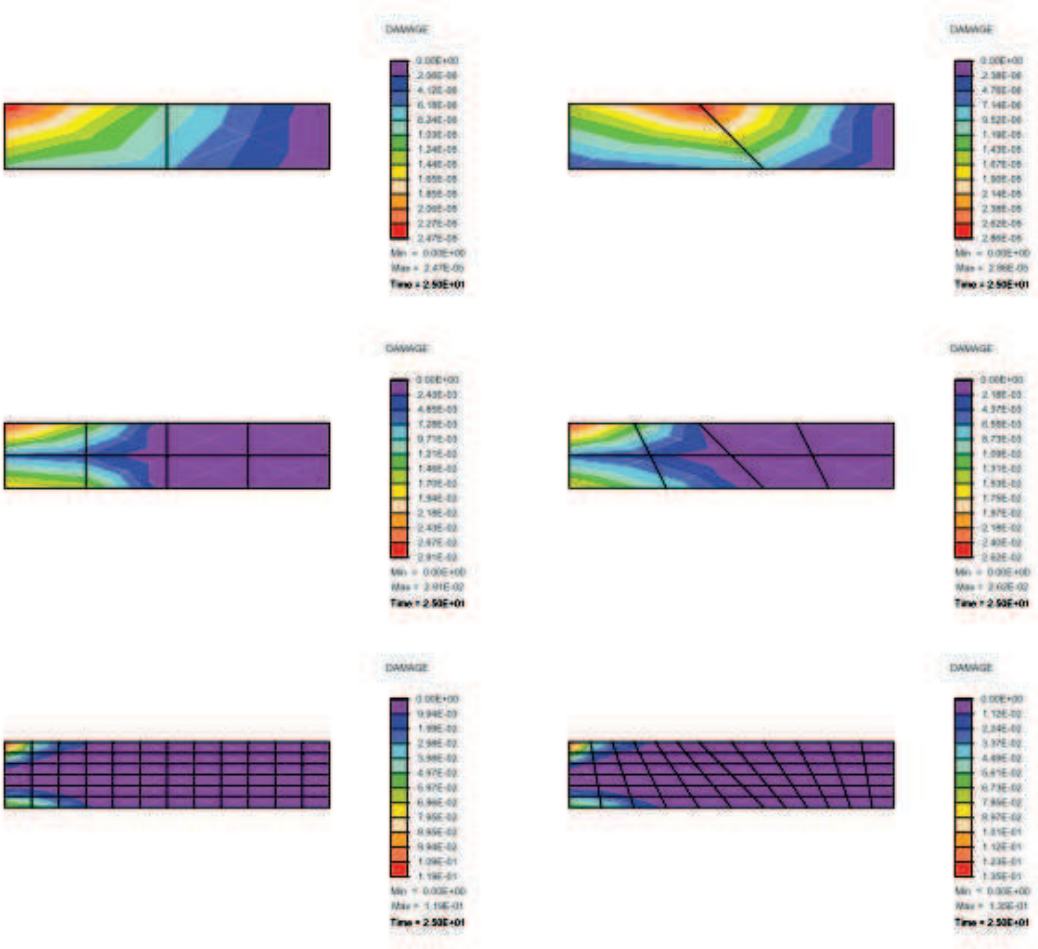

Figure 4.17: Yield contour of damage behavior q^d due to imposed shear loading for distorted and undistorted meshes.

5. CONCLUSIONS

In the present research, a comparative analysis between different types of cyclic loading has been performed by considering the coupled damage and plasticity behavior. The stress-based finite element formulation is used for the numerical analysis of the examples. Three basic effects: classical hysteresis curve, progressive relaxation to zero of the mean stress and strain ratcheting, are observed due to different loading types can be well captured by proposed model. Furthermore, plastic and damage zones considering the bending and shear loads are observed for the distorted and undistorted shape of mesh from coarse to fine size. We have presented that the developed model is efficient in representing the hysteresis loops for three kinds mentioned before by taking into account the coupled plasticity-damage behavior. In addition, we have demonstrated that we obtain very good results for the distorted mesh comparable the optimal results obtained with undistorted mesh of the structure undergoing the bending and shear loadings. We have shown that the stress interpolation function of Pian-Sumihara has a good performance for solving problems with dominant bending behavior.

We could extend this model of coupled damage-plasticity towards the applications whose accumulated damage might lead to softening as already done in 1D setting in [37].

REFERENCES

[1] **Wang, C. and Rose, L.** (1998). Transient and steady-state deformation at notch rood under cyclic loading, *Mechanics of Materials*, 20, 229–241.

[2] **Hill, R.** (1950). *The Mathematical Theory of Plasticity*, Oxford: Clarenden Press.

[3] **Lubliner, J.** (1990). *Plasticity Theory*, New York: Macmillan.

[4] **Simo, J.C. and Huges, T.** (1998). *Computational Inelasticity*, Berlin: Springer.

[5] **Lemaitre, J. and Chaboche, J.L.** (1990). *Mechanics of Solid Mechanics*, Cambridge: Cambridge University Press.

[6] **Krajcinovic, D.** (1996). *Damage Mechanics*, Amsterdam: North Holland.

[7] **Lemaitre, J.** (1985). Coupled elasto-plastic and damage constitutive equations, *Comput. Meth. Appl. Mech. Eng.*, 51, 31–49.

[8] **Ibrahimbegovic, A.**, **Markovic, D. and Gatuingt, F.** (2003). Constitutive model of coupled damge-plasticity and its finite element implementation, *Revue Europeenne des Elements Finis*, 12, 583–604.

[9] **Gurson, A.** (1977). Continuum theory of ductile rupture by void nucleation and growth:Part I-Yield criteria and flows rules for porous ductile media, *J. Eng. Mater. Tech.*, 99, 2–15.

[10] **Herve, G.**, **Gatuingt, F. and Ibrahimbegovic, A.** (2005). On numerical implementation of a coupled rate dependent damage-plasticity constitutive model for concrete in application to high-rate dynamics, *Engineering Computations*, 22, 381–405.

[11] **Meschke, G.**, **Lackner, R. and Mang., H.** (1998). An anisotropic elastoplastic damage model for plain concrete., *Int. J. Numer. Meth. Engng.*, 42, 703–727.

[12] **Simo, J.C.**, **Kennedy, J.G. and Taylor, R.L.** (1989). Complementary mixed finite element formulations for elastoplasticity, *Comput. Meth. Appl. Mech. Eng.*, 74, 177–206.

[13] **Einav, I.**, **Houlsby, G.T. and Nguyen, G.D.** (2007). Coupled damage and plasticity models derived from energy and dissipation potentials, *Int. J. Sol. Struct.*, 44, 2487–2508.

[14] **Chaboche, J.L.**, **Kruch, S.**, **Maire, J.F. and Pottier, T.** (2001). Towards a micromechanics based inelastic and damage modeling of composites, *Int. J. Plasticity*, 17, 411–439.

[15] **Litewka, A. and Szojda, L.** (2006). Damage, plasticity and failure of ceramics and cementitious composites subjected to multi axial state of stress, *Int. J. Plasticity*, 22, 2048–2065.

[16] **Voyiadjis, G.Z. and Dorgan, R.J.** (2007). Framework using functional forms of hardening internal state variables in modeling elasto-plastic-damage behavior, *Int. J. Plasticity*, 23, 1826–1859.

[17] **Haddag, B.**, **Abed-Meraim, F. and Balan, T.** (2009). Strain localization analysis using a large deformation anisotropic elastic plastic model coupled with damage, *Int. J. Plasticity*, 25, 1970–1996.

[18] **Yuanming, L.**, **Long, J. and Xiaoxiao, C.** (2009). Yield criterion and elasto-plastic damage constitutive model for frozen sandy soil, *Int. J. Plasticity*, 25, 1177–1205.

[19] **Badreddine, H.**, **Saanouni, K. and Dogui, A.** (2010). On non-associative anisotropic finite plasticity fully coupled with isotropic ductile damage for metal forming, *Int. J. Plasticity*, 23, 2058–2084.

[20] **Pyo, S.H. and Lee, H.K.** (2010). An elastoplastic damage model for metal matrix composites considering progressive imperfect interface under transverse loading, *Int. J. Plasticity*, 26, 25–41.

[21] **Zhu, Q.Z.**, **Shao, J.F. and Mainguy, M.** (2010). A micromechanics-based elastoplastic damage model for granular materials at low con?ning pressure, *Int. J. Plasticity*, 26, 586–602.

[22] **Brunig, M. and Gerke, S.** (2011). Simulation of damage evolution in ductile metals undergoing dynamic loading conditions, *Int. J. Plasticity*, 27, 479–491.

[23] **Naghdi, P.M. and Nikel, D.J.** (1984). Calculations for uniaxial stress and strain cyclic in plasticity, *Journal of Applied Mechanics*, 106, 487–493.

[24] **Naghdi, P.M. and Nikel, D.J.** (1986). Two dimensional strain cycling plasticity, *Journal of Applied Mechanics*, 108, 821–830.

[25] **Pirondi, A.**, **Bonora, N.**, **Steglich, D.**, **Brocks, W. and Hellmann, D.** (2006). Simulation of failure under cyclic plastic loading by damage models, *Int. J. Plasticity*, 22, 2146–2170.

[26] **Kang, G.**, **Kan, Q.**, **Zhang, J. and Sun, Y.** (2006). Time-dependent ratchetting experiments of SS304 stainless steel, *Int. J. Plasticity*, 22, 858–894.

[27] **Moreo, P.**, **Garcia-Aznar, J.M. and Doblare, M.** (2007). A coupled viscoplastic rate-dependent damage model for the simulation of fatigue failure of cement bone interfaces, *Int. J. Plasticity*, 23, 2058–2084.

[28] **D. J. Celentano, J.L.C.** (2007). Experimental and numerical characterization of damage evolution in steels, *Int. J. Plasticity*, 23, 1739–1762.

[29] **Chaboche, J.L.** (2008). A review of some plasticity and viscoplasticity constitutive theories, *Int. J. Plasticity*, 24, 1642–1693.

[30] **Jiang, Y.**, **Ott, W.**, **Baum, C.**, **Vormwald, M. and Nowack, H.** (2009). Fatigue life predictions by integrating EVICD fatigue damage model and an advanced cyclic plasticity theory, *Int. J. Plasticity*, 25, 780–801.

[31] **Henann, D.L. and Anand, L.** (2009). A large deformation theory for rate dependent elastic plastic materials with combined isotropic and kinematic hardening, *Int. J. Plasticity*, 25, 1833–1878.

[32] **Kang, G.**, **Liu, Y.**, **Ding, J. and Gao, Q.** (2009). Uniaxial ratcheting and fatigue failure of tempered 42CrMo steel: Damage evolution and damage coupled visco-plastic constitutive model, *Int. J. Plasticity*, 25, 838–860.

[33] **Zhang, J.**, **Yu, Q.**, **Jiang, Y. and Li, Q.** (2011). An experimental study of cyclic deformation of extruded AZ61A magnesium alloy, *Int. J. Plasticity*, 27, 768–787.

[34] **Dafalias, Y.F. and Feigenbaum, H.P.** (2011). Biaxial ratchetting with novel variations of kinematic hardening, *Int. J. Plasticity*, 27, 479–491.

[35] **Simo, J.C. and Ju, W.** (1987). Stress and strain-based continuum damage model I.Formulation II.Computational Aspect, *Int. J. Sol. Struct.*, 23, 821–869.

[36] **Ju, W.** (1987). On energy-based coupled elastoplastic damage theories: Constitutive modeling and computational aspects, *Int. J. Sol. Struct.*, 25, 803–833.

[37] **Ibrahimbegovic, A.**, **Jehel, P. and Davenne, L.** (2008). Coupled Damage-plasticity constitutive model and direct stiffness interpolation, *Comput. Mech.*, 42, 1–11.

[38] **Azzi, V.D. and Tsai, S.W.** (1995). Anisotropic strength of composites, *Exp. Mech.*, 5, 283–288.

[39] **R. M. Caddell, R.S.R. and Atkins, A.G.** (1973). Yield criterion for anisotropic and pressure dependent solids such as oriented polymers, *Journal of Materials Science*, 8, 1641–1646.

[40] **Orowan, E.** (1934). Zur kristallplastizitat III: Uber die mechanismus des gleitvorganges, *Zeitschrift fur Physik*, 89, 634–659.

[41] **Taylor, G.** (1934). The mechanism of plastic deformation of crystals, I. Theoretical, *Proceedings of the Royal Society A*, 145, 352–387.

[42] **Polanyi, M.** (1934). Uber eine art gitterstorung, die einem kristall plastisch machen konnte, *Zeitschrift fur Physik*, 89, 660–664.

[43] **Malvern, L.E.** (1969). *Introduction of the mechanics of a continuous medium*, New Jersey: Prentice Hall Inc.

[44] **Coussy, O.** (1995). *Mechanics of porous continua*, New York: John Wiley and Sons Ltd.

[45] **Strang, G.** (1986). *Introduction to Applied Mechanics*, Addison-Wesley.

[46] **Ibrahimbegovic, A.**, **Gharzeddine, F. and Chorfi, L.** (1998). Classical plasticity and viscoplasticity models reformulated: theoretical basis and numerical implementation, *Int. J. Numer. Meth. Engng.*, 42, 1499–1535.

[47] **Ibrahimbegovic, A.** (2009). *Nonlinear Solid Mechanics*, Springer.

[48] **Zienkiewicz, O.C.**, **Taylor, R.L. and Zhu, J.Z.** (2006). *The Finite Element Methods, vols. I,II,III*, Butterworth Heinemann, Oxford.

[49] **Pian, T.H.H. and Sumihara, K.** (1985). Rational approach for assumed stress finite elements, *Int. J. Numer. Meth. Engng.*, 20, 1685–1695.

[50] **Suita, K.**, **Kaneta, K. and Khozu, I.** (1992). The effect of strain rate in steel structural joints due to high speed cyclic loadings, *Proceedings of the 10th World Conference of Earthquake Engineering*, pp.2863–2866.

[51] **Ibrahimbegovic, A. and Wilson, E.L.** (1991). A modified method of incompatible modes, *Commun. Appl. Numer. Methods*, 7, 187–194.

[52] **Wilkins, M.L.** (1963). Calculation of elastic plastic flow, **Technical Report**, University of California.

[53] **de Borst, R.** (1991). The zero normal stress condition in plane stress and shell elastoplasticity, *Commun. Appl. Numer. Methods*, 7, 29–33.

APPENDICES

APPENDIX A : Von Mises Criterion

APPENDIX B :FEAP Codes

APPENDIX C : Interpolation Function

APPENDIX A: Von Mises Criterion

To fix ideas, the formulas given above are applied to the case of an isotropic material governed by Von Mises criterion with isotropic hardening. This is a particular case, but commonly used. We detail the different formulas and traps due to the passage of the indice notation to the vector notation of 6-component for the stresses. The Von Mises criterion is not sensitive to hydrostatic pressure. To simplify the equations, we decompose the stresses σ and deformations ε into two part; hydrostatic and deviatoric components, the latter being denoted s and e:

$$\begin{bmatrix}\sigma_{xx}\\ \sigma_{yy}\\ \sigma_{zz}\\ \tau_{xy}\\ \tau_{yz}\\ \tau_{xz}\end{bmatrix} = \begin{bmatrix}1\\ 1\\ 1\\ 0\\ 0\\ 0\end{bmatrix}\sigma_0 + \begin{bmatrix}s_{xx}\\ s_{yy}\\ s_{zz}\\ s_{xy}\\ s_{yz}\\ s_{xz}\end{bmatrix} \quad \begin{bmatrix}\varepsilon_{xx}\\ \varepsilon_{yy}\\ \varepsilon_{zz}\\ \gamma_{xy}\\ \gamma_{yz}\\ \gamma_{xz}\end{bmatrix} = \begin{bmatrix}\frac{1}{3}\\ \frac{1}{3}\\ \frac{1}{3}\\ 0\\ 0\\ 0\end{bmatrix} e_0 + \begin{bmatrix}e_{xx}\\ e_{yy}\\ e_{zz}\\ 2e_{xy}\\ 2e_{yz}\\ 2e_{xz}\end{bmatrix} \tag{A.1}$$

$$\sigma_0 = \frac{\sigma_{xx}+\sigma_{yy}+\sigma_{zz}}{3} \quad e_0 = \varepsilon_{xx}+\varepsilon_{yy}+\varepsilon_{zz}$$

The module of volume change connects the hydrostatic stress to hydrostatic deformation. Elastic law connecting deviatoric stresses can be written as:

$$\kappa = \frac{\sigma_{xx}+\sigma_{yy}+\sigma_{zz}}{3(\varepsilon_{xx}+\varepsilon_{yy}+\varepsilon_{zz})} = \frac{\sigma_0}{\varepsilon_0} = \frac{E}{3(1-2\nu)} \quad \begin{bmatrix}s_{xx}\\ s_{yy}\\ s_{zz}\\ s_{xy}\\ s_{yz}\\ s_{xz}\end{bmatrix} = \frac{E}{1+\nu}\begin{bmatrix}e_{xx}\\ e_{yy}\\ e_{zz}\\ e_{xy}\\ e_{yz}\\ e_{xz}\end{bmatrix} \tag{A.2}$$

The yield criterion is written in a non principal coordinate:

$$\begin{aligned} f &= \sqrt{\frac{1}{2}(\sigma_{xx}-\sigma_{yy})^2+(\sigma_{yy}-\sigma_{zz})^2+(\sigma_{zz}-\sigma_{xx})^2+6\tau_{xy}^2+6\tau_{yz}^2+6\tau_{xz}^2} \\ &= \sqrt{\frac{3}{2}[s_{xx}^2+s_{yy}^2+s_{zz}^2+2(s_{xy}^2+s_{yz}^2+s_{xz}^2)]} \end{aligned} \tag{A.3}$$

By using the indice notation, we write:

$$f = \sqrt{\frac{3}{2}s_{ij}s_{ij}} \tag{A.4}$$

The question is to see why there is a factor of 2 associated with the term s_{xy} which does not appear in the index notation. In fact, in the indice notation, i and j vary from 1 to 3 and if we develop the terms, we have a term s_{12} squared and squared term in s_{21}. Given the reciprocity of tangential stresses, these two terms are equal, which explains the factor 2. The variation of plastic deformation is given by:

$$
\begin{aligned}
d\varepsilon^{pl} &= d\gamma \frac{\partial f}{\partial \sigma} \\
&= \frac{d\lambda}{2f} \begin{bmatrix} 2\sigma_{xx} - \sigma_{yy} - \sigma_{zz} \\ 2\sigma_{xx} - \sigma_{yy} - \sigma_{zz} \\ 2\sigma_{xx} - \sigma_{yy} - \sigma_{zz} \\ 6\tau_{xy} \\ 6\tau_{yz} \\ 6\tau_{xz} \end{bmatrix} = \frac{3d\lambda}{2f} \begin{bmatrix} s_{xx} \\ s_{yy} \\ s_{zz} \\ 2s_{xy} \\ 2s_{yz} \\ 2s_{xz} \end{bmatrix}
\end{aligned} \tag{A.5}
$$

By using the indice notation, we have:

$$
d\varepsilon_{ij}^{pl} = \frac{3d\gamma}{2f} s_{ij} \tag{A.6}
$$

We see the same factor of 2 over the terms xy. In indice notation, it is the angular deformation ε_{xy}. Whie working with 6 components for stresses and strains, it is γ_{xy}, which explains the factor 2. By using the fact that the trace of deviators is zero, we deduce from these formulas the following result, in vector notation:

$$
\begin{aligned}
\sigma_{ij} \frac{\partial f}{\partial \sigma_{ij}} = (\sigma_0 \delta_{ij} + s_{ij}) \frac{\partial f}{\partial s_{ij}} = (\sigma_0 \delta_{ij} + s_{ij}) \frac{3s_{ij}}{2f} = \frac{3s_{ij}s_{ij}}{2f} = f \\
with \quad \frac{\partial f}{\partial \sigma_{ij}} = \frac{\partial f}{\partial s_{ij}}
\end{aligned} \tag{A.7}
$$

$$
\begin{aligned}
\sigma \frac{\partial f}{\partial \sigma} &= \frac{1}{2f} [\sigma_{xx}(2\sigma_{xx} - \sigma_{yy} - \sigma_{zz}) + \sigma_{yy}(2\sigma_{yy} - \sigma_{xx} - \sigma_{zz}) \\
&+ \sigma_{zz}(2\sigma_{zz} - \sigma_{xx} - \sigma_{yy}) + 6\tau_{xy}^2 + 6\tau_{xz}^2 + 6\tau_{yz}^2] \\
&= \frac{1}{2f} [(s_{xx} + p)3s_{xx} + (s_{yy} + p)3s_{yy} + (s_{zz} + p)3s_{zz} \\
&+ 6s_{xy}^2 + 6s_{xz}^2 + 6s_{yz}^2] \\
&= \frac{1}{2f} [3s_{xx}^2 + 3s_{yy}^2 + 3s_{zz}^2 + 6s_{xy}^2 + 6s_{xz}^2 + 6s_{yz}^2] = f
\end{aligned} \tag{A.8}
$$

The equation of the surface plasticity allows connecting the previous relationship to the current yield:

$$
\phi = 0 \rightarrow f - \sigma_y = 0 \rightarrow \sigma \frac{\partial f}{\partial \sigma} = f = \sigma_y \tag{A.9}
$$

G being the shear modulus can be calculated as:

$$H\frac{\partial f}{\partial \sigma} = \frac{E}{(1+\nu)(1-2\nu)} \begin{bmatrix} 1-\nu & \nu & \nu & 0 & 0 & 0 \\ \nu & 1-\nu & \nu & 0 & 0 & 0 \\ \nu & \nu & 1-\nu & 0 & 0 & 0 \\ 0 & 0 & 0 & \frac{1-2\nu}{2} & 0 & 0 \\ 0 & 0 & 0 & 0 & \frac{1-2\nu}{2} & 0 \\ 0 & 0 & 0 & 0 & 0 & \frac{1-2\nu}{2} \end{bmatrix} \frac{3}{2f} \begin{bmatrix} s_{xx} \\ s_{yy} \\ s_{zz} \\ 2s_{xy} \\ 2s_{yz} \\ 2s_{xz} \end{bmatrix}$$
$$= \frac{3E}{2(1+\nu)f} \begin{bmatrix} s_{xx} \\ s_{yy} \\ s_{zz} \\ s_{xy} \\ s_{yz} \\ s_{xz} \end{bmatrix} = \frac{3G}{f} \begin{bmatrix} s_{xx} \\ s_{yy} \\ s_{zz} \\ s_{xy} \\ s_{yz} \\ s_{xz} \end{bmatrix} \tag{A.10}$$

We deduce the expression of the numerator appearing in the expression of the tangential material law:

$$\frac{\partial f}{\partial \sigma} H \frac{\partial f}{\partial \sigma} = 3G \tag{A.11}$$

If we report these results in the expression of the tangential material theoretical law, we obtain:

$$H_T = H - \frac{9G^2}{f^2} \frac{ss^T}{3G+H'} \quad s^T = \begin{pmatrix} s_{xx} & s_{yy} & s_{zz} & s_{xy} & s_{yz} & s_{xz} \end{pmatrix} \tag{A.12}$$

Particularly, if the material has a negative hardening, which means, if the yield decreases when the equivalent plastic strain increases, there is a limit on the module H that cannot be less than $-3G$. There can also be an expression of the variation of equivalent plastic strain which is obtained by the equivalence of plastic work:

$$Y d\bar{\varepsilon}^p = \sigma_{ij} d\varepsilon_{ij}^p = \sigma_{ij} d\gamma \frac{\partial f}{\partial \sigma_{ij}} = d\gamma f = d\gamma \sigma_y \rightarrow d\bar{\varepsilon}^p = d\gamma \tag{A.13}$$

At the numerical integration, the first equation of the nonlinear system to be solved in each integration point is:

$$\sigma_{n+1} = \sigma^{TR} - \Delta\gamma H \frac{\partial f}{\partial \sigma_{n+1}} \tag{A.14}$$

It is divided between volumetric and deviatoric part:

$$\begin{bmatrix} 1 \\ 1 \\ 1 \\ 0 \\ 0 \\ 0 \end{bmatrix} \sigma_{0,n+1} + \begin{bmatrix} s_{xx,n+1} \\ s_{yy,n+1} \\ s_{zz,n+1} \\ s_{xy,n+1} \\ s_{yz,n+1} \\ s_{xz,n+1} \end{bmatrix} = \begin{bmatrix} 1 \\ 1 \\ 1 \\ 0 \\ 0 \\ 0 \end{bmatrix} \sigma_0^{TR} + \begin{bmatrix} s_{xx}^{TR} \\ s_{yy}^{TR} \\ s_{zz}^{TR} \\ s_{xy}^{TR} \\ s_{yz}^{TR} \\ s_{xz}^{TR} \end{bmatrix} \frac{3G\Delta\bar{\varepsilon}^p}{f_{n+1}} \begin{bmatrix} s_{xx,n+1} \\ s_{yy,n+1} \\ s_{zz,n+1} \\ s_{xy,n+1} \\ s_{yz,n+1} \\ s_{xz,n+1} \end{bmatrix} \tag{A.15}$$

The criterion depends only on the deviatoric stress, the second equation to satisfy is written:

$$f(s_{n+1}) - \sigma_y(\bar{\varepsilon}_n^p + \Delta\bar{\varepsilon}^p) = 0 \tag{A.16}$$

We deduce that the hydrostatic test stress is good, it is logical for a material whose plasticity criterion of Von Mises since it does not occur. Taking into account this equality, and the quadratic form of f as a function of s, we rewrite the first equation of the form:

$$\begin{aligned} s_{n+1} = s^{TR} - \frac{3G}{f_{n+1}}\Delta\bar{\varepsilon}^p s_{n+1} \rightarrow s_{n+1} = \frac{1}{frac1 + 3G\Delta\bar{\varepsilon}^p f_{n+1}} s^{TR} \\ f_{n+1} = \frac{1}{\frac{1+3G\Delta\bar{\varepsilon}^p}{f_{n+1}}} f^{TR} \rightarrow f_{n+1} + 3G\Delta\bar{\varepsilon}^p = f^{TR} \end{aligned} \tag{A.17}$$

This relationship is introduced in the second equation:

$$f^{TR} - 3G\Delta\bar{\varepsilon}^p - \sigma_y(\bar{\varepsilon}^p + \Delta\varepsilon^p) = 0 \tag{A.18}$$

Finally, the system to be solved is reduced to a scalar equation. If hardening is more linear, in other words if the hardening modulus is constant, this equation is linear. If hardening is nonlinear and if the curvature of the curve Y as a function of the plastic deformation is negative, the Newton resolution always converges. When we solve with a Newton scheme, we see the factor $(3G+H)$ appearing, which is also involved in theoretical tangential law. If there is no hardening, there is no problem for the integration of the constitutive law. This algorithm is known as the radial return [52]. In the deviatoric plane, the Von Mises criterion is a circle. Test stress (elastic predictor) gives a point outside the circle. The plastic corrector returns the point on the circle, in a way perpendicular to the circle, giving the name of radial. If the criterion is not Von Mises or if the material is not isotropic, elastic scheme predictor / plastic corrector is no longer equal to the radial return. The equations were established in the three-dimensional case. In stress state plane, it is a bit more complicated: the total deformation is not known in the transverse direction but the stress must be nowhere. The resolution of this case is beyond the scope of this work [53]. While the criterion is Von Mises, plasticity surface is an ellipse in the plane $(\sigma_I\sigma_{II})$, the radial return is not equivalent to a pattern elastic predictor/plastic corrector. For shells, layers are in stress state plane, thus the form of the Von Mises criterion is an ellipse in a plane of principal stresses. The algorithm elastic predictor - plastic corrector does not correspond to a radial return which has no theoretical justification for being used.

APPENDIX B:FEAP Codes

c*Id* : *sld*2*d*2.*f*, *v*1.12001/08/0117 : 16 : 18*rltExp*

subroutine elmt09(d,ul,xl,ix,tl,s,r,ndf,ndm,nst,isw)

c * * F E A P * * A Finite Element Analysis Program

c——[–.—-+—-.—-+—-.———————————————————]

c Purpose: Pian-Sumiohara elasto-plastic-damage small deformation element c

c Inputs:
c d(*) - Element parameters
c ul(ndf,*) - Current nodal solution parameters
c u0 - Initial solution state
c xl(ndm,*) - Nodal coordinates
c ix(*) - Global nodal connections
c tl(*) - Nodal temp vector
c ndf - Degree of freedoms/node
c ndm - Mesh coordinate dimension
c nst - Element array dimension
c isw - Solution option switch

c Outputs:
c s(nst,*) - Element array
c r(ndf,*) - Element vector

c——[–.—-+—-.—-+—-.———————————————————]

implicit none

include ’augdat.h’
include ’bdata.h’
include ’cdata.h’
include ’cdat1.h’
include ’comblk.h’
include ’dahi.h’
include ’elbody.h’
include ’eldata.h’
include ’elengy.h’
include ’elplot.h’
include ’eltran.h’
include ’fdata.h’
include ’hdata.h’
include ’iofile.h’
include ’laginf.h’
include ’macro.h’
include ’part0.h’
include ’pmod2d.h’
include ’prld1.h’
include ’tdata.h’

```
include 'upointer.h'


integer ndf,ndm,nst,isw,i,i1,j,jj,j1,l,lint,nhi,nhv,nn,npm
integer ix(*)
real*8 augfp, epp, b1,b2, dv,dl,d1, third, xsj(25), type
real*8 dsigtr, mpress, dmass, dmshp, dtheta, cfac,lfac, fac
real*8 d(*), ul(ndf,nen,*), xl(ndm,*), tl(*), s(nst,*)
real*8 sg(3,25), r(ndf,*), xx(2) , shp(3,4,25)
real*8 bbd(2,7), aa(6,6,5,25), dd(7,7) , dvol(25)
real*8 sigm(9), sigl(16,25), bpra(3) , bbar(2,16,25)
real*8 al(2), ac(2), vl(2) , x0(2)
real*8 phi(6,25), theta(3,25), hh(6,6)
real*8 press(25),pbar(25),hsig(6),eps(6,25),gru(6,3,25)
real*8 irad(25), ta(25), epsd(4), epsv(25)
integer carama,uprm,mplus,k,pom1,ip,ii
real*8 rpo1,ss(4,4,4),x1(2),x2(2),rpom,lagv(4),xn(4),btan(5,5)
real*8 gp1,gp2,ap,tjac(2,2),bet(5),strsh(6,25),bsig(4,25)
real*8 tan1(4,4,25),peps(4,5),stb(5,ndf,nel),betdd(5,nst)
real*8 bres(5),btpg(5,25),btgg(25),brg(25),sig33(25),gama(25)
real*8 ep(25),ep1(25),yield,fisig,kapa,odf(4,25),brnom,tol
real*8 odkapa
real*8 pres(5),RP(7),peps2(4,5),peps3(5),odf2(4,4),rod,kdv
real*8 ksid(25),ksid1(25),dam(25),dml(2),dodf(4,25),dfisig
real*8 betn(5),dbet(4),sig33n(25),dama(25),peps4(5),bsign(4,25)
real*8 dep(4,25),dissp,dissd,td(20)
logical noconv,errck,pinput
integer ni
character wd(2),yyy*120
real*8 dalph
real*8 kappaP(4,25),kappaP1(4,25),alphaP(4,25),alphaP1(4,25)
real*8 ksip1, ksipn
real*8 q(2,4) !to plot the ksip and ksid
real*8 damq(4) !to obtain the D parameter
real*8 hpom(2,4)

save

data third / 0.3333333333333333d0 /
data nhi / 2 / , ni /5/ , kdv /0.81649658092772603273/

uprm = ndd-nud

c TEMPORARY SET OF TEMPERATURE

data ta / 25*0.0d0 /
data gp2 /0.7886751345948128822 5d0/
data gp1 /0.2113248654051871177 5d0/


c position to the beginning of ud() array
uprm = ndd-nud
```

```
ccccccccccccccccccccccccccc ISW = 1 ccccccccccccccccccccccccccccc

if(isw.eq.1) then
if(ior.lt.0) write(*,3000)
c call pintio(yyy,10)


errck = pinput(td,12)


do i = 1,12
d(uprm+i) = td(i)
enddo ! i
d(uprm + 1) = 2.0d0*d(uprm + 1)


nh1 = 2*8 + 5 + 2*8


return 11 print*,'ERROR IN ELMT09' stop

ccccccccccccccccccccccccccc ISW = 2 ccccccccccccccccccccccccccccc

c check the mesh

elseif(isw.eq.2) then
call ckisop(ix,xl,ap,ndm)


elseif(isw.eq.32 .or. isw.eq.30) then
call pzero(shp,3*4*25)

r(1,1) = (xl(1,1)+xl(1,2)+xl(1,3)+xl(1,4))/4.0d0
r(2,1) = (xl(2,1)+xl(2,2)+xl(2,3)+xl(2,4))/4.0d0


do i = 1,4
do j = 1,4
do k = 1,4
ss(k,j,i) = 0.0d0
enddo
enddo
enddo


c.....assuming 2 g.p. integration

do i = 1,nlag
x1(1) = xl(1,plag(i))
x1(2) = xl(2,plag(i))
x2(1) = xl(1,mplus(plag(i),1,nen))
x2(2) = xl(2,mplus(plag(i),1,nen))


rpom = (x2(1)-x1(1))*(x2(1)-x1(1))
rpom = rpom + (x2(2)-x1(2))*(x2(2)-x1(2))
```

```
rpom = dsqrt(rpom)/2.0d0

xn(1) = gp1*(x2(1) - x1(1)) + x1(1)
xn(2) = gp1*(x2(2) - x1(2)) + x1(2)

xn(3) = gp2*(x2(1) - x1(1)) + x1(1)
xn(4) = gp2*(x2(2) - x1(2)) + x1(2)

c Lag. mult. fun. gp 1
call lagran_int(xn,lagi(1,1,i),lagi(1,2,i),lagv,2,ndm)

c Lag. mult. fun. gp 2
call lagran_int(xn(3),lagi(1,1,i),lagi(1,2,i),lagv(3),2,ndm)

c Disp. fun.
shp(1,1,i) = gp2
shp(2,1,i) = gp2
shp(1,2,i) = gp1
shp(2,2,i) = gp1
shp(1,3,i) = gp1
shp(2,3,i) = gp1
shp(1,4,i) = gp2
shp(2,4,i) = gp2

do k = 1,2
do j = 1,2
ss(2*j-1,2*k-1,i) = shp(1,2*j-1,i)*lagv(k )*rpom + shp(1,2*j ,i)*lagv(k+2)*rpom
ss(2*j ,2*k ,i) = shp(2,2*j-1,i)*lagv(k )*rpom + shp(2,2*j ,i)*lagv(k+2)*rpom
enddo ! j
enddo ! k
enddo ! i

pom1 = nst*nst ! 4x4x4
call cpmat(ss,s,pom1)

c endif

c Compute tangent stiffness and residual force vector

elseif(isw.eq. 3 .or. isw.eq. 4 .or. isw.eq. 6 .or.isw.eq. 8 .or. isw.eq.14) then

c Set element quadrature order

npm = 1
l = 2 ! prej
c l = d(5)
call int2d(l,lint,sg)
```

```
nhv = 8 !kappaP(4)-kinematic variable

ccccccccccccccccccccccccccc ISW = 14 ccccccccccccccccccccccccccccc

if(isw.eq.14) then

c damage parameter
do i = 1,lint
hr(nh1+ni + (i-1)*nhv + 3) = 1.0d0/9.0d0/d(uprm+1)
hr(nh2+ni + (i-1)*nhv + 3) = hr(nh1+ni + (i-1)*nhv + 3)
enddo ! i


endif
ccccccccccccccccccccccccc END ISW = 14 ccccccccccccccccccccccccccc

c stress interpolation parameters
do i = 1,ni
bet(i) = hr(nh2-1+i)
betn(i) = hr(nh1-1+i)
end do

c sig33
do i = 1,lint
sig33(i) = hr(nh2+ni + (i-1)*nhv + 1)
sig33n(i) = hr(nh1+ni +(i-1)*nhv + 1)
enddo ! i

c plastic isotropic hardening parameter
do i = 1,lint
ep(i) = hr(nh1+ni + (i-1)*nhv )
ep1(i) = ep(i)
c write(iow,*)'hr(nh1+(i-1)*nhv = ', ep(i)
enddo ! i

c damage hardening parameter
do i = 1,lint
ksid(i) = hr(nh1+ni + (i-1)*nhv + 2)
ksid1(i) = ksid(i)
c write(iow,*)'hr(nh1+(i-1)*nhv+2 = ', ksid(i)
enddo ! i

c damage parameter
do i = 1,lint
dam(i) = hr(nh1+ni + (i-1)*nhv + 3)
c write(iow,*)'hr(nh1+(i-1)*nhv+3 = ', dam(i)
enddo ! i

c plastic isotropic hardening parameter
do i=1,lint
q(1,i) = hr(nh1+ni + (l-1)*nhv ) !plasticity harden
```

```
c damage hardening parameter
q(2,i) = hr(nh1+ni + (l-1)*nhv + 2) !damage harden

ccccccccccccccccc DAMAGE PARAMETER-IJP
c damq(l) = hr(nh1+ni + (l-1)*nhv + 3) !damage parameter

ccccccccccccccccc DAMAGE PARAMETER-IJP
enddo

cccccccc CHANGEMENT ccccccccccccccccccc
c get alphaP1 at g.p

c kinematic hardening variable
do i = 1,lint
do j = 1,4
kappaP(j,i) = hr(nh1+ni+(i-1)*nhv+3+j)
kappaP1(j,i) = kappaP(j,i)
enddo ! j
enddo ! i

ccccccc FIN

c get the Jacobian in the middle
call shp2d(x0,xl,shp(1,1,1),xsj(1),ndm,nel,ix,.true.)
call pzero(tjac,4)

do j = 1,2
do i = 1,2
do l = 1,nel
tjac(i,j) = tjac(i,j) + xl(i,l)*shp(j,l,1)
enddo ! l
enddo ! i
enddo ! j


c————-TEST
do i = 1,7
RP(i) = d(i)
enddo ! i
c————-TEST

do l = 1,lint

c Shape functions and derivatives

call shp2d(sg(1,l),xl,shp(1,1,l),xsj(l),ndm,nel,ix,.false.)

dvol(l) = xsj(l)*sg(3,l)

c strains
call strn2d_ps(d,xl,ul,shp(1,1,l),ndf,ndm,nel,xx(1),xx(2),gru(1,1,l))

c constants for stress shape functions calculations
strsh(1,l) = sg(2,l)*tjac(1,1)**2
strsh(2,l) = sg(1,l)*tjac(1,2)**2
strsh(3,l) = sg(2,l)*tjac(2,1)**2
strsh(4,l) = sg(1,l)*tjac(2,2)**2
```

```
strsh(5,l) = sg(2,l)*tjac(1,1)*tjac(2,1)
strsh(6,l) = sg(1,l)*tjac(2,2)*tjac(1,2)


end do ! l

c Tangent and residual computations

if(isw.eq.3 .or. isw.eq.6 .or. isw.eq.14) then

ccccccccccccccccccccccccccc ISW = 3 or 6 ccccccccccccccccccccccccccc
if(isw.eq.3 .or. isw.eq.6) then

noconv = .true.
ii = 0

do while(noconv)
ii = ii + 1

c put beta residual/tangent to 0
call pzero(bres,5)
call pzero(brg,lint)
call pzero(btan,25)
call pzero(btpg,5*lint)
call pzero(btgg,lint)


c BOUCLE SUR LES POINTS D'INTEGRATION
do l = 1,lint

c CALCUL DU RESIDU

c deformation projection SÎ Eps(Sig)

c get Sig in g.p.
bsig(1,l) = bet(1)+strsh(1,l)*bet(2)+strsh(2,l)*bet(4)
bsig(2,l) = bet(3)+strsh(3,l)*bet(2)+strsh(4,l)*bet(4)
bsig(3,l) = sig33(l)
bsig(4,l) = bet(5)+strsh(5,l)*bet(2)+strsh(6,l)*bet(4)


c store strain and stress at NGP
do i = 1,4
tt(11*(l-1)+2*(i-1)+1) = gru(i,1,l)
tt(11*(l-1)+2*(i-1)+2) = bsig(i,l)
end do

do i = 1,2
tt(11*(l-1)+8+i) = q(i,l)     !hardening param of plasticity and damage
enddo

tt(11*(l-1)+11) = dam(l) !D parameter

c get Sig in g.p. at the previous increment
bsign(1,l) = betn(1) + strsh(1,l)*betn(2) + strsh(2,l)*betn(4)
bsign(2,l) = betn(3) + strsh(3,l)*betn(2) + strsh(4,l)*betn(4)
bsign(3,l) = sig33n(l)
```

```
bsign(4,l) = betn(5) + strsh(5,l)*betn(2) + strsh(6,l)*betn(4)

c correct elastic properties
dml(1) = 1.0d0/(1.0d0/d(uprm+1) + 9.0d0*dam(l))
dml(2) = d(uprm+2)

c get d sig in g.p.
dbet(1) = bsig(1,l) - bsign(1,l)
dbet(2) = bsig(2,l) - bsign(2,l)
dbet(3) = bsig(3,l) - bsign(3,l)
dbet(4) = bsig(4,l) - bsign(4,l)

c get Eps (and Sig33) in g.p.
call epsig(dml,dbet,eps(1,l),tan1(1,1,l))

c constant part
bres(1) = bres(1) - eps(1,l)*dvol(l)
bres(3) = bres(3) - eps(2,l)*dvol(l)
bres(5) = bres(5) - 2.0d0*eps(4,l)*dvol(l)

c linear part
bres(2) = bres(2) - strsh(1,l)*eps(1,l)*dvol(l)
bres(2) = bres(2) - strsh(3,l)*eps(2,l)*dvol(l)
bres(2) = bres(2) - 2.0d0*strsh(5,l)*eps(4,l)*dvol(l)

bres(4) = bres(4) - strsh(2,l)*eps(1,l)*dvol(l)
bres(4) = bres(4) - strsh(4,l)*eps(2,l)*dvol(l)
bres(4) = bres(4) - 2.0d0*strsh(6,l)*eps(4,l)*dvol(l)

brg(l) = -eps(3,l)*dvol(l)

c ———— trial part

c constant part
bres(1) = bres(1) + gru(1,3,l)*dvol(l)
bres(3) = bres(3) + gru(2,3,l)*dvol(l)
bres(5) = bres(5) + 2.0d0*gru(4,3,l)*dvol(l)

c linear part
bres(2) = bres(2) + strsh(1,l)*gru(1,3,l)*dvol(l)
bres(2) = bres(2) + strsh(3,l)*gru(2,3,l)*dvol(l)
bres(2) = bres(2) + 2.0d0*strsh(5,l)*gru(4,3,l)*dvol(l)

bres(4) = bres(4) + strsh(2,l)*gru(1,3,l)*dvol(l)
bres(4) = bres(4) + strsh(4,l)*gru(2,3,l)*dvol(l)
bres(4) = bres(4) + 2.0d0*strsh(6,l)*gru(4,3,l)*dvol(l)

c plastic constitutive part
```

```
c compute alpha
do i = 1,4
call alph(d(uprm+12),kappaP(i,l),alphaP(i,l))
enddo

yield = fisig(bsig(1,l),alphaP(1,l))+kdv*kapa(d(uprm+3),ep(l))

gama(l) = 0.0d0
if(yield.gt.0.0d0) then
write(iow,*) 'plastification'
write(iow,*)'ksip1 = ', ep1(l)

call gamacomp(d(uprm+3),bsig(1,l),ep(l),ep1(l),kappaP(1,l),kappaP1(1,l),gama(l))

do i = 1,4
call alph(d(uprm+12),kappaP1(i,l),alphaP1(i,l))
enddo

yield = fisig(bsig(1,l),alphaP1(1,l)) + kdv*kapa(d(uprm+3),ep1(l))


call odfisig(bsig(1,l),alphaP1(1,l),odf(1,l))


c constant part
bres(1) = bres(1) - gama(l)*odf(1,l)*dvol(l)
bres(3) = bres(3) - gama(l)*odf(2,l)*dvol(l)
bres(5) = bres(5) - gama(l)*odf(4,l)*dvol(l)


c linear part
bres(2) = bres(2) - strsh(1,l)*gama(l)*odf(1,l)*dvol(l)
bres(2) = bres(2) - strsh(3,l)*gama(l)*odf(2,l)*dvol(l)
bres(2) = bres(2) - strsh(5,l)*gama(l)*odf(4,l)*dvol(l)

bres(4) = bres(4) - strsh(2,l)*gama(l)*odf(1,l)*dvol(l)
bres(4) = bres(4) - strsh(4,l)*gama(l)*odf(2,l)*dvol(l)
bres(4) = bres(4) - strsh(6,l)*gama(l)*odf(4,l)*dvol(l)


brg(l) = brg(l) - gama(l)*odf(3,l)*dvol(l)
endif

c damage constitutive part

yield = dfisig(bsig(1,l)) + kapa(d(uprm+8),ksid(l))

dama(l) = 0.0d0
if(yield.gt.0.0d0) then
write(iow,*) 'endommagement'
write(iow,*) 'ksid1= ', ksid(l)
c write(iow,*) 'ksid1(2)= ',ksid1(2)
c write(iow,*) 'ksid1(3)= ',ksid1(3)
c write(iow,*) 'ksid1(4)= ',ksid1(4)


call damacomp(d(uprm+8),bsig(1,l),ksid(l),ksid1(l),dama(l))
```

```
yield = dfisig(bsig(1,l)) + kapa(d(uprm+8),ksid1(l))

call dodfisig(bsig(1,l),dodf(1,l))

c constant part
bres(1) = bres(1) - dama(l)*dodf(1,l)*dvol(l)
bres(3) = bres(3) - dama(l)*dodf(2,l)*dvol(l)
bres(5) = bres(5) - dama(l)*dodf(4,l)*dvol(l)

c linear part
bres(2) = bres(2) - strsh(1,l)*dama(l)*dodf(1,l)*dvol(l)
bres(2) = bres(2) - strsh(3,l)*dama(l)*dodf(2,l)*dvol(l)
bres(2) = bres(2) - strsh(5,l)*dama(l)*dodf(4,l)*dvol(l)


bres(4) = bres(4) - strsh(2,l)*dama(l)*dodf(1,l)*dvol(l)
bres(4) = bres(4) - strsh(4,l)*dama(l)*dodf(2,l)*dvol(l)
bres(4) = bres(4) - strsh(6,l)*dama(l)*dodf(4,l)*dvol(l)


brg(l) = brg(l) - dama(l)*dodf(3,l)*dvol(l)
endif

c BETA TANGENT

c initialize peps arrays
call pzero(peps,20)
call pzero(peps2,20)
call pzero(peps3,5)
call pzero(peps4,5)

c C^(-1)*S dV
do i = 1,4
peps(i,1) = tan1(i,1,l)*dvol(l)
peps(i,3) = tan1(i,2,l)*dvol(l)
peps(i,5) = 2.0d0*tan1(i,4,l)*dvol(l)


peps(i,2) = peps(i,2) + strsh(1,l)*tan1(i,1,l)*dvol(l)
peps(i,2) = peps(i,2) + strsh(3,l)*tan1(i,2,l)*dvol(l)
peps(i,2) = peps(i,2) + 2.0d0*strsh(5,l)*tan1(i,4,l)*dvol(l)


peps(i,4) = peps(i,4) + strsh(2,l)*tan1(i,1,l)*dvol(l)
peps(i,4) = peps(i,4) + strsh(4,l)*tan1(i,2,l)*dvol(l)
peps(i,4) = peps(i,4) + 2.0d0*strsh(6,l)*tan1(i,4,l)*dvol(l)
enddo ! i

if(gama(l).gt.0.0d0) then
call odfisig2(bsig(1,l),alphaP1(1,l),odf2)


c d^2 f/d sig^2 * S * gama
do i = 1,4
peps2(i,1) = odf2(i,1)*dvol(l)*gama(l)
peps2(i,3) = odf2(i,2)*dvol(l)*gama(l)
```

```
peps2(i,5) = odf2(i,4)*dvol(l)*gama(l)

peps2(i,2) = peps2(i,2) + strsh(1,l)*odf2(i,1)*dvol(l)*gama(l)
peps2(i,2) = peps2(i,2) + strsh(3,l)*odf2(i,2)*dvol(l)*gama(l)
peps2(i,2) = peps2(i,2) + strsh(5,l)*odf2(i,4)*dvol(l)*gama(l)

peps2(i,4) = peps2(i,4) + strsh(2,l)*odf2(i,1)*dvol(l)*gama(l)
peps2(i,4) = peps2(i,4) + strsh(4,l)*odf2(i,2)*dvol(l)*gama(l)
peps2(i,4) = peps2(i,4) + strsh(6,l)*odf2(i,4)*dvol(l)*gama(l)
enddo ! i
c d f/d sig S
peps3(1) = odf(1,l)
peps3(3) = odf(2,l)
peps3(5) = odf(4,l)

peps3(2) = strsh(1,l)*odf(1,l)
peps3(2) = peps3(2) + strsh(3,l)*odf(2,l)
peps3(2) = peps3(2) + strsh(5,l)*odf(4,l)

peps3(4) = strsh(2,l)*odf(1,l)
peps3(4) = peps3(4) + strsh(4,l)*odf(2,l)
peps3(4) = peps3(4) + strsh(6,l)*odf(4,l)
endif ! gama>0
if(dama(l).gt.0.0d0) then
c d f/d sig S
peps4(1) = dodf(1,l)
peps4(3) = dodf(2,l)
peps4(5) = dodf(4,l)

peps4(2) = strsh(1,l)*dodf(1,l)
peps4(2) = peps4(2) + strsh(3,l)*dodf(2,l)
peps4(2) = peps4(2) + strsh(5,l)*dodf(4,l)

peps4(4) = strsh(2,l)*dodf(1,l)
peps4(4) = peps4(4) + strsh(4,l)*dodf(2,l)
peps4(4) = peps4(4) + strsh(6,l)*dodf(4,l)
endif ! dama>0
c ST̂ * (Ĉ-1)*S)
do j = 1,5
btan(1,j) = btan(1,j) + peps(1,j)
btan(3,j) = btan(3,j) + peps(2,j)
btan(5,j) = btan(5,j) + 2.0d0*peps(4,j)
```

```
btan(2,j) = btan(2,j) + strsh(1,l)*peps(1,j)
btan(2,j) = btan(2,j) + strsh(3,l)*peps(2,j)
btan(2,j) = btan(2,j) + 2.0d0*strsh(5,l)*peps(4,j)

btan(4,j) = btan(4,j) + strsh(2,l)*peps(1,j)
btan(4,j) = btan(4,j) + strsh(4,l)*peps(2,j)
btan(4,j) = btan(4,j) + 2.0d0*strsh(6,l)*peps(4,j)

btpg(j,l) = peps(3,j)

enddo ! j

c elastic
btgg(l) = tan1(3,3,l)*dvol(l)

if(gama(l).gt.0.0d0) then

c S^ * d^2 f/d sig^2 * S * gama do j = 1,5 btan(1,j) = btan(1,j) + peps2(1,j)
btan(3,j) = btan(3,j) + peps2(2,j)
btan(5,j) = btan(5,j) + peps2(4,j)

btan(2,j) = btan(2,j) + strsh(1,l)*peps2(1,j)
btan(2,j) = btan(2,j) + strsh(3,l)*peps2(2,j)
btan(2,j) = btan(2,j) + strsh(5,l)*peps2(4,j)

btan(4,j) = btan(4,j) + strsh(2,l)*peps2(1,j)
btan(4,j) = btan(4,j) + strsh(4,l)*peps2(2,j)
btan(4,j) = btan(4,j) + strsh(6,l)*peps2(4,j)

btpg(j,l) = btpg(j,l) + peps2(3,j)
enddo ! j

btgg(l) = btgg(l) + odf2(3,3)*gama(l)*dvol(l)

c S^ d f/d sig d f/d sig S
rod = dvol(l)/(kdv*kdv*odkapa(d(uprm+3),ep1(l)) + dalph(d(uprm+12)) )
do j = 1,5
do i = 1,5
btan(i,j) = btan(i,j) - peps3(i)*peps3(j)*rod
enddo ! i
btpg(j,l) = btpg(j,l) - odf(3,l)*peps3(j)*rod
enddo ! j

btgg(l) = btgg(l) - odf(3,l)*odf(3,l)*rod
endif ! gama>0

c damage contribution
if(dama(l).gt.0.0d0) then

c S^ d f/d sig d f/d sig S
rod = dvol(l)/odkapa(d(uprm+8),ksid1(l))
```

```
do j = 1,5
do i = 1,5
btan(i,j) = btan(i,j) - peps4(i)*peps4(j)*rod
enddo ! i
btpg(j,l) = btpg(j,l) - dodf(3,l)*peps4(j)*rod
enddo ! j

btgg(l) = btgg(l) - dodf(3,l)*dodf(3,l)*rod
endif ! dama>0

c compute directly the inverse of the g.p. submatrix
c elastic part
btgg(l) = 1.0d0/btgg(l)
c FIN DE LA BOUCLE SUR LES POINTS D'INTEGRATION
enddo ! l
call statcongg(btan,btpg,btgg,bres,brg,ni,lint)

c copy residual
do i = 1,ni
pres(i) = bres(i)
enddo ! i
c solve for the corrections of beta
call gaussj(btan,5,5,bres,1,1)

c residual energy bres*dbeta
brnom = 0.0d0
do i = 1,ni
brnom = brnom + abs(bres(i)*pres(i))
enddo ! i
do i = 1,5
bet(i) = bet(i) + bres(i)
enddo ! i
call getsig33(btpg,btgg,brg,bres,sig33,ni,lint)
tol = 1.0e-20
if(brnom.lt.tol) then
noconv = .false.
elseif(ii.gt.20) then
write(*,*) 'elmt08: main(isw=3,6): NO CONVERGENCE FOR LOCAL ITER.'
write(*,*) 'no. of iterations: ',ii
read(*,*)
stop
endif

if(ii.eq.15) noconv = .false.
```

```
c FIN DES ITERATION POUR ANNULER LE RESIDU EN CONTRAINTES
enddo ! while - iterations

c stress interpolation parameters
do i = 1,ni
hr(nh2-1+i) = bet(i)
end do

c sig33
do i = 1,lint
hr(nh2+ni + (i-1)*nhv + 1) = sig33(i)
enddo ! i

c plastic hardening parameter
do i = 1,lint
c isotropic hardening
hr(nh2+ni + (i-1)*nhv ) = ep1(i)
c kinematic hardening
do j = 1,4
hr(nh2+ni+(i-1)*nhv+3+j) = kappaP1(j,i)
enddo ! j
enddo ! i

c damage hardening parameter
do i = 1,lint
hr(nh2+ni + (i-1)*nhv + 2) = ksid1(i)
enddo ! i

c damage parameter
do i = 1,lint
rpom = bsig(1,i) + bsig(2,i) + bsig(3,i)
c for our dfisig dodf(1)=dodf(2)=dodf(3)
if(rpom.ne.0.0d0) then
rpom = dama(i)*dodf(1,i)/3.0d0/rpom
endif ! rpom ne 0
dam(i) = dam(i) + rpom
hr(nh2+ni + (i-1)*nhv + 3) = dam(i)
enddo ! i


c plastic strain increment
do i = 1,lint
do j = 1,4
dep(j,i) = gama(i)*odf(j,i)
enddo ! j
enddo ! i

cc AJOUTER ECROUISSAGE CINEMATIQUE DANS LA DISSIPATION PLAS-
TIQUE cc

c Dissipation calculations

c plastic dissipation
do i = 1,lint
```

```
call dissincps(bsign(1,i),bsig(1,i),dep(1,i),ep(i),ep1(i),d(uprm+3),dissp)
delo(2) = delo(2) + dissp*dvol(i)
enddo ! i

c damage dissipation
do i = 1,lint
call dissdamps(bsign(1,i),bsig(1,i),hr(nh1+ni+(i-1)*nhv+3)
,dam(i),ksid,ksid1,d(uprm+8),dissd)
delo(3) = delo(3) + dissd*dvol(i)
enddo ! i

c return

call pzero(stb,ndf*nel*5)

c Compute the stiffness
do l = 1,lint

c int ST̂ B dV
do i = 1,nel

c bet 1
stb(1,1,i) = stb(1,1,i) + shp(1,i,l)*dvol(l)

c bet 2
stb(2,1,i) = stb(2,1,i) + strsh(1,l)*shp(1,i,l)*dvol(l)
stb(2,1,i) = stb(2,1,i) + strsh(5,l)*shp(2,i,l)*dvol(l)
stb(2,2,i) = stb(2,2,i) + strsh(3,l)*shp(2,i,l)*dvol(l)
stb(2,2,i) = stb(2,2,i) + strsh(5,l)*shp(1,i,l)*dvol(l)

c bet 3
stb(3,2,i) = stb(3,2,i) + shp(2,i,l)*dvol(l)

c bet 4
stb(4,1,i) = stb(4,1,i) + strsh(2,l)*shp(1,i,l)*dvol(l)
stb(4,1,i) = stb(4,1,i) + strsh(6,l)*shp(2,i,l)*dvol(l)
stb(4,2,i) = stb(4,2,i) + strsh(4,l)*shp(2,i,l)*dvol(l)
stb(4,2,i) = stb(4,2,i) + strsh(6,l)*shp(1,i,l)*dvol(l)

c bet 5
stb(5,1,i) = stb(5,1,i) + shp(2,i,l)*dvol(l)
stb(5,2,i) = stb(5,2,i) + shp(1,i,l)*dvol(l)
enddo ! i

enddo ! l

c Compute residual
do j = 1,nel
do i = 1,5
r(1,j) = r(1,j) - stb(i,1,j)*bet(i)
r(2,j) = r(2,j) - stb(i,2,j)*bet(i)
enddo ! i
enddo ! j

c return

ccccccccccccccccccccccccccc ISW = 3 ccccccccccccccccccccccccccccc
```

```
c Compute mixed tangent stiffness matrix

if(isw.eq.3) then

call pzero(betdd,nst*5)

c compute d bet/d u = btan(-1) sgt
do j = 1,nel
do l = 1,ndf
do i = 1,5
do ii = 1,5
betdd(i,2*(j-1) + l) = betdd(i,2*(j-1) + l) + btan(i,ii)*stb(ii,l,j)
enddo ! ii
enddo ! i
enddo !l
enddo ! j

c K = stbT d bet/d u call stiff_ps(stb,betdd,s,nst)

endif ! isw = 3

ccccccccccccccccccccccccccc END ISW = 3 ccccccccccccccccccccccccccccc

endif ! isw = 3 or 6

ccccccccccccccccccccccccccc END ISW = 3 or 6 ccccccccccccccccccccccccc

c Output stresses.

ccccccccccccccccccccccccccc ISW = 4 or 8 ccccccccccccccccccccccccccccc

elseif(isw.eq.4 .or. isw.eq.8) then

do i = 1,9
sigm(i) = 0.0d0
end do ! i
do i = 1,3
bpra(i) = 0.0d0
end do ! i
epp = 0.0d0
dtheta = 0.0d0

ccccccccccccccccccccccccccc ISW = 4 ccccccccccccccccccccccccccccccccc
c Output stresses

if (isw .eq. 4) then

sigm(1) = bet(1)
sigm(2) = bet(3)
sigm(4) = bet(5)
sigm(3) = 0.0d0


do l = 1,lint
sigm(3) = sigm(3) + sig33(l)
enddo ! l
sigm(3) = sigm(3)/3.0d0
```

```
write(iow,*) 'sig11 = ',sigm(1),' sig22 = ',sigm(2),' sig33 = ',sigm(3),' sig12 =
',sigm(4)
if(ior.lt.0) then
write(*,*) 'sig11 = ',sigm(1),' sig22 = ',sigm(2),' sig33 = ',sigm(3),' sig12 = ',sigm(4)
endif

ccccccccccccccccccccccccccc ISW = 8 ccccccccccccccccccccccccccccc
c Project stresses onto nodes

else do l = 1,lint
bsig(1,l) = bet(1)+strsh(1,l)*bet(2)+strsh(2,l)*bet(4)
bsig(2,l) = bet(3)+strsh(3,l)*bet(2)+strsh(4,l)*bet(4)
bsig(3,l) = sig33(l)
bsig(4,l) = bet(5)+strsh(5,l)*bet(2)+strsh(6,l)*bet(4)
hist(1,l) = hr(nh2+ni + (l-1)*nhv )
hist(14,l)= hr(nh2+ni + (l-1)*nhv + 2)


c plastic isotropic hardening parameter

q(1,l) = hr(nh2+ni + (l-1)*nhv ) !plasticity harden

c damage hardening parameter

q(2,l) = hr(nh2+ni + (l-1)*nhv + 2) !damage harden

ccccccccccccccccc DAMAGE PARAMETER-IJP

damq(l) = hr(nh2+ni + (l-1)*nhv + 3) !damage parameter

ccccccccccccccccc DAMAGE PARAMETER-IJP

enddo ! l

c q is added in order to plot ksip and ksid
call slcn2d09(ix,bsig,shp,dvol,r,s,r(nen+1,1),lint,nel,4,q)

endif

ccccccccccccccccccccccccccc END ISW = 8 ccccccccccccccccccccccccccc

c Compute J-integrals and material forces

ccccccccccccccccccccccccccc ISW = 16 ccccccccccccccccccccccccccccc

elseif(isw.eq.16) then

call pjint2d(d,ul,tl,shp,dvol,epsv,sigl,r,ndf,ndm,lint)

elseif(isw.eq.25) then

call stcn2z(xl,sigl,shp,dvol,lint,ndm,nel,16)

endif ! isw = 4 or 8

ccccccccccccccccccccccccccc END ISW = 4 or 8 ccccccccccccccccccccccccccccc

endif ! isw = 3 or 4 or 6 or 8 or 14 or 16

c Formats 1000 format(11f10.0)

2001 format(a1,20a4//5x,'Element Stresses'//' Elmt Mat Angle',
'11-stress 22-stress 33-stress 12-stress',
```

```
'1-stress'/' 1-coord 2-coord 11-strain',
'22-strain 33-strain 12-strain 2-stress') 2002 for-
mat(i8,i4,0p,f6.1,1p,5e12.3/0p,2f9.3,1p,5e12.3/1x)

3000 format(' Input: e, nu, rho, th, is (1=pl.stress,2=pl.strain)'/
1 3x,'mate>',)
end
ccccccccccccccccccccccccccccccccccccccccccccccccccccccccc
c define the material model eps = eps(sigma) subroutine epsig(d,sig,eps,tan1)
implicit none
real*8 d(*),sig(*),eps(*),psig(4),tre,trs
integer i,j
real*8 dvag,tan1(4,*),stis3,g,stig,c1,c2

call pzero(tan1,16)
call pzero(eps,4)
stis3 = 3.0d0 * d(1)
dvag = 2.0d0 * d(2)
stig = 4.0d0 * d(2)
g = d(2)
c1 = (stis3 + g)/(3.0d0*stis3*g)
c2 = 1.0d0/stis3/3.0d0 - 1.0d0/dvag/3.0d0

do j = 1,3
do i = 1,3
tan1(i,j) = c2
enddo ! i
enddo ! j
do i = 1,3
tan1(i,i) = c1
enddo ! i
tan1(4,4) = 1.0d0/stig
do j = 1,3
do i = 1,3
eps(i) = eps(i) + tan1(i,j)*sig(j)
enddo ! i
enddo ! j
eps(4) = eps(4) + 2.0d0*tan1(4,4)*sig(4)
end ! sub epsig
ccccccccccccccccccccccccccccccccccccccccccccccccccccccccc
c strain subroutine strn2d_ps(d,xl,ul,shp,ndf,ndm,nel,xx,yy,eps)
implicit none
```

```
include 'cdata.h'
include 'incshp.h'
include 'pmod2d.h'


integer ndf,ndm,nel, j
real*8 d(*),xl(ndm,*),ul(ndf,nen,*),shp(3,*)
real*8 eps(6,*), xx,yy


save

c Compute strains and coordinates

do j = 1,4
eps(j,1) = 0.0d0
eps(j,3) = 0.0d0
end do
xx = 0.0d0
yy = 0.0d0
do j = 1,nel
xx = xx + shp(3,j)*xl(1,j)
yy = yy + shp(3,j)*xl(2,j)
eps(1,1) = eps(1,1) + shp(1,j)*ul(1,j,1)
eps(2,1) = eps(2,1) + shp(2,j)*ul(2,j,1)
c eps(3,1) = eps(3,1) + shp(3,j)*ul(1,j,1)
eps(4,1) = eps(4,1) + 0.5d0*(shp(2,j)*ul(1,j,1) + shp(1,j)*ul(2,j,1))

c increment
eps(1,3) = eps(1,3) + shp(1,j)*ul(1,j,2)
eps(2,3) = eps(2,3) + shp(2,j)*ul(2,j,2)
c eps(3,3) = eps(3,3) + shp(3,j)*ul(1,j,2)
eps(4,3) = eps(4,3) + 0.5d0*(shp(2,j)*ul(1,j,2) + shp(1,j)*ul(2,j,2))
end do

c Strain at t_n
eps(1,2) = eps(1,1) - eps(1,3)
eps(2,2) = eps(2,1) - eps(2,3)
eps(3,2) = eps(3,1) - eps(3,3)
eps(4,2) = eps(4,1) - eps(4,3)

end ! sub strn2d_ps

ccccccccccccccccccccccccccccccccccccccccccccccccccccccccccc

c compute the stiffness

subroutine stiff_ps(stb,betdd,s,nst)

implicit none

integer nst,i,j,ii
real*8 stb(5,*),betdd(5,*),s(nst,*)

c call pzero(s,nst*nst)
```

```
do j = 1,nst
do i = 1,j
do ii = 1,5
s(i,j) = s(i,j) + stb(ii,i)*betdd(ii,j)
enddo ! ii
enddo ! i
enddo ! j

c Compute lower part by symmetry
do i = 1,nst
do j = 1,i
s(i,j) = s(j,i)
end do ! j
end do ! i

end ! sub stiff_ps

ccccccccccccccccccccccccccccccccccccccccccccccccccccccccccc

c stress part of the yield function
real*8 function fisig(sig,alpha)


implicit none

real*8 sig(*),alpha(1,4),psig(4),trs,dsqrt
integer i

trs = (sig(1) + sig(2) + sig(3))/3.0d0

do i = 1,3
psig(i) = sig(i) - trs + alpha(1,i)
enddo ! i
psig(4) = sig(4) + alpha(1,4)

fisig = 0.0d0
do i = 1,3
fisig = fisig + psig(i)*psig(i)
enddo ! i
fisig = dsqrt(fisig + 2.0d0*psig(4)*psig(4))

end ! fun fisig

ccccccccccccccccccccccccccccccccccccccccccccccccccccccccccc

c stress part of the yield function
real*8 function dfisig(sig)

implicit none

real*8 sig(*)
integer i

dfisig = (sig(1) + sig(2) + sig(3))/3.0d0


end ! fun dfisig

ccccccccccccccccccccccccccccccccccccccccccccccccccccccccccc
```

```
c 1. odvod
subroutine odfisig(sig,alpha,odf)

implicit none

real*8 sig(*),odf(*),trs,dsqrt,devn
real*8 alpha(4)
integer i

trs = (sig(1) + sig(2) + sig(3))/3.0d0

do i = 1,3
odf(i) = sig(i) - trs + alpha(i)
enddo ! i
odf(4) = sig(4) + alpha(4)

devn = 0.0d0
do i = 1,3
devn = devn + odf(i)*odf(i)
enddo ! i
devn = dsqrt(devn + 2.0d0*odf(4)*odf(4))

do i = 1,3
odf(i) = odf(i)/devn
enddo ! i
odf(4) = 2.0d0*odf(4)/devn

end ! sub odfisig

ccccccccccccccccccccccccccccccccccccccccccccccccccccccccccccc

subroutine dodfisig(sig,odf)

implicit none

real*8 sig(*),odf(*)
integer i

do i = 1,3
odf(i) = 1.0d0/3.0d0
enddo ! i
odf(4) = 0.0d0

end ! sub dodfisig

ccccccccccccccccccccccccccccccccccccccccccccccccccccccccccccc

c 2. odvod
subroutine odfisig2(sig,alpha,odf2)

implicit none

real*8 sig(*),alpha(4),odf2(4,*),trs,dsqrt,devn
real*8 psig(4),devn3
integer i,j

do j = 1,4
do i = 1,4
```

```
odf2(i,j) = 0.0d0 enddo ! i
enddo ! j

trs = (sig(1) + sig(2) + sig(3))/3.0d0


do i = 1,3
psig(i) = sig(i) - trs + alpha(i)
enddo ! i psig(4) = sig(4) + alpha(4)


devn = 0.0d0
do i = 1,3
devn = devn + psig(i)*psig(i)
enddo ! i
devn = 1.0d0/dsqrt(devn + 2.0d0*psig(4)*psig(4))
devn3 = devn**3

do i = 1,3
odf2(i,i) = devn
enddo ! i
odf2(4,4) = 2.0d0*devn - 4.0d0*devn3*psig(4)*psig(4)

do j = 1,3
do i = 1,3
odf2(i,j) = odf2(i,j) - devn/3.0d0 - devn3*psig(i)*psig(j)
enddo ! i
enddo ! j

do j = 1,3
odf2(j,4) = - 2.0d0 * devn3 * psig(j) * psig(4)
odf2(4,j) = odf2(j,4)
enddo ! j

end ! sub odfisig2

ccccccccccccccccccccccccccccccccccccccccccccccccccccccccccccc

c kinematic part of the yield criterion


subroutine alph(H1,kappaP,alphaP)

implicit none

real*8 kappaP,H1,kdv,alphaP

data kdv /0.81649658092772603273/

alphaP = -kdv*kdv*H1*kappaP

end

ccccccccccccccccccccccccccccccccccccccccccccccccccccccccccccc

c derivee de la contrainte de rappel est ajoutee

real*8 function dalph(H1)

implicit none
```

```
real*8 kdv,H1

data kdv /0.81649658092772603273/

dalph = -kdv*kdv*H1

end

ccccccccccccccccccccccccccccccccccccccccccccccccccccccccccccc

c hardening part of the yield function
real*8 function kapa(d,ksip)

implicit none

real*8 d(*),ksip,dsqrt

c kapa = - dsqrt(2.0d0/3.0d0)
kapa = -(d(1) + (d(2)-d(1))*(1.0d0-exp(-d(3)*ksip)) + d(4)*ksip)

end ! fun kapa

ccccccccccccccccccccccccccccccccccccccccccccccccccccccccccccc

c odvod
real*8 function odkapa(d,ksip)

implicit none

real*8 d(*),ksip,dsqrt

c odkapa = - dsqrt(2.0d0/3.0d0)
odkapa = -(d(3)*(d(2)-d(1))*exp(-d(3)*ksip) + d(4))

end ! fun odkapa

ccccccccccccccccccccccccccccccccccccccccccccccccccccccccccccc

c static condensation

subroutine statcongg(btan,btpg,btgg,bres,brg,np,ng)

implicit none

integer np,ng,i,j,k
real*8 btan(np,np),btpg(np,*),btgg(*)
real*8 bres(np),brg(*)

do i = 1,np
do j = 1,ng
bres(i) = bres(i) - btpg(i,j)*brg(j)*btgg(j)
enddo ! j
enddo ! j


do j = 1,np
do i = 1,np
do k = 1,ng
btan(i,j) = btan(i,j) - btpg(i,k)*btgg(k)*btpg(j,k)
enddo ! k
```

```
enddo ! i
enddo ! j

end ! sub statcongg

ccccccccccccccccccccccccccccccccccccccccccccccccccccccccccccccccc

c get the sig33 component in each g.p.

subroutine getsig33(btpg,btgg,brg,bet,sig33,np,ng)

implicit none

integer np,ng,i,j
real*8 btpg(np,*),btgg(*),brg(*),bet(*)
real*8 sig33(ng),psig(ng)


do i = 1,ng
psig(i) = 0.0d0
do j = 1,np
psig(i) = psig(i) - btpg(j,i)*bet(j)
enddo ! j
enddo ! i

do i = 1,ng
psig(i) = btgg(i)*(brg(i) + psig(i))
enddo ! i

do i = 1,ng
sig33(i) = sig33(i) + psig(i)
enddo ! i

end ! sub getsig33

ccccccccccccccccccccccccccccccccccccccccccccccccccccccccccccccccc

c get gama from the compatibility equation

subroutine damacomp(d,sig,ksidn,ksid1,gama)

implicit none

real*8 sig(*),ksidn,dfisig,h,ksid1,tol,dg
real*8 kapa,gama,d(*),odkapa,fiss
logical noconv
integer ii

tol = 1.0d-12
gama = 0.0d0
dg = 0.0d0
ksid1 = ksidn
noconv = .true.

fiss = dfisig(sig)

ii = 0
do while(noconv)
ii = ii + 1
```

```
gama = gama + dg
ksid1 = ksidn + gama
h = fiss + kapa(d,ksid1)
if( abs(h) .le. tol*d(1) ) then
noconv = .false.
c write(*,*) 'ksid1= ',ksid1
c read(*,*)
elseif(ii.gt.20) then
write(*,*) 'elmt09: damacomp: NO CONVERGENCE FOR GAMMA'
write(*,*) 'no. of iterations: ',ii
write(*,*) 'residual = ',h
write(*,*) 'tolerance= ',tol,' kapa= ',kapa(d,ksidn)
read(*,*)
stop
else
dg = odkapa(d,ksid1)
dg = - h/dg
endif
enddo ! while

end ! sub damacomp

ccccccccccccccccccccccccccccccccccccccccccccccccccccccccccccc

subroutine gamacomp(d,sig,ksipn,ksip1,kappapn,kappap1,gama)

implicit none

real*8 sig(*),ksipn,fisig,h,ksip1,tol,dg,iow
real*8 kappapn(4),kappap1(4),alphapn(4),alphap1(4)
real*8 kapa,gama,d(*),odkapa,fiss,kdv,odf(4),dalph
logical noconv
integer i,ii

kdv = dsqrt(2.0d0/3.0d0)
tol = 1.0d-12
gama = 0.0d0
dg = 0.0d0
ksip1 = ksipn
do i = 1,4
kappap1(i) = kappapn(i)
call alph(d(10),kappap1(i),alphap1(i))
enddo
noconv = .true.

call odfisig(sig(1),alphap1(1),odf(1))

fiss = fisig(sig,alphap1)

ii = 0
do while(noconv)
ii = ii + 1
gama = gama + dg
ksip1 = ksipn + kdv*gama
```

```
do i = 1,4
kappap1(i) = kappapn(i) + gama*odf(i)
call alph(d(10),kappap1(i),alphap1(i))
enddo h = fiss + dalph(d(10))*gama + kdv*kapa(d,ksip1)
c print*,'h =',h
if( abs(h) .le. tol*d(1) ) then
noconv = .false.
c write(iow,*)'kisp1 = ', ksip1

elseif(ii.gt.20) then
write(*,*) 'elmt09: gamacomp: NO CONVERGENCE FOR GAMMA'
write(*,*) 'no. of iterations: ',ii
write(*,*) 'residual = ',h, ' tolerance= ',tol
write(*,*) 'alphap1(1)= ',alphap1(1),' kapa= ',kapa(d,ksipn)
write(*,*) 'kappap1(1)= ',kappap1(1),' odf(1)= ',odf(1)
write(*,*) 'kappap1(2)= ',kappap1(2),' odf(2)= ',odf(2)
write(*,*) 'kappap1(3)= ',kappap1(3),' odf(3)= ',odf(3)
write(*,*) 'kappap1(4)= ',kappap1(4),' odf(4)= ',odf(4)
write(*,*) 'sig(1)= ',sig(1)
write(*,*) 'sig(2)= ',sig(2)
write(*,*) 'sig(3)= ',sig(3)
write(*,*) 'sig(4)= ',sig(4)
write(*,*) 'sig(5)= ',sig(5)
write(*,*) 'sig(6)= ',sig(6)
read(*,*)
stop
else
c print*,'dalph =',dalph(d(10))
c ii = ii + 1 !ajoute
dg = kdv*kdv*odkapa(d,ksip1) + dalph(d(10))
dg = - h/dg
c print*,'dg =',dg
c gama = gama + dg !ajoute
endif
enddo ! while


end ! sub gamacomp

ccccccccccccccccccccccccccccccccccccccccccccccccccccccccccccccccc

c plastic dissipation
subroutine dissincps(sig1,sig2,dep,ksi,ksi2,d,diss)

implicit none

integer i,j
real*8 sig1(*),sig2(4),ka,mu,dot,dep(*),d(*)
real*8 trsig,trepse,sigp(6),diss,ksi,ksi2
real*8 sy,sinf,beta,rp,sig(4),kp,tt,kapa
```

```
c average stress
do i = 1,4
sig(i) = (sig1(i) + sig2(i))/2.0d0
enddo !i

diss = dot(dep,sig,3) + 2.0d0*dep(4)*sig(4)


C TEST
tt = dsqrt(2.0d0/3.0d0)
rp = -tt/2.0d0*(kapa(d,ksi2) + kapa(d,ksi)+2.0d0*d(1))
rp = rp*(ksi2 - ksi)
diss = diss - rp
end ! sub dissincps


ccccccccccccccccccccccccccccccccccccccccccccccccccccccccccccccccccccccc

c damage dissipation
subroutine dissdamps(sgin,sig1,damn,dam1,ksi,ksi2,d,diss) implicit none integer i,j
real*8 sgin(*),sig1(*),dot,damn(*),dam1(*)
real*8 trsig,sigp(4),diss,ksi,ksi2,kd,ddam
real*8 d(*),rp,ed(4),tred,kapa,sig(4)
do i = 1,4
sig(i) = (sig1(i) + sgin(i))/2.0d0
enddo !i

trsig = (sig(1) + sig(2) + sig(3))/3.0d0

ddam = dam1(1) - damn(1)

tred = 3.0d0*ddam*trsig

do i = 1,3
ed(i) = tred
enddo !i
ed(4) = 0.0d0

C TEST

diss = dot(ed,sig,3) + 2.0d0*ed(4)*sig(4)

rp = -(kapa(d,ksi2) + kapa(d,ksi) + 2.0d0*d(1))/2.0d0
rp = rp*(ksi2 - ksi)

c TEST

if(rp.gt.diss .and. rp.gt.0.0) then
endif

C TEST

if(rp.gt.0.0d0) then
diss = diss - rp
else
diss = 0.0d0
endif
```

end ! sub dissdamps

ccccccccccccccccccccccccccccccccccccccccccccccccccccccccccccccccccccccccc

APPENDIX C:Interpolation Function

Pian-Sumihara is the two-field elements interpolation of the full stress and displacement fields. A four-node plane rectangular element where interpolations may be given directly in terms of Cartesian coordinates is shown in Fig.B.1.

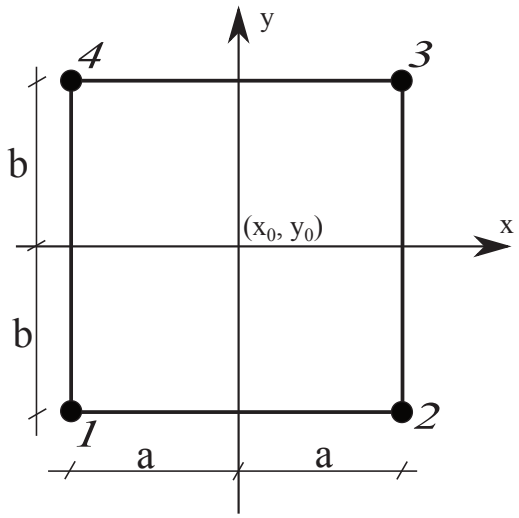

Figure B.1: Displacement directions of yhe plasticity surface

Displacement interpolation is given by

$$u = \sum_{i=1}^{4} N_i(x,y)\bar{u}_i \tag{A.1}$$

so that the shape functions are;

$$\begin{aligned}
N_1(x,y) &= \frac{1}{4}\left\{1-\frac{x-x_0}{a}\right\}\left\{1-\frac{y-y_0}{b}\right\} \\
N_2(x,y) &= \frac{1}{4}\left\{1+\frac{x-x_0}{a}\right\}\left\{1-\frac{y-y_0}{b}\right\} \\
N_3(x,y) &= \frac{1}{4}\left\{1+\frac{x-x_0}{a}\right\}\left\{1+\frac{y-y_0}{b}\right\} \\
N_4(x,y) &= \frac{1}{4}\left\{1-\frac{x-x_0}{a}\right\}\left\{1+\frac{y-y_0}{b}\right\}
\end{aligned} \tag{A.2}$$

where x_0 and y_0 are the cartesian coordinate of the element centre. From the Eq. **A.2** the strains are obtained;

$$\begin{aligned} \varepsilon_x &= \alpha_1 + \alpha_2 y \\ \varepsilon_y &= \alpha_3 + \alpha_4 x \\ \varepsilon_{xy} &= \alpha_5 + \alpha_6 x + \alpha_7 y \end{aligned} \tag{A.3}$$

Here, α_i are expressed in terms of $\bar{u}$. We use 5β parameter as explained in [49].

$$\begin{bmatrix} \sigma_x \\ \sigma_y \\ \tau_{xy} \end{bmatrix} = \begin{bmatrix} 1 & 0 & 0 & y-y_0 & 0 \\ 0 & 1 & 0 & 0 & x-x_0 \\ 0 & 0 & 1 & 0 & 0 \end{bmatrix} \begin{bmatrix} \beta_1 \\ \beta_2 \\ \beta_3 \\ \beta_4 \\ \beta_5 \end{bmatrix} \tag{A.4}$$

CURRICULUM VITAE

Name Surname: Bahar Ayhan Tezer

Place and Date of Birth: Ankara and 18.11.1979

E-Mail: ayhanb@itu.edu.tr

B.Sc.: Istanbul Technical University,2003

Professional Experience
2003-2006 – Civil Engineer, Tekser Construction Company
2007- – Research/Teaching Assistant, Istanbul Technical University

Rewards

- Foreign Student Scholarship of French Government (Joint Ph.D. student)
- The Scientific and Technological Research Council of Turkey(TUBITAK) BIDEB 2211 and 2214 scholarship (Ph.D Studies)

List of Publications and Patents

- **B. Ayhan**, P. Jehel, D. Brancherie, A. Ibrahimbegovic, 'Coupled Damage-Plasticity Model for Cyclic Loading Applications: Theoretical Formulation and Numerical Implementation', Int. J. Engineering Structures, in press, (2013)
- **B. Ayhan**., P. Jehel, A. Ibrahimbegovic, 'The energy dissipation in metal membrane under cyclic loading', IASS-IACM 2012: 7th Int. Conference on Computational Mechanics for Spatial Structures, Sarajevo, April 2-4, (2012)
- **B. Ayhan**, P. Jehel, A. Ibrahimbegovic, H. Engin, 'Coupled Damage-Plasticity Based Constitutive Modeling of Metallic Membrane Element Under Cyclic Loading', COMPDYN 2011 Computational Methods in Structural Dynamics and Earthquake Engineering, Corfu, May 26-28, (2011).